Analysis of the uncharacterized La-related protein, Slr1p from *Schizosaccharomyces pombe*

Lidia Siniavskaia

A THESIS SUBMITTED TO FACULTY OF GRADUATE STUDIES IN PARTIAL FULFILMENT OF THE REQUIREMENTS FOR THE DEGREE OF

MASTER OF SCIENCE

GRADUATE PROGRAM IN BIOLOGY
YORK UNIVERSITY
TORONTO, ONTARIO

August 2013

ABSTRACT

La is a ubiquitous RNA-binding phosphoprotein found in nearly all eukaryotes. La binds to nascent polymerase III transcripts via their UUU-3'OH motif and protects these RNAs from 3'exonucleolytic digestion. La also exhibits RNA chaperone activity, is involved in intracellular trafficking, and stimulates the translation of certain subsets of mRNA via unknown mechanisms. Structurally, all La proteins harbour an N-terminal La module consisting of a La motif (LAM) and an RNA recognition motif. The LAM displays a high degree of conservation, not only among genuine La proteins but also in La-related proteins (LARPs) of which 4 families have been identified: LARP 1, 4, 6 and 7. Although they fulfill important cellular functions, LARPs are generally poorly understood. In an effort to characterize LARPs in greater detail, a simple LARP from *Schizosaccharomyces pombe*, Slr1p, was chosen as an ideal candidate to study. From an evolutionary perspective, we propose that Slr1p constitutes an ancestor to LARPs in higher eukaryotes, and therefore, characterization of its function may provide insight into the divergent roles of its extended relatives. We performed RNA chaperone assays, electromobility shift assays, localization studies via indirect immunofluorescence, as well as co-immunoprecipitation and mass spectrometry to determine Slr1p associated factors. Taken together, our results suggest that Slr1p is an RNA chaperone, it associates with fatty acid synthase as well as translation initiation factors in the cytoplasm, and that it binds to RNAs in a UUU'3-OH independent manner.

Acknowledgements

Foremost, I would like to express my gratitude to my supervisor Dr. Mark Bayfield for giving me the opportunity to work in his lab and for the patient guidance, encouragement and advice he has provided throughout this thesis. His immense knowledge and enthusiasm have inspired me to become a better researcher and I could not have imagined having a better supervisor and mentor for my Master's thesis.

I would like to thank Marlene Oeffinger at the IRCM for her collaboration as her method of RNP isolation was fundamental to this project. Also, a special thanks to my thesis committee members: Dr. Yi Sheng, Dr. Peter Cheung and Dr. Gerald Audette for contributing their time and effort towards my thesis.

If it were not for the support and friendship of my fellow lab mates, completing this work would have been so much more difficult. I want to thank all the past and present members of the lab for their continuous support, willingness to help and all the fun times we shared together.

Finally, I would like to thank my family and friends for always supporting me and encouraging me with their best wishes. They have been there for me throughout the good and bad times of my research and have pushed me to never give up. I am forever grateful for your constant love and support.

TABLE OF CONTENTS

LIST OF ABBREVIATIONS

Ala	Alanine
Amp	Ampicillin
Asp	Aspartic acid
bp	Base pairs
BSA	Bovine serum albumin
CCA	Cytosine-cytosine-adenine
CIP	Calf intestinal alkaline phosphatase
CK2	Casein kinase 2
Co-IP	Co-immunoprecipitation
Cm	Chloramphenicol
CTD	C-terminal domain
DAG	Diacylglycerol
DAPI	4',6-diamidino-2-phenylindole
ddH_2O	Double-distilled water
DNA	Deoxyribonucleic acid
dNTP	Deoxyribonucleoside Triphosphate
DTT	Dithiothreitol
ECL	Enhanced chemiluminescence
EDTA	Ethylenediamine tetra-acetic acid
eIF	Eukaryotic initiation factor
EMM	Edinburgh minimal media
EMSA	Electrophoretic mobility shift assay
F	Free
FAS	Fatty acid synthase
Fas1	Fatty acid synthase β-subunit
Fas2	Fatty acid synthase α-subunit
FRET	Fluorescence resonance energy transfer
g	Force of Gravity (centrifugal speed unit)
Gln	Glutamine
HCV	Hepatitis C virus
His	Histidine
hLA	Human La
HRP	Horseradish peroxidase
IgG	Immunoglobulin G
IPTG	Isopropyl thiol galactopyranoside
IRES	Internal Ribosomal Entry Site
Kan	Kanamycin
kDa	Kilodaltons
LAM	La-motif
LARP	La-related protein
LB	Luria-Bertani growth medium (Luria Broth)
LC-MS	Liquid chromatography - mass spectrometry

LC-MS/MS	Liquid chromatography – tandem mass spectrometry
Leu	Leucine
Mdm2	Murine double minute oncogene
Met	Methionine
mRNA	Messenger RNA
NEB	New England Biolabs
NLS	Nuclear localization signal
NRE	Nuclear retention element
NTD	N-terminal Domain
OD	Optical density
ORF	Open reading frame
PA	Phosphatidic acid
PABP	Poly-A binding protein
PAP	Peroxidase anti-peroxidase
PBSBL	1X PBS,1% BSA,100 mM lysine-HCl
PC	Phosphatidylcholine
PCR	Polymerase chain reaction
PE	Phosphatidylethanolamine
PG	Phosphatidylglycerol
PI	Phosphatidylinositol
PL	Phospholipid
PMSF	Phenylmethylsulfonyl fluoride
PrA	Protein A
pre-tRNA	Precursor transfer RNA
PS	Phosphatidylserine
RNA	Ribonucleic acid
RNP	Ribonucleoprotein
RRM	RNA- recognition motif
RRM-L	RRM-Like
SBM	Short basic motif
SD	Standard deviation
SDS-PAGE	Sodium dodecyl sulfate polyacrylamide gel electrophoresis
Ser	Serine
TAG	Triacylglyceride
TEMED	N, N, N', N'- Tetramethylethylenediamine
Tet	Tetracycline
TOP	Terminal oligopyrimidine
tRNA	Transfer RNA
Tyr	Tyrosine
uORF	Upstream open reading frame
ura	Uracil
UTR	Untranslated region
YES	Yeast extract with supplements

LIST OF TABLES

LIST OF FIGURES

INTRODUCTION

La is a ubiquitously expressed nuclear phosphoprotein found in in nearly all eukaryotes studied. Human La (hLa) was originally identified as an autoantigen in patients affected by autoimmune diseases such as systemic lupus erythrematosus and Sjogren's syndrome (Mattioli and Reichlin, 1974; Alspaugh and Tan, 1975). Although it is not clear why La is targeted as an autoantigen in these diseases, functions of La in various intracellular processes involving RNA have been extensively studied. Genuine La is essential in higher eukaryotes, such as *Drosophila* and mice (Bai and Tolias, 2000; Park et al., 2006), but it becomes dispensable for growth in lower eukaryotic species (Yoo and Wolin, 1994; Van Horn et al., 1997). Therefore, budding and fission yeast serve as good model organisms to study La and La-related proteins (LARPs) where genetic manipulations are made possible and La deletion is viable.

Structurally, La proteins share the highly conserved La motif with La-related proteins of which 4 human families have been identified so far: LARP 1, 4, 6 and 7 (Bousquet-Antonelli and Deragon, 2009). Although they fulfill important cellular functions, LARPs are generally poorly understood. In an effort to characterize LARPs in greater detail, a simple LARP from *Schizosaccharomyces pombe,* Slr1p, was studied and has been shown to exhibit RNA chaperone activity and bind to translation initiation factors and fatty acid synthase in the cytoplasm.

A. Genuine La protein

1. La protein structure

La proteins contain a highly conserved N-terminal La module that consists of a La motif (LAM) and an adjacent RNA recognition motif (RRM), separated by a short linker (Teplova et al., 2006) (Figure 1A). Studies show that both the LAM and RRM1 are required for high-affinity RNA binding (Alfano et al., 2004). Structural studies on human La have revealed that the LAM, an approximately 80 residue RNA binding domain adopts a winged helix-turn-helix architecture and the RRM1, approximately 90 amino acids long, harbours a classic $\beta_1\alpha_1\beta_2\beta_3\alpha_2\beta_4$ topology of canonical RRMs (Alfano et al., 2004; Maris et al., 2005). These two motifs work synergistically to form a tight RNA-binding pocket that recognizes and binds to RNAs ending in UUU-3'OH (Kotik-Kogan et al., 2008) (Figure 1B). A co-crystal structure of the La module from human La, bound to a short RNA containing a UUU-3'OH tail demonstrates that its mode of RNA binding is more complex than other RNA-binding proteins, leaving the canonical nucleic acid binding surfaces accessible (Teplova et al., 2006).

Structure-based mutagenesis studies and biochemical tactics reveal that La proteins have two separate ways to engage their target RNAs: UUU-3'OH dependent and independent RNA binding modes (Bayfield and Maraia, 2009). In human La, residues in the conserved aromatic patch of the LAM (Gln20, Tyr23 and Asp33) are essential for pre-tRNA binding in a UUU-3'OH dependant manner. More specifically, Gln20 makes contacts to the penultimate base of the RNA which is uridylate specific, Tyr23 stacks on the uracil and makes a direct hydrogen bond protein-protein contact between the LAM

and RRM1 and Asp33 makes bidentate contacts to the 2'OH and 3'OH groups of the terminal sugar residue of the RNA, simultaneously discriminating between DNA ends and RNA ends (Bayfield et al., 2010). Conversely, the UUU-3'OH independent mode can be attributed to one or more of the basic residues in the loop (loop-3 in hLa) that connects the β_2 and β_3 strands of RRM1 (Bayfield and Maraia, 2009). Mutational analysis has shown that this binding mode interacts with unknown regions on the main body of the pre-tRNA by making contacts to residues in the RRM1 β-sheet surface which projects in the same plane as the conserved aromatic side chains (Bayfield and Maraia, 2009). As a result, the coordinated function of LAM and RRM1 produce higher affinity RNA-binding and increased stability (Alfano et al., 2004; Bayfield and Maraia, 2009).

The C-terminal domain (CTD) of La proteins is more divergent and varies greatly in length between different eukaryotes for reasons that are not well understood. The variability of the CTD can be observed in the size of La proteins, ranging from about 32 kDa in yeast to approximately 50 kDa in humans (Dong et al., 2004). The CTD of human La contains an atypical RRM (RRM2) followed by a long unstructured terminal region (Jacks et al., 2003). In addition, the structural features of the C-terminus include a short basic motif (SBM) that incorporates a Walker A motif, a nuclear localization signal (NLS), a nuclear retention element (NRE) and a regulatory phosphorylation site on serine 366 (Maraia and Intine, 2001; Wolin and Cedervall, 2002; Intine et al., 2002). The majority of the motifs found in the CTD of La proteins are not conserved across species which demonstrates the variability of the C-terminal region and complements the functional divergence of La proteins (Jacks et al., 2003).

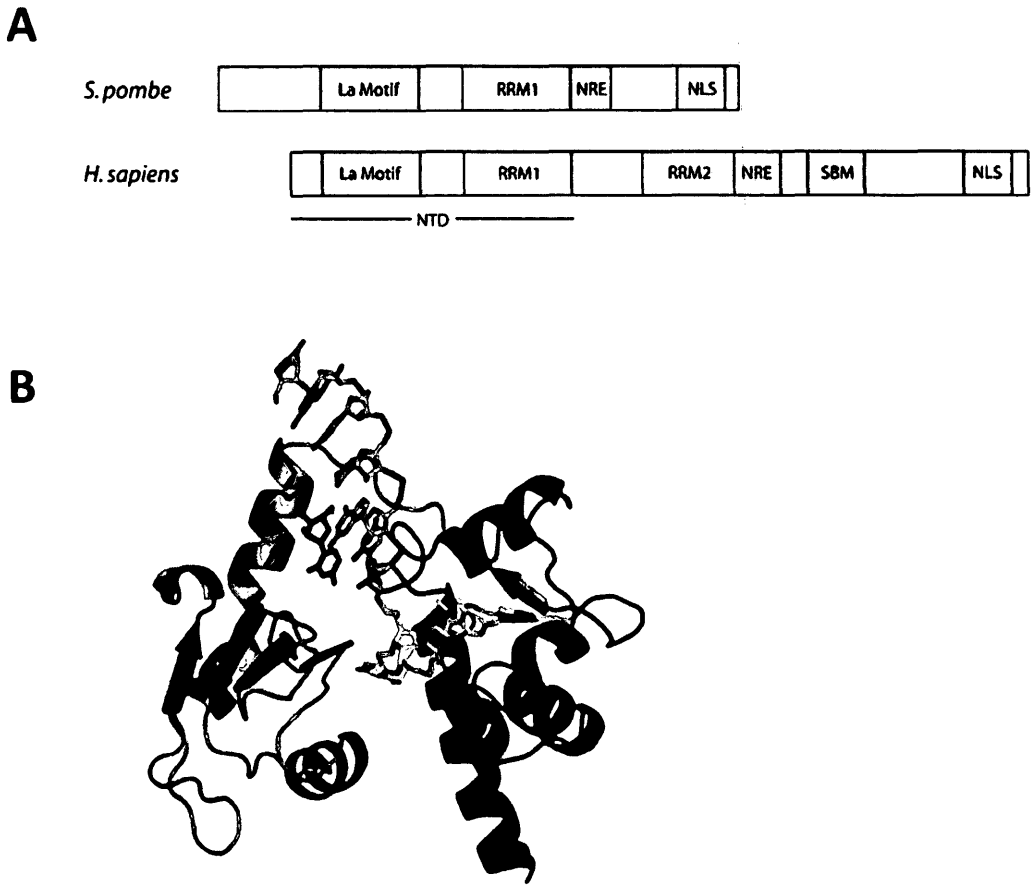

Figure 1 - General architecture of La proteins and structure of the N-terminal domain of human La bound to the UUU-3'OH trailer of an RNA. (A) A schematic alignment depicting the architectural organization of human La and the *S. pombe* homolog, Sla1p. The La module in the N-terminal domain (NTD), comprised of a La motif (LAM) and an adjacent RNA recognition motif (RRM1) is conserved across species, while the C-terminus is more divergent and increases in size from yeast to higher organisms. Human La has an additional RRM (RRM2) that is absent in yeast. NRE, nuclear retention element; SBM, short basic motif; NLS, nuclear localization signal (NLS). (B) The LAM (right) and RRM1 (left) form a pocket that recognizes and interacts with the RNA containing a poly U 3'trailer (yellow). The La motif can be mapped to a UUU-3'OH dependent binding mode which uses two surfaces to interact with the RNA. The RRM1 can be mapped to a UUU-3'OH independent binding mode that binds the RNA via the interface between RRM1 and LAM and Loop 3. The structure of the NTD of hLa bound to a 9mer RNA was solved to 1.85 Å (PDB ID code 1YTY). Figure adapted from Maraia and Bayfield, *Mol Cell* 2006; Teplova et al., *Mol Cell* 2006.

2. La function in the processing and metabolism of a variety of RNA targets

La proteins bind to a number of noncoding RNAs and mRNAs which promote their remarkable functional versatility. Genuine La preferentially binds to RNAs containing up to four terminal uridylates, a universal characteristic of nascent RNA polymerase III transcripts (Stefano, 1984). Ligands most abundantly bound to La include tRNA precursors, 5S rRNA, SRP RNA, the Y RNAs, 7SK RNA, U6 RNA as well as several cellular and viral mRNAs (Bayfield et al., 2010). Studies reveal that La has a conserved role in tRNA processing, it exhibits RNA chaperone activity, is involved in intracellular trafficking, and that it stimulates the translation of certain mRNAs via unknown mechanisms (Maraia and Intine, 2001).

2.1 La's role in precursor tRNA processing and maturation

Nascent pre-tRNAs undergo excessive processing prior to their function in the cytoplasm. Processing involves 5'-end removal by RNase P, 3'-end processing, splicing of introns, base modifications, 3'CCA addition, aminoacylation and nuclear export (Wolin and Matera, 1999). Since La is the first protein to interact with pre-tRNAs, it is involved in several steps of the pre-tRNA processing pathway (Bayfield and Maraia, 2009). The number of uridylate residues at the 3' terminus defines La binding affinity to pre-tRNA, which consequently determines if the RNA species will be processed in a La-dependent or La-independent pathway.

La binds nascent RNAs at the UUU-3'OH terminus and facilitates their maturation by protecting them from 3' exonucleolytic digestion (Yoo and Wolin, 1997). Studies show that the presence of La protein bound to the 3' end of a pre-tRNA ensures

the primary pathway for 3' –end processing in eukaryotes is endonucleolytic (Van Horn et al., 1997). This La-dependent processing pathway begins with the pre-tRNA 5' leader first being removed by RNase P, followed by the excision of the 3' trailer by the endonuclease RNase Z (Maraia and Intine, 2001) (Figure 2). La then dissociates from the mature tRNA and recycles to re-associate with new pre-tRNAs, facilitating their maturation (Bayfield et al., 2010). Since La uses two binding sites, LAM and RRM1 to produce high affinity stable binding of nascent pre-tRNAs, either site alone results in lower affinity and less stable binding. Therefore, once the 3' trailer is cleaved, La now binds two RNAs, the processed tRNA and the cleaved 3' trailer with a lower affinity, therefore allowing it to recycle onto a new pre-tRNA (Bayfield and Maraia, 2009). The mature tRNA undergoes further processing of CCA addition to the new 3'-end, aminoacylation and nuclear export to the cytoplasm. However, in the absence of La the order of processing is altered, where the 3' trailer is removed by exonuclease activity prior to 5'leader cleavage by RNase P (Yoo and Wolin, 1997) (Figure 2).

Additional studies in yeast have shown that La deletion is synthetically lethal with mutations in essential tRNAs that disrupt the secondary structure (Yoo and Wolin, 1997). Originally discovered in *Saccharomyces cerevisiae* (*S. cerevisiae*), a genetic screen identified a mutation in the anticodon stem of an essential $tRNA^{Ser}$ that causes yeast cells to require Lhp1p, a La homolog, for growth (Yoo and Wolin, 1997). In the absence of La, the structurally impaired pre-tRNA becomes prone to degradation by a second class of 3' exonucleases, thus highlighting the importance of La (Bayfield et al., 2010). In support of this, when La is overexpressed in cells, it is able to rescue the defective pre-tRNAs and

allow for their processing and maturation into functional tRNAs (Van Horn et al., 1997). It has been suggested that La stabilizes pre-tRNAs in conformations that facilitate endonucleolytic cleavage (Yoo and Wolin, 1997). Consequently, the fate of many RNAs in the cell is mediated by La, making La an important protein in tRNA processing and maturation.

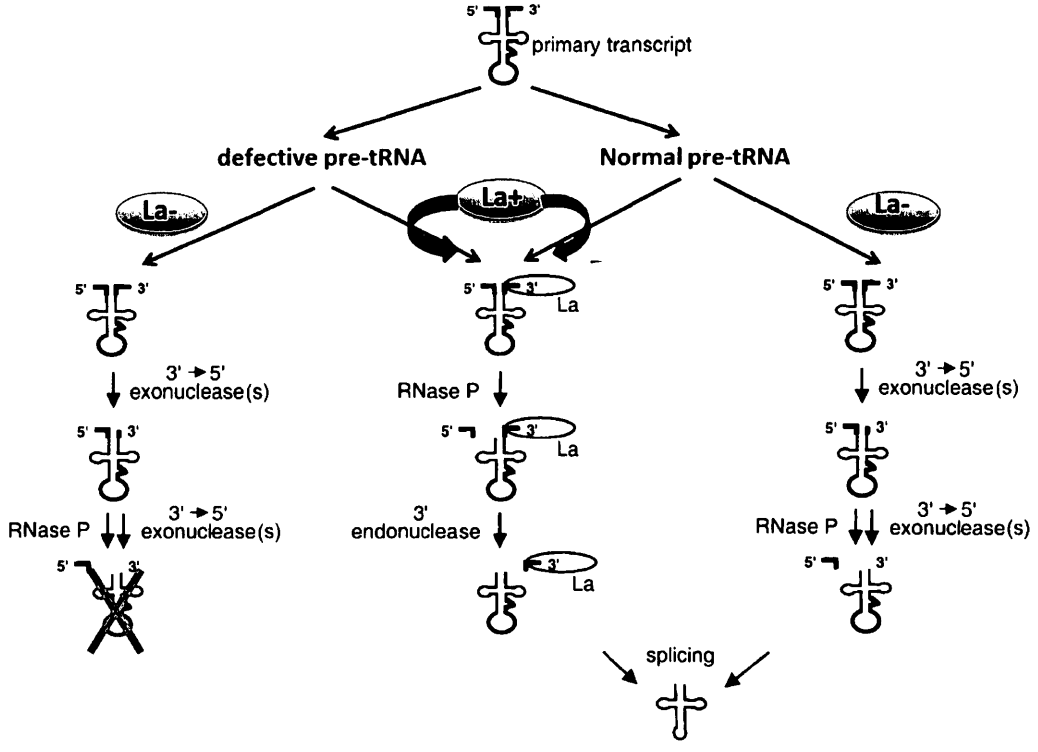

Figure 2 - Precursor-tRNA processing pathways in the presence and absence of La. Four possible pathways exist that determine the fate of the pre-tRNA. The pre-tRNA fate is determined by the length of poly U 3' end, where the interaction between pre-tRNA and La is established with a minimum of three terminal Us. The normal pathway of pre-tRNA processing occurs in the presence and absence of La, but processing of a defective pre-tRNA is only made possible in the presence of La. La engages nascent pre-tRNA transcripts and protects them from 3'exonuclease activity causing the 5' leader to be cleaved first by RNase P followed by 3' end processing by 3' endonuclease Rnase Z. In the absence of La, cleavage of the 5'leader and 3'trailer sequences occurs in the reverse order. A defective pre-tRNA cannot get properly processed in the absence of La, thus resulting in degradation. Figure adapted from Yoo and Wolin, *Cell* 1997.

2.2 La shuttles between the nucleus and the cytoplasm

Immunofluorescence studies have described the subcellular localization of human La as predominately confined to the nucleus, and less in the nucleolus and cytoplasm (Maraia and Intine, 2001; Wolin and Cedervall, 2002). The distribution of La in the cytoplasm becomes increased during certain situations such as apoptosis or certain viral infections (Meerovitch et al., 1993; Ayukawa et al., 2000). The localization of human La can be correlated to its phosphorylation status. When La is present in the nucleus, it is phosphorylated on serine-366 by protein kinase CK2 and associates with nascent pre-tRNAs. Non-phosphorylated La is mostly concentrated in the nucleolus and cytoplasm and associates with several viral and cellular mRNAs (Bayfield et al., 2007).

Intracellular trafficking signals in human La map to the C-terminus and include a nuclear localization signal (NLS) and a nuclear retention element (NRE) (Simons et al., 1996). Although trafficking of human La is important for its wide array of functions, not much is known about La trafficking in specific RNA pathways. Nonetheless, mutational studies have shown that disruption of the normal trafficking of La causes deleterious effects on tRNA processing (Intine et al., 2002). However, it has yet to be shown that wild type La brings tRNAs to the cytoplasm. Consistent with this, studies show that in fission yeast, deletion of the NRE causes nuclear export of La. As a result dysfunctional pre-tRNA processing occurs where the tRNA is spliced out but not 5'-end and 3'end processed, leading to tRNA mediated suppression and degradation (Intine et al., 2002). Therefore, when La is associated with pre-tRNAs and not retained in the nuclei, it causes disorder in the normal pattern of pre-tRNA processing.

2.3 La is an RNA Chaperone

RNA chaperones are proteins that help RNAs attain their native conformations either by preventing kinetic traps or preventing and opening up misfolded structures (Semrad, 2011). *In vivo* data suggests that La binds to the 3' poly U tail of newly synthesized polymerase III transcripts and stabilizes them from 3'exonucleolytic digestion at the precursor stage. In doing so, it maintains them through the critical maturation process. After trailer dissociation, further processing continues and the mature species can accumulate in the cytoplasm and function in the absence of La (Wolin and Cedervall, 2002). In addition, La is able to rescue structurally impaired pre-tRNAs. As aforementioned, La is not essential in yeast, but in the presence of mutations that compromise pre-tRNA structure, La becomes essential (Yoo and Wolin, 1997). When pre-tRNAs acquire certain mutations, they become unstable in the absence of La, and as a result require La for correct folding and subsequent processing (Bayfield and Maraia, 2009). Therefore, in addition to binding and protecting the UUU-3'OH tails of pre-tRNAs, footprinting experiments suggest that La contacts and stabilizes the correctly folded anticodem stem-loop of pre-tRNAs (Chakshusmathi et al., 2003).

Additionally, human La was shown to harbour RNA chaperone activity in an *in vitro* cis-splicing assay, *in vitro* fluorescence resonance energy transfer assay (FRET) and an *in vivo* folding trap assay (Belisova et al., 2005; Bayfield and Maraia, 2009; Naeeni et al., 2012). In addition to protecting pre-tRNA 3' trailers, La proteins function as RNA chaperones to correct the folding of misfolded pre-tRNAs (Naeeni et al., 2012). Besides binding to pre-tRNAs, La also has a role in the enhancement of translation of several

cellular (Holcik and Korneluk, 2000; Intine et al., 2003; Trotta et al., 2003; Inada and Guthrie, 2004) and viral RNAs (Craig et al., 1997; Ali et al., 2000; Costa-Mattioli et al., 2004). A proposed mechanism for this is that La acts as an RNA chaperone to assist in the correct folding of RNA structures required for optimal translation of these mRNAs (Costa-Mattioli et al., 2004; Svitkin et al., 1994; Holcik and Sonenberg, 2005; Martino et al., 2012). Using FRET based assays, it has been shown that the RNA chaperone activity is a conserved feature between *S. pombe* and human La (Naeeni et al., 2012). Also, it has been demonstrated that La-dependent RNA chaperone activity does not require UUU-3'OH mediated RNA binding and human La exhibits both strand annealing and strand dissociation activities in the assay. Mutational analysis revealed that the NTD and CTD both harbour RNA chaperone activity. In the N-terminus, the RRM1 motif, an atypical α-helix C-terminal to the RRM1 (α3-helix) and a subsequent unstructured region are sufficient for strand annealing and strand displacement activities (Figure 3) (Naeeni et al., 2012). In the C-terminus, the intrinsically disordered region is important for RNA chaperone activity (Kucera et al., 2011). However, because the C-terminal half of human La is not conserved and is absent in yeast, suggests a generality for RNA chaperone activity of La proteins. Budding and fission yeast La homologs lack an RRM2 and yet they exhibit RNA chaperone activity. Therefore, a general trend can be observed in both yeast and human La, where the disordered region after an RRM is important for RNA chaperone activity (Naeeni et al., 2012; Kucera et al., 2011). As a result, the combined results from various experiments suggest that La functions redundantly with other

proteins that also contact nascent polymerase III transcripts to stabilize the RNAs and assist their assembly into functional ribonucleoproteins (RNPs).

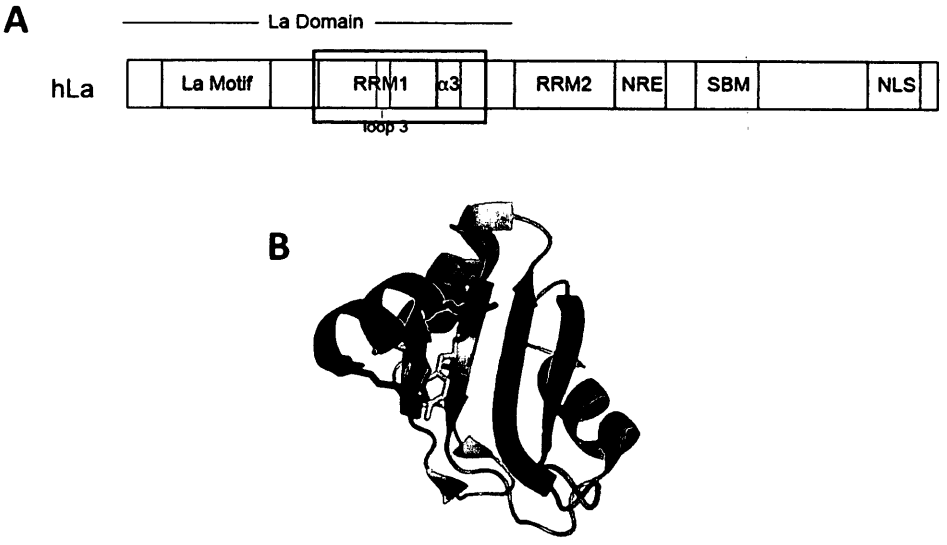

Figure 3 - The canonical RRM1 RNA binding surface and atypical α3-helix are required for RNA chaperone activity. (A) A schematic diagram depicting the architecture of human La. hLa has both N-terminal and C-terminal RNA chaperone activity. NTD activity relies on RRM1 with α3-helix and subsequent disordered region (boxed in red). (B) Structure of the hLa RRM1. β strands are shown in red and the α3-helix in blue. Figure adapted from Naeeni et al., *J Biol Chem* 2012.

2.4 La function in mRNA metabolism

In addition to La's roles in pre-tRNA processing and maturation, La can directly facilitate translation of specific cellular and viral mRNA by binding to internal ribosomal entry sites (IRES), 5'-terminal oligopyrimidine sites (5'TOPs) and upstream open reading frames (uORFs) (Maraia and Intine, 2001; Wolin and Cedervall, 2002). Although first described for poliovirus mRNA (Meerovitch et al., 1993), studies have expanded the list to cellular IRES-containing mRNAs that encode cell cycle-dependent transcripts such as the X-Linked inhibitor of apoptosis (XIAP) and viral mRNAs including hepatitis C virus (HCV), rubella virus, human immunodeficiency virus, influenza virus and vesicular stomatitis (Holick and Korneluk, 2000; Maraia and Intine, 2001). In addition, La has been shown to associate with an Mdm2 mRNA isoform that contains two upstream open reading frames and promotes Mdm2 translation resulting in a downregulation of p53 and consequently an increase in leukemia progression (Trotta et al., 2003). In general, La binds to these atypical translation initiation start sites in the 5' untranslated region of target mRNAs and stimulates their translation, although the molecular mechanism involved remains obscure.

The majority of the work on the interaction between human La and IRES has been done with HCV, reporting that human La bound to the IRES element leads to a significant level of stimulation of the HCV IRES-dependent translation (Ali et al., 2000). More specifically, studies suggest that La binding to the IRES is in the vicinity of the AUG start codon of IRES domain IV (Ali et al., 1997; Ali et al., 2000). Interestingly, this RNA does not contain a UUU-3'OH end, suggesting that La's cytoplasmic binding

capabilities are rather different when compared to its RNA binding mode to substrates in the nucleus (Martino et al., 2012). Moreover, it has been suggested that the C-terminus of human La may be implicated in interactions with mRNAs harbouring atypical translation initiation start sites. This is consistent with La involvement in poliovirus RNA translation which has been correlated to the C-terminal end of human La (Ali et al., 2000). Nonetheless, definitive evidence has yet to be produced that the CTD of human La mediates the interaction to HCV IRES (Martino et al., 2012).

La binds to 5'TOP motifs which are found on a family of mRNAs that encode ribosomal proteins and other factors involved in the translational apparatus (Cardinali et al., 2003). TOP-containing mRNAs generally have extremely short 5'UTRs of about 30 nucleotides with no upstream AUGs (Meyuhas et al., 2000). Ribosome biogenesis is controlled by the regulation of 5'TOP-containing mRNA which directly affects translation; however, the modular mechanisms remain unclear. Data suggests that non-phosphorylated La was found to associate with 5'TOP mRNA in HeLa cells, but not the phosphorylated isoform, suggesting that the phosphorylation status of La may control the capability of La to interact with 5'TOP mRNA (Intine et al., 2003). Furthermore, in *Xenopus* La, there was a positive effect on TOP-mRNA translation whereas in human La, there was an inhibitory effect (Zhu et al., 2001). The role of La in the translational control of TOP mRNAs as either a positive or negative effector has been established, however, future investigations may uncover the different mechanisms involved.

B. La-related proteins

1. Conservation of the La module in La-related proteins

The La motif has been identified in other proteins that are structurally unrelated to La, revealing a family of La-related proteins, called LARPs. LARPs are conserved amongst eukaryotes. Through bioinformatics and structural studies, LARPs have been classified into four distinct classes: LARP 1, 4, 6 and 7 (Bousquet-Antonelli and Deragon, 2009). Based on sequence homology, LARP7 proteins are most closely related to genuine La proteins bearing a canonical RRM1 adjacent to its La motif. Conversely, LARP4 is most divergent lacking a classical RRM (Bayfield et al., 2010) (Figure 4). Human LARPs 1, 4 and 6, as well as LARPs in lower systems contain an RRM-like (RRM-L) motif in place of the canonical RRM, and a few LARPs lack the RRM altogether (Bayfield et al., 2010) (Figure 4). Except for the conserved La motif, these proteins are structurally and functionally different from each other and genuine La proteins. Since LARPs have varying RNA targets, the function of each LARP family is still poorly understood and to date, only a few LARPs have been characterized (Nykamp et al., 2008).

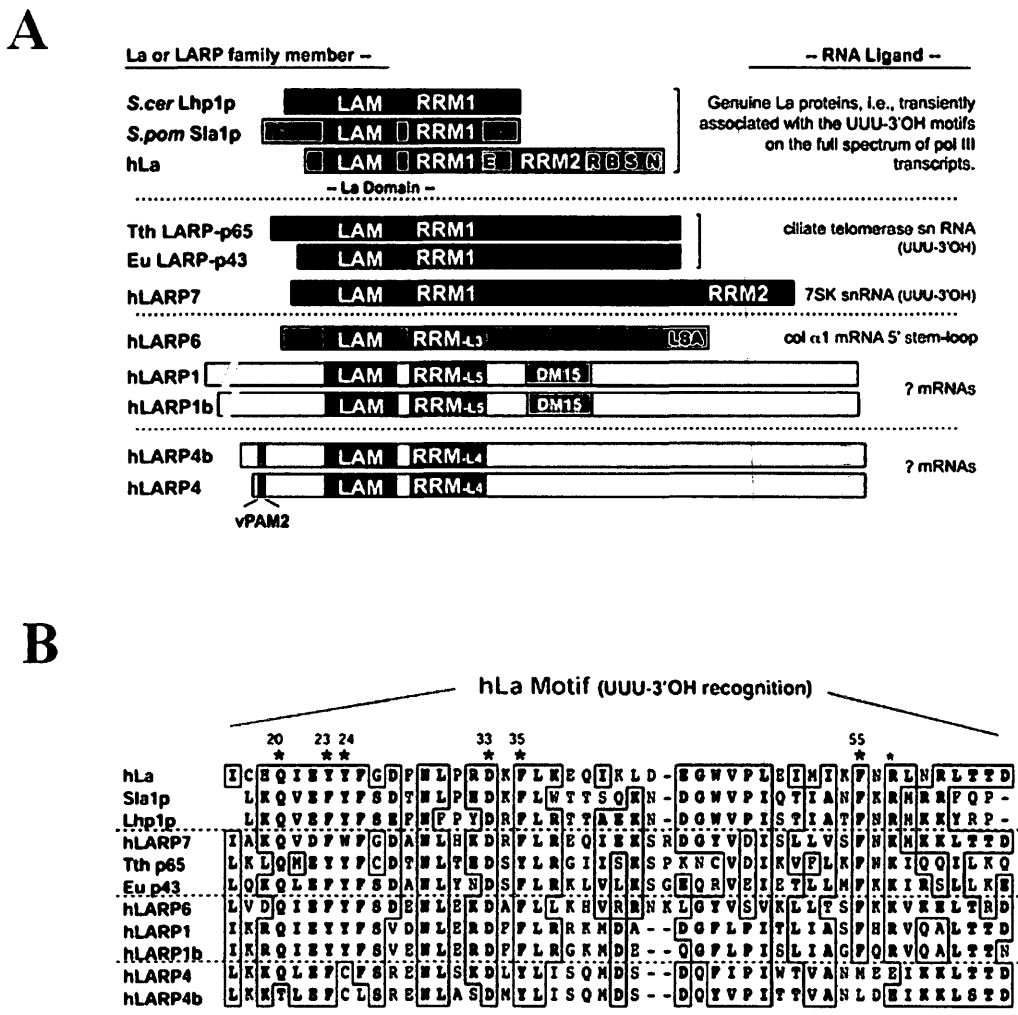

Figure 4 - Schematic alignment of the architecture of the conserved La module of genuine La proteins and LARPs and a clustal-W alignment of the LAM of genuine La and LARPs. (A) LARPs are arranged in the order of their sequence conservation in their LAM compared to genuine La. Genuine La proteins of three species are at the top, *S. cerevisiae*, Lh1p1, *S. pombe,* Sla1p and human La. Human LARPs 1, 6 and 4 exhibit variations from the canonical RRM1, thus having RRM-Like motifs numbered, RRM-L3, RRM-L4 and RRM-L5. LARP7 is the best characterized LARP, thus three members of the LARP7 family are shown, Tth: *Tetrahymena thermophilia* LARP-p65 and Eu: *Eupliotes aediculatus* LARP-p43. LARP4 is most divergent from genuine La. (B) The residues involved in recognizing and binding UUU-3'OH termination motifs are indicated by astericks and numbered according to hLa. Figure adapted from Bayfield, M.A., *et al.*, BBAGene Reg. Mech, 2010.

1.1 La-related proteins 1, 4, 6 and 7

Contrary to the well characterized authentic La proteins, functional and structural data on LARPs is very limited, even though they fulfill crucial cellular functions (Bousquet-Antonelli and Deragon, 2009). To date only a few LARPs have been characterized, of which LARP7 has been the most extensively studied. Studies reveal that LARP7 is part of the 7SK RNP complex, and the complex interacts with the transcription elongation factor b (P-TEFb) (He et al., 2008; Krueger et al., 2008; Markert et al., 2008). P-TEFb is a kinase that is recruited to sites of active transcription and phosphorylates the CTD of RNA polymerase II, thereby relieving a block in transcriptional elongation (Peterlin and Price, 2006). The 7SK snRNP is composed of 7SK RNA, HEXIM 1 and 2 proteins and the 5' methylphosphate capping enzyme, MeCPE. LARP7 specifically binds to and enhances the stability of nuclear 7SK snRNA in a UUU-3'OH dependant manner. This is critical because within the complex, 7SK RNA mediates the interaction of P-TEFb with HEXIM1, which consequently inhibits P-TEFb kinase activity and results in transcriptional attenuation (He et al., 2008). In addition, LARP7 was shown to have an antigrowth/antitumor function that correlates with its negative impact on P-TEFb. Knockdown of hLARP7/PIP7S in human cells resulted in a significant increase in active P-TEFb, leading to elevated expression of key tumour-promoting genes such as PTHLH and TGM-2, unsuppressed cell growth and malignant transformation (He et al., 2008). As a result, LARP7 has been shown to act as a negative transcriptional regulator of polymerase II genes, acting by means of the 7SK RNP system. Moreover, other well studied LARP7 family members include the ciliate homologs p43 from *Euplotes*

aediculatus and p65 from *Tetrahymena thermophile*. These LARP7 homologs have been shown to enhance telomerase activity by assisting in the correct folding of telomerase RNA and hierarchal assembly of the RNP (Aigner et al., 2000; Singh et al., 2012). Human LARP7 and ciliate LARPs have both shown to recognize and bind to the UUU-3'OH termination motif of newly synthesized polymerase III RNA transcripts, suggesting a binding mechanism similar to that of genuine La (Singh et al., 2012).

Other LARP families demonstrate distinct roles in mRNA metabolism, rather than noncoding RNA metabolism. Specifically, LARP6 in the moth *Meduca sexta* homolog Acheron, has been implicated in muscle development where it interacts with transcription factors and functions upstream of the transcription factor MyoD (Valavanis et al., 2007). In humans, LARP6 has been shown to specifically bind with high-affinity to a highly conserved stem-loop motif located in the 5'UTR of α1 collagen mRNAs and presumably coordinate localized translation (Cai et al., 2010). Studies indicate that LARP6 can be a translational repressor if expressed at high levels, but at physiological levels it acts to stimulate collagen synthesis, thus establishing this protein as an important regulator of mRNA translation (Cai et al., 2010; Manojlovic et al., 2012).

Originally identified in *Drosophila*, LARP1 was found to be important for spermatogenesis, embryogenesis and cell cycle progression (Ichihara et al., 2007; Chauvet et al., 2000; Blagden et al., 2009). Biochemical analysis has demonstrated that LARP 1 binds Poly-A binding protein (PABP) and is in complex with eIF4E (Burrows et al., 2010). More recently it has been shown that LARP1 specifically recognizes and binds the 3'terminus of poly(A) mRNA, suggesting that LARP1 may be involved in post-

transcriptional regulation of gene expression as well as mRNA translation (Aoki et al., 2013). Furthermore, LARP1 in *C. elegans* has posed a role in germline development, specifically oogenesis, where it co-localizes with cytoplasmic granules called P-bodies which function in RNA degradation. Interestingly, both eIF4E and PABP have been identified within the cytoplasmic granules (Nykamp et al., 2008). Therefore, LARP1 is hypothesized to affect the stability of certain mRNAs through its association with germline bodies (Nykamp et al., 2008). Overall, LARP1 has been implicated in several processes of mRNA metabolism; however, the function and mechanism for RNA-binding remain unclear.

LARP1 is closest in homology to LARP4 as both display roles in mRNA stability and translation, however, the LARP4 family is also highly divergent from genuine La (Bayfield et al. 2010). Biochemical studies have shown that human LARP4 is a cytoplasmic protein that co-sediments with polysomes and accumulates upon stress induction in stress granules (Schaffler et al., 2010). Also, LARP4 interacts with two key factors of the translational machinery, PABP and the receptor for activated C kinase, acting as a general transcription factor and stimulating the translation of several cellular mRNAs (Schaffler et al., 2010). Some LARP4 proteins harbour an atypical PABP-interacting motif 2 (PAM2) sequence near their N-terminal region (Bayfield et al., 2010). PAM2 motifs generally bind to the MLLE peptide-binding domain found at the C-terminus of PABP, and this interaction enhances the ability of PABP to recruit translation factors and proteins involved in translation regulation and mRNA stability (Merret et al., 2013). Yang et al., 2011 has suggested that LARP4 exhibits a different recognition mode

to its RNA substrates from that of La proteins. NMR and crystallography of a peptide representing the PAM2w motif of human LARP4 and the MLLE domain of PABP showed a distinct interaction, suggesting that LARP4 binds to PABP via an interaction similar to those of other PAM2-MLLE complexes (Yang et al., 2011). Consequently, evidence suggests that LARP4 promotes translation, in part by stabilizing mRNA.

Overall, a general theme emerges from these studies, implicating La-motif containing proteins in mRNA metabolism; however, the mechanism involved and how they recognize various substrates to fulfill their functions still need to be resolved.

1.2 La-related proteins in budding and fission yeast

The two LARPs in *S. cerevisiae*, Sro9p and Slf1p, belong to an unclassified family of LARPs as they do not comprise any other predicted domain besides the La motif, which is positioned more C-terminally (Schenk et al., 2012). Most closely related to LARP1, Sro9p and Slf1p have been implicated in several processes involved in mRNA metabolism (Bayfield et al., 2010). Genetic experiments reveal that these two proteins are not synthetically lethal with the La homolog in *S. cerevisiae*, Lhp1p, suggesting that these three La motif containing proteins do not function in a single essential process (Sobel and Wolin, 1999). Studies show that Sro9p and Slf1p are functionally redundant RNA-binding proteins that associate with translating ribosomes and bind to poly(U) and poly(G) RNA in vitro (Sobel and Wolin, 1999). Immunolocalization data suggests that Sro9p engages in nucleocytoplasmic shuttling where it interacts with protein complexes in the nucleus and cytoplasm that are involved in gene expression (Rother et al., 2010). Sro9p is transported to transcribed genes, and accompanies the nascent transcript to the

cytoplasm where it modulates translation of the bound mRNA (Rother et al., 2010). As a result, Sro9p has been demonstrated to interact with various complexes involved in transcription, translation, and mRNA transport; however, potential Sro9p mRNA targets have not been identified to date (Rother et al., 2010). In contrast to Sro9p, much less is known about Slf1p. RIP-chip analysis has identified potential mRNA targets of Sro9p and Slf1p, and it was shown that the most predominant mRNAs specifically associated with Slf1p were key regulators of the copper-detoxification system (Schenk et al., 2012). It was further demonstrated that the La motif of Slf1p is critical for the interaction and stability of mRNAs that code for proteins involved in copper homeostasis (Schenk et al., 2012). Therefore, Sro9p and Slf1p comprise an evolutionary family of proteins that may function in mRNA translation, although further experimentation is required to fully understand the mechanisms involved.

Whereas *S. cerevisiae* has 2 LARPs, *S. pombe* only has one LARP, which we have named *Schizosaccharomyces pombe* La-related protein 1 (Slr1p). Slr1p is an RNA-binding protein that consists of a C-terminal La motif and lacks an adjacent RRM. Its N-terminal region is rich in positively charged residues, which may also contribute to RNA binding by either specific or non-specific interactions. Structurally, Slr1p does not belong to any of the families of LARPs, thus belonging to the family of unclassified LARPs along with Sro9p and Slf1p. Based on sequence homology, Slr1p is most closely related to LARP1. Slr1p is an uncharacterized LARP and while the present data point to a role in mRNA metabolism and translation, possible mechanisms for target RNA binding and recognition and complete functions of this protein are still unclear.

2. An overview of eukaryotic translation initiation

Protein synthesis and translational control of gene expression is mainly regulated at the initiation stage, rather than during elongation or termination (Svitkin et al., 2009). Efficient translation initiation requires a series of interactions with various translation initiation factors as well as the mRNA itself. Eukaryotic translation initiation has three fundamental steps and the two structural determinants characteristic of eukaryotic mRNAs include the 5'cap and the 3'poly(A) tail, which synergize to stimulate translation (Svitkin et al., 2009). First, the 43S preinitiation complex is formed when the 40S small ribosomal subunit binds the specific initiator Met-$tRNA_i^{Met}$. Second, the resulting complex recognizes and binds to the 5'cap of mRNA which promotes ribosomal scanning to locate the AUG initiation codon. Finally, the 60S large ribosomal subunit joins to create the 80S translation-competent ribosome (Sonenberg and Dever, 2003).

More specifically in the second step, eIF4E is the translation initiation factor that recognizes the m^7G cap and PABP recognizes the poly(A) tail at the 3' end. eIF4E is a cap-binding subunit of the eIF4F complex, which also includes eIF4A, an RNA-dependent helicase as well as eukaryotic translational initiation factor 4G (eIF4G) which functions as a scaffold for binding eIF4A and eIF4E (Wells et al., 1998) (Figure 5). Interestingly, eIF4G also interacts with PABP and functions to recruit the 40S ribosome subunit through an interaction with eIF3 (Hershey et al, 1996) (Figure 5). Thus, the PABP–eIF4G interaction is critical to bring about the circularization of the mRNA and stimulate translation.

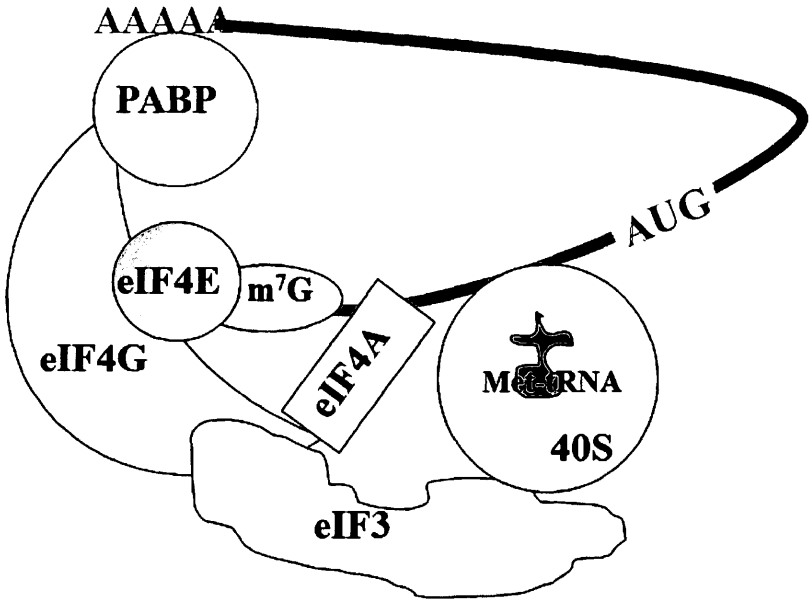

Figure 5 - Eukaryotic translation initiation complex. The eIF4F complex, which is composed of eIF4E, eIF4A and eIF4G recruits capped mRNAs. eIF4E is the cap binding protein that binds the mRNA at the 5' end via the m^7G cap. eIF4A is a helicase and eIF4G acts as a scaffold and interacts with PABP, eIF4A and eIF3. Translation initiation begins once the mRNA is bound to the 40S ribosome, the ribosome and associated factors then scan along the mRNA until an initiation codon is encountered. The 60S ribosomal subunit binds the complex to form the 80S ribosome. Figure adapted from Robaglia and Caranta, *Cell* 2005.

3. Structural and functional analysis of fatty acid synthase

Fatty acids are vital molecules of the cell that are essential for nearly all organisms. They are the major constituents of cell membranes and they provide an ideal form to store metabolic energy in organisms (Lomakin et al., 2007). In addition, specific fatty acids may serve as precursors for biologically more active compounds thus harbor signalling functions and they may also be used for posttranslational protein modifications, thereby directly linking fatty acid homeostasis to cell proliferation and potentially disease (Tehlivets et al., 2006; Johansson et al., 2008).

The *de novo* synthesis of fatty acids is carried out by fatty acid synthase (FAS), a multienzyme complex that catalyzes a series of cyclic chemical reactions that are conserved across species (Lomakin et al., 2007). Specifically, FAS catalyzes the synthesis of saturated long-chain fatty acids from acetyl-CoA and malonyl-CoA as an intermediate supply of carbon atoms and each reaction cycle elongates the fatty acid by a C2 unit (Niwa et al., 1998). Yeast cytosolic FAS is composed of two subunits in equimolar amounts, Fas1 (β subunit) and Fas2 (α subunit) which are organized as a $\alpha_6\beta_6$ dodecamer of 2.6 MDa (Figure 6). As a member of the fungal type I FAS family, FAS contains six copies of eight independent functional domains which catalyze all reactions required for synthesis of fatty acids in yeast, namely; activation, priming, multiple cycles of elongation and termination (Lomakin et al., 2007).

Synthesis of long chain fatty acids is a remarkable event; however, the molecular basis for chain length determination is still not clear and studying this process is made more difficult as the ability of an organism to manipulate its fatty acid composition is

dependent on many aspects of metabolism. In *S. pombe,* it was found that oleic acid (18:1) was the predominant fatty acid species under normal growth conditions and much less palmitic acid (16:0) was observed (McDonough and Roth, 2004). Lynen et al. (1969) showed that lowering the ratio of malonyl-CoA/acetyl-CoA resulted in an increase in the proportion of shorter chain fatty acids. Moreover, studies in *S. cerevisiae* have shown that under normal conditions, the products of FAS are palmitate (60%) and stearate (40%), but the ratio becomes significantly altered upon changing the incubation temperature (Okuyama et al., 1979). Therefore, liquid chromatography coupled with mass spectrometry (LC-MS) has become an advantageous technique in studying the lipidome of various organisms (Shui et al., 2010). Lipidomics is able to compare and detect dynamic changes of TAG species, DAG species, free fatty acids, as well as various phospholipids (PL), including PC, PE, PS, PG, PI and PA (Shui et al., 2010). In *S. pombe*, the closest pathway to the reaction step that is catalyzed by FAS is the formation of phosphatidic acid (PA), thus serving as a good marker to detect differences in lipid composition between different strains and growth conditions. Since very little is known about the regulation and mechanism of FAS, using *S. pombe* as a model organism, we may be able to fill in the gaps on the metabolic map of lipid synthesis.

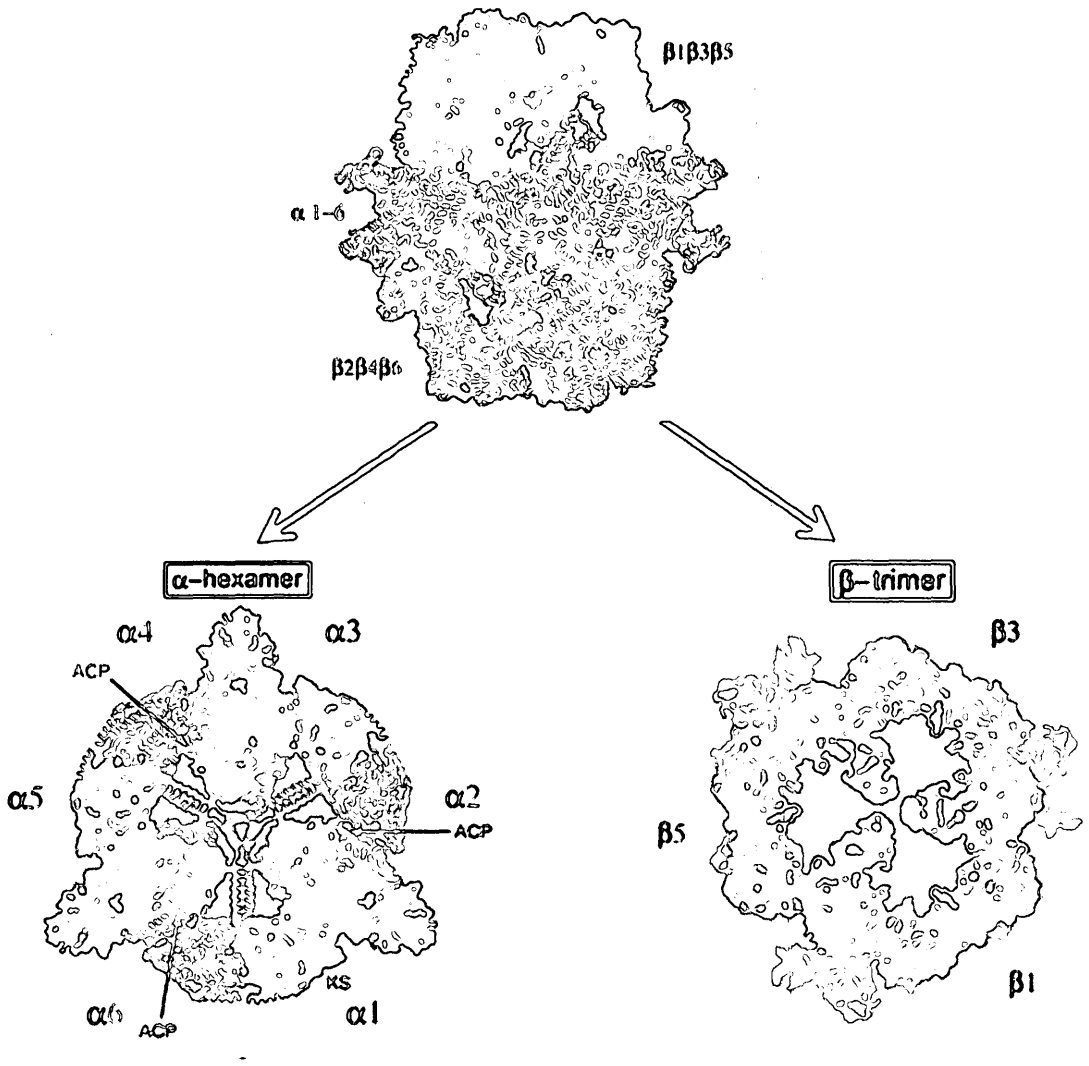

Figure 6 – Overall structure of yeast fatty acid synthase. Yeast FAS, a member of the fungal type I FAS family, is a 2.4 MDa $\alpha_6\beta_6$ dodecamer harbouring a barrel-shape structure. The structure was solved by X-ray diffraction at 4 Å resolution (PDB ID code 2PFF). FAS has two domes, each composed of β subunit trimers (green, purple and blue) and an equatorial wheel composed of α subunits (yellow) (top). On the left, is the α subunit hexamer from a top view, and on the right is the β subunit trimer viewed from the top. The acyl carrier protein (ACP), located at the N-terminus of the α subunit plays a central role in the entire synthesis process by shuttling all of the substrate intermediates between the catalytic centers of the FAS complex. Figure adapted from Lomakin et al., *Cell* 2007

C. Thesis Proposal

While the function of La in the metabolism of newly synthesized polymerase III transcripts has been well studied, the characterization of LARPs is lacking as very little is known about what these proteins are doing in the cell. In the hope of characterizing a general function for all LARPs, it is worthwhile to investigate homologs in simple eukaryotes such as yeast. *S. pombe* only has one LARP, which makes it an ideal model organism for functional studies. From an evolutionary perspective, we propose that Slr1p constitutes an ancestor to LARPs in higher eukaryotes, and therefore, characterization of its function may provide insight into the divergent roles of its extended relatives. It is therefore important to understand the function of Slr1p, which is the overall aim of this project. A variety of methodologies were used to elucidate the function of Slr1p. Focus was placed on identifying Slr1p associated factors by means of co-IP and mass spectrometry, identifying Slr1p's RNA targets by RNA-sequencing, and analyzing RNA-protein interactions by electrophoretic mobility shift assays. In addition, Slr1p localization was determined by indirect immunofluorescence and RNA chaperone activity was tested by fluorescent resonance energy transfer (FRET) based RNA chaperone assays.

A general trend has emerged suggesting a conserved function of La and LARPs as RNA chaperones involved in modulating RNA stability. To determine if this is also true for Slr1p, FRET-based RNA chaperone assays were performed where strand annealing and strand dissociation capabilities were measured *in vitro*. Furthermore, Slr1p mutants

were tested for RNA chaperone activity to determine which region of the protein is important for this function.

Using electrophoretic mobility shift assays, the RNA-protein interactions of Slr1p were determined. Poly(A), poly(U), poly(C) and poly(G) 10 mer and 20 mer RNA homopolymers were tested for binding with increasing concentrations of Slr1p. Also, a more structured substrate, a tRNA was tested for binding and Sla1p, the La homolog in *S. pombe* was used as a positive control. Based on these data, it was unclear whether Slr1p preferentially binds tRNAs or whether Slr1p binds to any RNA encompassing a secondary structure. Therefore, to determine Slr1p's endogenous RNA targets, RNA-sequencing was performed. Using a Slr1p-PrA tagged strain, where the PrA was integrated into the endogenous SLR1 locus in *S. pombe*, co-IP was performed to isolate RNAs pulled down with Slr1p. This technique had the advantage of assaying Slr1p-RNA complexes formed *in vivo,* and due to a very rapid and efficient isolation procedure, there was less chance of rearrangement between RNAs and their binding proteins (Oeffinger at al., 2007). As a result, Slr1p RNA targets were identified; however, bioinformatic analysis is still underway.

Immunolocalization studies of Slr1p were performed using indirect immunofluorescence. The *S.cerevisiae* homologs have been shown to localize to the cytoplasm, in support of a role in translation (Sobel and Wolin, 1999). Similarly, data suggests that Slr1p is localized to the cytoplasm which may also implicate this protein to have a role in translation.

Identification of potential protein interactors may provide valuable clues pertaining to the molecular pathway(s) the protein is involved in. For the purpose of this experiment, as previously mentioned, a PrA tag was inserted into the SLR1 gene locus so that it may be endogenously expressed and thus reflect physiological conditions. Co-IP experiments were performed using IgG-conjugated magnetic beads and lyophilized elutions were subjected to mass spectrometry analysis. Mass spectrometry revealed that Slr1p interacts with several translation initiation factors, as well as fatty acid synthase. These results were validated by recombinant co-IP experiments and subsequent experiments focused on the interaction between Slr1p and FAS.

Using recombinant co-IP experiments of full length Slr1p and Slr1p mutants, the interaction between Slr1p and FAS was mapped. In addition, lipid extraction was performed on a wild strain and an SLR1 null strain at two different temperatures. Lipidomics analysis was utilized to check for differences in lipids and free fatty acyls between the two strains. Based on the data, significant differences were observed, however, analysis of several more replicates is required to validate the results.

Since Slr1p is an uncharacterized protein, we have employed several biochemical methods to determine its function. We have shown that Slr1p is an RNA chaperone that interacts with translation initiation factors and FAS in the cytoplasm and it exhibits a UUU-3'OH independent binding mode.

EXPERIMENTAL METHODS

2.1 Strains, Plasmids, Antibiotics and Data Analysis

Yeast strains yAS99 and yAS99ΔSLR1, plasmids pET28a, pREP41X, pREP42X, pMO13 PrA Kan MX4 originally a gift from Marlene Oeffinger (IRCM), BL21 Star (DE3) pLysS or RosettaBlue (DE3) pLysS cells were obtained from the sources listed in Table 1. Refer to Table 1 for a complete list of yeast strains, bacterial strains and plasmids used in this study. Table 2 outlines all the primers used in this study. The final concentration of antibiotics used are as follows; Ampicillin (Amp; 50μg/mL), Kanamycin (Kan; 50μg/ml), Tetracycline (Tet; 10 μg/ml) and Chloramphenicol (Cm; 20 μg/ml).

A Carl Zeiss LSM 700 confocal microscope was used for immunofluorescence imaging analysis. All fluorescence readings for the FRET assays were obtained by a Cary Eclipse fluorimeter. Tandem mass spectrometry analysis was performed at the Proteomics Discovery Platform, Institut de Recherches Cliniques de Montréal (IRCM). Illumina RNA- sequencing was performed at McGill University, the Genome Quebec Innovation Center. Lipid analysis was performed by the Kansas Lipidomics Research Center.

Table 1 - *Schizosaccharomyces pombe* strains, *Escherichia coli* strains and plasmids used in this study*

YEAST STRAINS	DESCRIPTION	SELECTIVE MARKER (s)	REFERENCE
yAS99	h^- ade6-704 leu1-32 ura4$^-$ sla1		Lab Stock
yAS99ΔSLR1	h^- ade6-704 leu1-32 ura4$^-$ sla1	G418+	This study
yLS001	h^- ade6-704 leu1-32 ura4$^-$ sla1 with SLR1-PrA	G418+	This study
BACTERIAL STRAINS			
BL21 Star (DE3) pLysS	F- *ompT hsdS*B (rB-mB-) *gal dcm rne131* (DE3) pLysS (CamR)	Cm	Invitrogen
RosettaBlue (DE3) pLysS	*endA1 hsdR17* (r_{K12}^- m_{K12}^+) *supE44 thi-1 recA1 gyrA96 relA1 lac* (DE3) F'[*proA*$^+$*B*$^+$ *lacI*^{q}*ZΔM15*::Tn*10*] LysSRARE (Cam^R, Tet^R)	Tet, Cm	Clonetech
RbCl XL-1 Gold	TetrD(*mcrA*)*183* D(*mcrCB-hsdSMR-mrr*)*173 endA1 supE44 thi-1 recA1 gyrA96 relA1 lac* Hte [F′ *proAB lacI*qZD*M15* Tn*10* (Tetr) Amy Camr]	Tet, Cm	Stratagene
PLASMIDS			
pET28a	Bacterial expression vector with T7lac promoter, adds N-terminal His tag, thrombin cleavage site, internal T7 epitope tag, C-terminal His tag	Kan	Novagen
pREP41X pREP42X	REP-X derivatives derived from the REP/RIP series. Yeast origin ars1. nmt med strength.	Amp, LEU2 Amp, ura4+	Basi, 1993 and Forsburg, 1993
pMO13 PrA Kan MX4	YCp50 (*CEN URA3*)-P*TDH3-GFP-HDEL*	Kan, G418+	Oeffinger 2007

* The relevant characteristics, antibiotics and selection markers of the various *S. pombe* strains, *E. coli* strains and various vectors obtained from the referenced source.

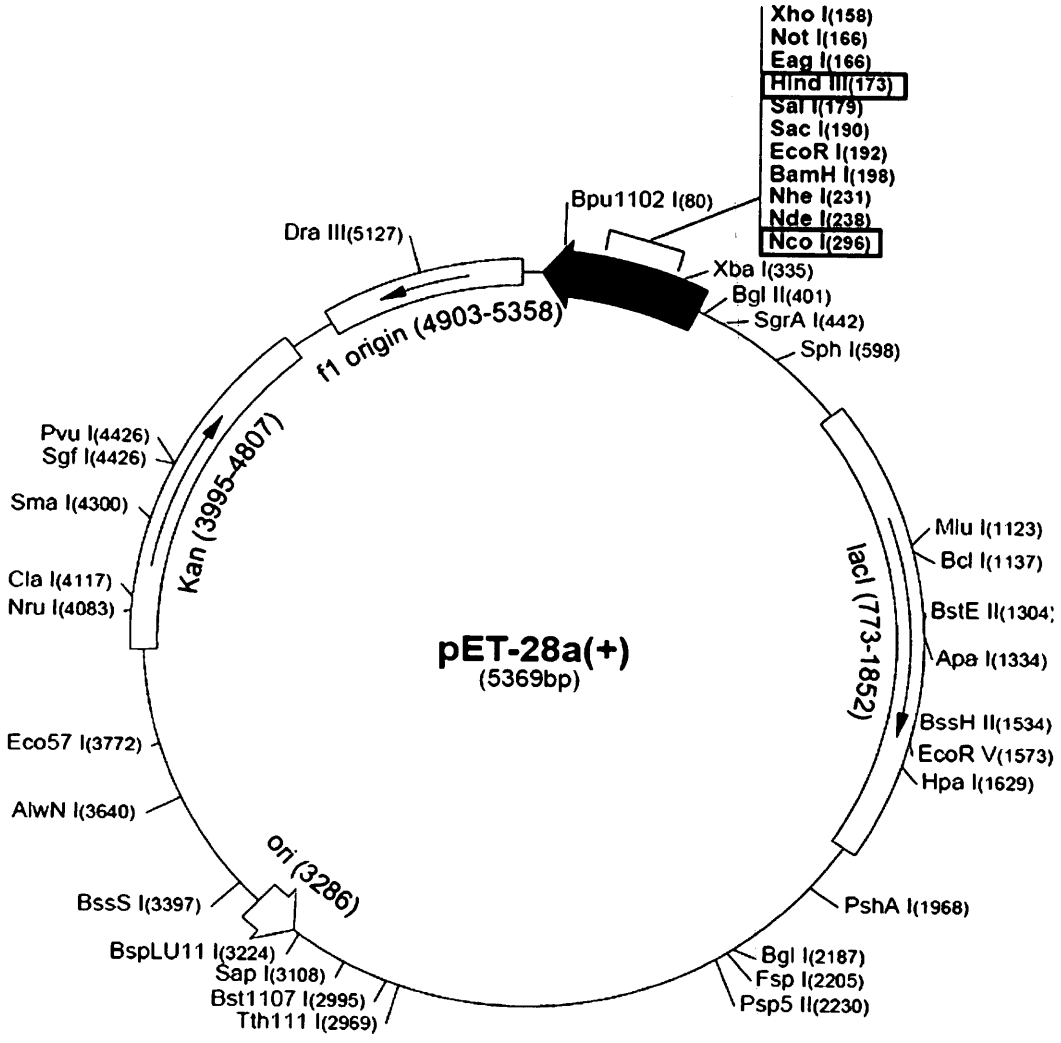

Figure 7 - Plasmid pET28a used for expression of Slr1p. The restriction sites, HindIII and NcoI used for cloning are highlighed in red. Image from Novagen.

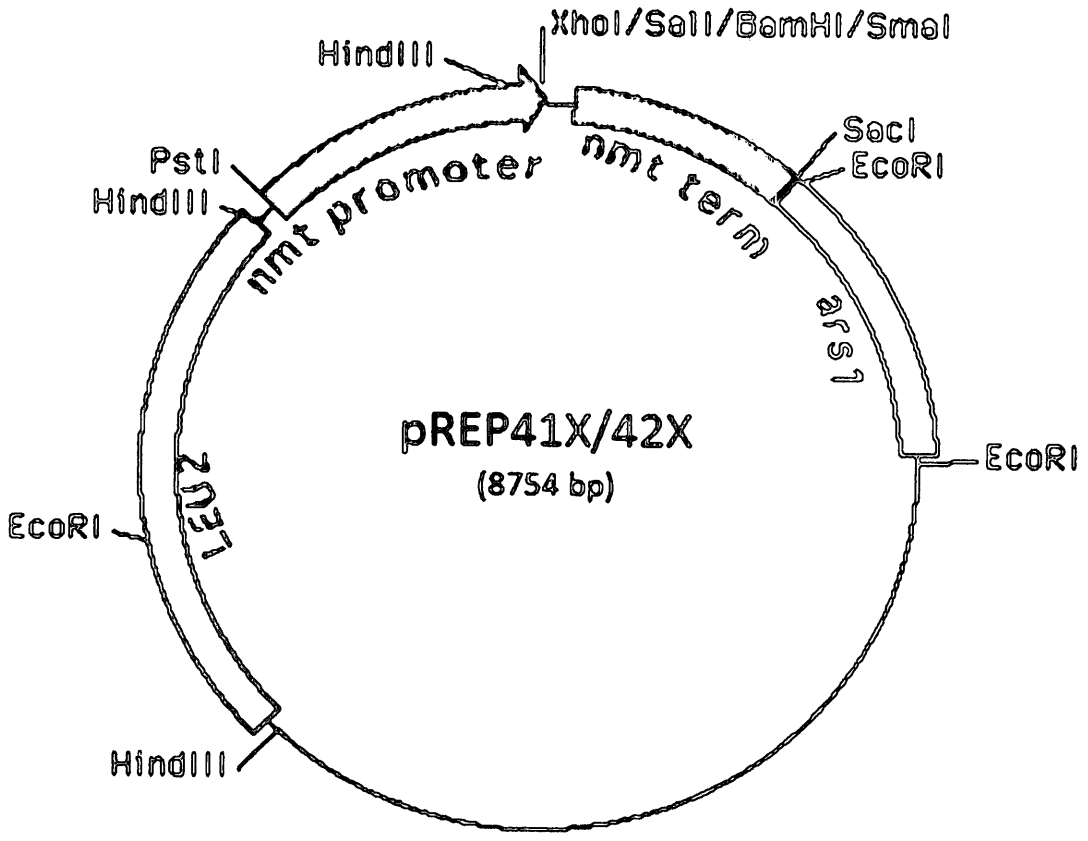

Figure 8 – Plasmid map for pREP41X/pREP42X. Plasmids pREP41X and pREP42X used for expression of Fas1, Fas2, eIF3B, eIF4G, eIF4A and aconitate hydratase. Either XhoI and XmaI or SalI and XmaI restriction enzymes were used. Image from Forsburg PombeNet.

Table 2 - Primers used in this Study*

CONSTRUCT	PRIMER
pET28 SLR1 For	5'-GCGCCCATGGCATCTCATAAAGAACCAAGTGCTGAAACTTC-3'
pET28 SLR1 Rev	5'-GCGAAGCTTCTAATGGTGATGGTGATGGTGAACAGTAAGT TTATC CTCAACCTCAGTTTB -3'
pET28 1-130 Rev	5'GCGAAGCTTCTAATGGTGATGGTGATGGTGTGACAATTTCCT ATCTTCAACCTGTTTTTC-3'
pET28 130-312 For	5'-GCGCCCATGGCATCAGATGATTCACAAAAGCCTTTAGCACCC - 3'
pET28 312 Rev	5'-GCGAAGCTTCTAATGGTGATGGTGATGGTGGACAGGATAGT TTGGAAATGGACCTTGTAT-3'
pET28 312-414 For	5'-GCGCCCATGGCAGTCGTCAATGGTAATGGCGTTAATCCTTAC CT-3'
pET28 312-414 Rev	5'-GCGAAGCTTCTAATGGTGATGGTGATGGTGTAAAATCCAAG GAGACCAAGTTTCCTTTCT-3'
pREP41 Fas1-HA For	5'-CGCCTCGAGATGGTTGAGGCTGAACAAGTTCATCAGTCGCT GAGGTCGTTGG-3'
pREP41 Fas1-HA Rev	5'- CGCCCCGGGTTAAGCGTAATCTGGAACATCGTATGGTAGGATG ACTCATATTCATCCCAGTTTTGCAAAATC-3'
pREP42 Fas2-FLAG For	5'-CGCCTCGAGATGAGACCAGAAGTTGAGCAGGAGCTTGCTCA TACTTTATTAT-3'
pREP42 Fas2-FLAG Rev	5'-CGCCCCGGGTTACTTATCGTCGTCATCCTTGTAATCCTTGTG AGCCAAAGCAACACTGACACTTTGATTATCATCGTG-3'
pREP41 eIF3B-HA For	5'-CGCCTCGAGATGTCGGAAATCCTAATTGAGGAAATTAAGGA TCAAA-3'
pREP41 eIF3B-HA Rev	5'-CGCCCCGGGTTAAGCGTAATCTGGAACATCGTATGGTGAATC TTCAACGGGTTCTATCTCTTCAGAGATTACTTC-3'
pREP41 eIF4G-FLAG For	5'-GCGCGTCGACATGTCTTCAAAACCACCGTCAAATACTCCAA AGTTTAGTT-3'
pREP41 eIF4G-FLAG Rev	5- CGCCCCGGGTTACTTATCGTCGTCATCCTTGTAATCCGAACTAG TTTTTGAGTTAGAATCTTTTTGACCCCCATCATTAT-3'
pREP41 aconitate-FLAG For	5'-CGCCTCGAGATGGCTACATTCGCTAGAATGAAGCTTTGCCTT TCGGGCTCTTC-3'
pREP41 aconitate-FLAG Rev	5'- CGCCCCGGGTTACTTATCGTCGTCATCCTTGTAATCGTTCAGTTT GAGTTCCGTAACCCTTAAAATAGTATACG-3'
pREP42 eIF4A-HA For	5'-CGCCTCGAGATGGTAGACCAACTGGAGGATTCGGTTATTG-3'
pREP42 eIF4A-HA Rev	5'-CGCCCCGGGTTAAGCGTAATCTGGAACATCGTATGGTAA ATCAAGTCAGCAATGTTCATAGGCATTTC-3'
SLR1 Tag For	5'-TTCTCCTCCATTCATTCCTTCTTCTGTGGATTCAATTATAAAA AGAGATGTTCAAACTGAGGTTGAGGATAAACTTACTGTTCGTA CGCTGCAGGTCGAC-3'
SLR1 Tag Rev	5'- GTACAGGCGTCAATAAAAGAACAGACCCAGAATGAACGAA AAATATTGATGCCTCGAGAAATAAAAAAAATATCAAAAATTAT CGATGAATTCGAGCTCG-3'
SLR1 Int ORF For	5'-GTGATGTCCAAGCATTTCTCACTTC-3'
SLR1 Int Tag Rev	5'-GTCGACCTGCAGCGTACG-3'
SLR1 Int Tag For	5'-CGAGCTCGAATTCATCGAT-3'
SLR1 Int 3UTR Rev	5'-CCTGCGGCCTTTAAATATAGAATAGC-3'

Marker In For	5'-GCTAGGATACAGTTCTCACATCACATCCG-3'

*Restriction enzyme cleavage sites are underlined (NcoI:CCATGG, HindIII: AAGCTT, XhoI: CTCGAG , SalI: GTCGAC, XmaI: CCCGGG), 6x-His tag is in green, HA tag in blue, FLAG tag in red, PrA tag in purple and Kanamycin cassette in orange. All primers were obtained from Integrated DNA Technologies.

2.2 Cloning pET28a SLR1-6xhis

SLR1 with a C-terminal 6x-His tag was cloned into a pET28a plasmid. The PCR primers pET28 SLR1 For and pET28 SLR1 Rev were used to amplify the SLR1 sequence from a pFS118-SLR1-FLAG construct containing overhangs for the restriction enzymes NcoI and HindIII. The PCR reaction outlined in Table 3 was set up and PCR parameters in Table 4 were used with an annealing temperature of 53°C and an extension of 3 minutes.

Table 3 - PCR Reaction Components

COMPONENT	FINAL CONCENTRATION	VOLUME
Template DNA	<250 ng	1 µL
5X Phusion HF Buffer	1X	10 µL
20 µM Forward Primer	0.5 µM	1 µL
20 µM Reverse Primer	0.5 µM	1 µL
10 mM dNTPs	200 µM	1 µL
Phusion enzyme	0.5 units/50 µL PCR	0.5 µL
ddH_2O		35.5 µL
TOTAL		**50 µL**

Table 4 – General PCR Cycling Conditions*

CYCLE STEP	TEMPERATURE	TIME	NUMBER OF CYCLES
Lid	103°C		
Initial Denaturation	98°C	2 min	1
Denaturation	98°C	15 sec	30
Annealing	Varied	15 sec	
Extension	72°C	Varied	
Final Extension	72°C	10 min	1
Hold	4°C		

* All PCR reactions were carried out using an Eppendorf Mastercycler personal 5332. The annealing temperature of each reaction was dependent on the T_m of the product. The extension was dependent on the size of the PCR product.

DNA extraction was then performed on the amplified SLR1-6xhis insert PCR product. The reaction volume was brought up to 200 µL with ddH_2O and an equal volume of phenol:chloroform:isoamyl alcohol (25:24:1) was added. The reaction was vortexed for 20 seconds and centrifuged at 13,000 x g for 10 minutes. The aqueous layer was transferred to a clean microfuge tube and re-extracted with chloroform. The DNA was precipitated overnight using 3M sodium acetate at $1/10^{th}$ the volume of DNA, 100% ethanol at 2.5 times the volume of DNA and 1 µL of 15 mg/mL GlycoBlue Coprecipitant. The DNA was pelleted by centrifugation at 13,000 x g for 10 minutes and washed with 70% ethanol. The pellet was air dried for 5 minutes and resuspended in 20 µL of ddH_2O. The pET28a plasmid was extracted from the *E.coli* strain XL-1-Gold RbCl cells and mini-prepped using Omega E.Z.N.A. Plasmid MiniPrep Kit I, following the manufacturer's protocol. Next, double digest reactions were set up for the SLR1-6xhis insert and pET28a plasmid as outlined in Table 5; the reactions were incubated at 37°C overnight.

Table 5 - Digestion Reactions for SLR1-6xhis insert and pET28a vector

SLR1-6xhis Insert		pET28a Vector	
Plasmid pET28a	20 µL	pET28a vector	87 µL
10X NEB Buffer 2	3 µL	10X NEB Buffer 2	10 µL
100X BSA	0.3 µL	100X BSA	1 µL
NcoI	1 µL	NcoI	1 µL
HindIII	1 µL	HindIII	1 µL
ddH_2O	4.7 µL	ddH_2O	0 µL
TOTAL	**30 µL**	**TOTAL**	**100 µL**

The pET28a vector was treated with 1 µL of CIP for 2 hours at 37°C to remove the terminal phosphate. The insert and vector were then electrophoresed on a 1% agarose gel and further purified using Omega E.Z.N.A. MicroElute Gel Extraction Kit, following the manufacturer's protocol. Both insert and vector were analyzed and quantified on a 1% agarose gel. A 10 µL ligation reaction was prepared using 100 ng of vector DNA with a 1:3 vector to insert ratio, 1 µL of 10X T4 DNA ligase buffer, 1 µL of T4 ligase and 4 µL of ddH_2O. The reaction was incubated at room temperature for 1 hour.

2.2.1 Transformation into *Escherichia coli*

The ligation reaction was transformed into RbCl ultra-competent *E. coli* XL-1 Gold cells. Briefly, 4 µL of the ligation reaction was added to 50 µL of competent cells and incubated on ice for 30 minutes. The cells were heat shocked for 90 seconds at 37°C and chilled on ice for 2 minutes to take up the plasmid. 400 µL of Luria Bertani (LB) broth was added to the cells and incubated at 37°C for 1 hour. The cells were then plated on selective media for Kan resistance and incubated at 37°C overnight.

Six colonies were selected and mini-prepped to isolate the plasmid DNA. The plasmid DNA was digested again with NcoI and HindIII and visualized on a 1% agarose gel. Two candidates that displayed both the insert and vector on the agarose gel were chosen and confirmed by sequencing at the molecular core facility (York University Core Facility).

2.2.2 Cloning SLR1 mutants into pET28a

The SLR1 mutant constructs (Figure 9) were created using the PCR primers pET28 SLR1 For with pET28 1-130 Rev, pET28 130-312 For with pET28 312 Rev, pET28 SLR1 For with pET28 312 Rev, pET28 312-414 For with pET28 312-414 Rev and pET28 312-414 For with pET28 SLR1 Rev (refer to Table 2). To amplify the SLR1 regions by PCR, pET28a SLR1-6xhis was used as the template. The PCR reactions and PCR parameters used are outlined in Table 3 and Table 4, respectively. An annealing temperature of 55°C and a 3 minute extension was used. Subsequent steps followed were the same as those listed above (refer to Section 2.2).

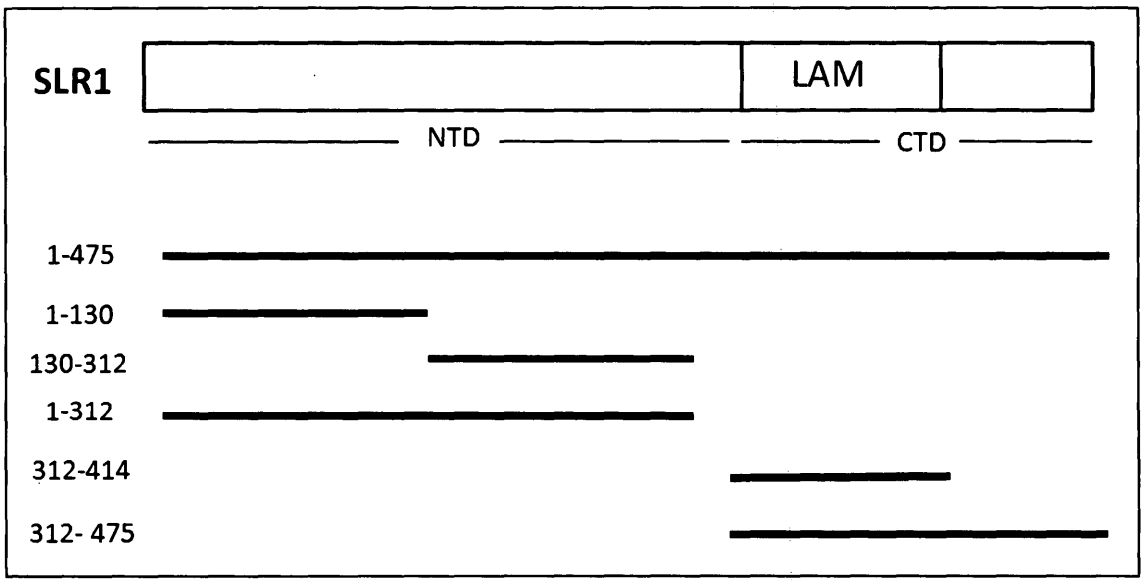

Figure 9 – Schematic presentation of the SLR1 mutants used in this study. The SLR1 mutants were cloned into pET28a with a C-terminal His-tag. Full length SLR1 (475aa) is represented at the top and the SLR1 mutants below. The name of each mutant corresponds to the amino acid residues of SLR1 that it contains.

2.2.3 Expression of SLR1, SLR1 mutants and hLa

SLR1 and SLR1 mutants cloned into the NcoI and HindIII sites of pET28a were transformed into RosettaBlue (DE3) pLysS cells as outlined in Section 2.2.1. Overnight cultures were prepared from the transformed colonies and used to seed 500 mL of LB containing Kan and Cm at 37°C with shaking until mid-log phase was reached (OD_{600} 0.5-0.6). Protein expression was induced with 0.1 mM IPTG for 3 hours at 37 degrees.

hLa, cloned into pET30, was transformed into BL21 Star (DE3) cells as outlined in Section 2.2.1. An overnight culture was prepared from the transformed colonies and used to seed 500 mL of LB containing Amp at 37°C with shaking until mid-log phase was reached (OD_{600} 0.5-0.6). Protein expression was induced with 1 mM IPTG for 3 hours at 37 degrees.

The induced cells were harvested by centrifugation at 6,000 x g for 15 minutes and washed with 50 mL of 50 mM Tris-HCl pH 7.5, 100 nM NaCl. The pellets obtained were stored at -80°C.

2.2.4 Protein Purification

Proteins were purified using affinity chromatography. The pellets from induction were resuspended in 5 mL of lysis buffer (50 mM Tris-HCl pH 7.5, 500 mM NaCl, 0.05% IGEPAL, 10 mM Imidazole, 0.1 mM β-mercaptoethanol, 1X protease inhibitor (Sigma Catalogue # P8849). Cell lysis was accomplished by sonication (Branson Digital Sonifier) at a frequency of 20 kHz, amplitude 30% and 6 cycles of 15 second pulses followed by 30 seconds on ice. The cell debris was separated by centrifugation at 7,500 x g for 30 minutes at 4°C. The supernatant was added to 250 µL Co-NTA beads which were 3 times washed in binding buffer (50 mM Tris-HCl pH 7.5, 500 mM NaCl, 0.05% IGEPAL, 10 mM Imidazole, 0.1 mM β-mercaptoethanol). The samples were incubated on a nutator at 4°C for 30 minutes. The beads were then pelleted by centrifugation at 4,000 x g for 3 minutes at 4°C and washed 3 times in 1 mL of wash buffer (50 mM Tris-HCl pH 7.5, 1 mM EDTA, 500 mM NaCl, 10 mM β-mercaptoethanol, 10 mM imidazole). For the fourth wash, 500 µL of Micrococcal nuclease (MCN) buffer (50 mM Tris-HCl pH 7.5, 25 mM NaCl, 5 mM $CaCl_2$, 1% BSA, 10 mM imidazole) with 1 µL of MCN enzyme was added to the beads and incubated at 37°C for 10 minutes. Then, four more washes were performed, followed by 2 elutions where the beads were incubated with 750 µL of elution buffer (50 mM Tris-HCl pH 7.5, 1 mM EDTA, 500 mM NaCl, 10

mM β-mercaptoethanol, 150 mM imidazole) for 5 minutes. The elutions were pooled together and the proteins were concentrated and desalted into RNA Chaperone buffer (50 mM Tris-HCl pH 7.5, 1.5 mM $MgCl_2$, 1 mM DTT). The proteins were quantified using SDS-PAGE and Coomassie staining.

2.2.5. Coomassie staining of polyacrylamide gels

Twelve microliters of each protein sample was mixed with 3 μL of 5X Laemmli Buffer (10 % SDS, 0.25 M Tris-HCl, pH 6.8, 0.25 % bromophenol blue, 0.5 M DTT, 50% glycerol), heated at 95°C for 10 minutes, centrifuged at 13000 x g for 1 minute and loaded onto a 10% Tris-Tricine polyacrylamide gel. After running the SDS-PAGE gel, the samples were visualized with Coomassie staining (45% methanol, 10% acetic acid, 0.25% Coomassie Brilliant Blue, R-250) for 40 minutes and then destained with destain solution (40% methanol, 10% acetic acid) until optimal band versus background was achieved. Glycerol was added to the concentrated proteins to 10% final and the proteins were stored at -80°C. Protein concentrations were estimated by comparing the band intensities to known bovine serum albumin (BSA) concentrations, also using SDS-PAGE and Coomassie staining.

2.3 FRET assays

RNA Chaperone assays were performed as described by Rajkowitsch and Schroeder, (2007). Briefly, two synthesized fluorophore-tagged RNA substrates (Cy5-AUGUGGAAAAUCUCUAGCAGU and Cy3-ACUGCUAGAGAUUUUCCACAU)

were annealed in a Cary Eclipse fluorimter at 37 degrees in a buffer containing 50 mM Tris-HCl pH 7.5, 1.5 mM $MgCl_2$ and 1 mM DTT. Annealing was initiated by combining 25 nM Cy3 RNA with 25 nM Cy5 RNA, and 100 nM (final concentration) of the protein to be tested in a final reaction volume of 400 µL. The reaction was allowed to proceed for 180 seconds where the Cy3 dye was excited at wavelength 535 nm and the level of fluorescence emission at 680 nm and 590 nm were recorded at half-second time points. Then, 20 µL of 20 µM non-labelled competitor RNA was added to the reaction and readings were measured for another 180 seconds at half-second time points. The ratio of fluorescence emissions (FRET index: emission at 680 nm/emission at 590 nm) was normalized to 1 at t_{180s} and least-square fitted with Prism 5.0 (GraphPad Software Inc). For phase I, the second order reaction equation for equimolar initial reactant concentrations was used: $y=A[1-1/(k_{ann,1}\, t+1)]$, where $k_{ann,1}$ is the observed annealing reaction constant and A is the maximum reaction amplitude. Phase II was assessed to be either describing continuing RNA annealing (FRET index increasing) or strand displacement (FRET index decreasing) and fitted accordingly with a single-exponential function for signal increase $y=y_0+A[1-\exp(-k_{ann,2}t)]$ or signal decay $y=y_0+A\exp(k_{SD}t)]$. Values plotted on histograms with rate constants are shown as mean ± standard deviation (SD) as derived from three independent experiments.

2.4 Electrophoretic mobility shift assays (EMSA)

In the first set of gel shifts, varying Slr1p concentrations were incubated with a constant amount of labelled 10 mer and 20 mer RNA homopolyers that were: poly (U), poly (G), poly (C) and poly (A). In the second set of gel shifts, varying protein (Sla1p and Slr1p) concentrations were incubated with constant amounts of labelled *in vitro* transcribed T7 $tRNA^{Ala}AGC$. In order to make the different concentrations, the protein(s) was diluted in La dilution buffer (10 µL of 10X EMSA Buffer, 15 µL of 80% Glycerol, 85 µL of RNase free water). 10X EMSA buffer (200 mM Tris pH 7.9, 1M KCl, 10 mM EDTA, 50 mM β-mercaptoethanol) was prepared in order to make the subsequent buffers used in the assay. The final volume of each reaction was 20 µL which consisted of: 2µL 10X EMSA, 2.5 µL of 80% Glycerol, 0.2 µL labelled tRNA substrate, 2 µL of the protein and RNase free water. While the 10% native gel (1X TBE, 40% polyacrylamide, ddH_2O up to a final volume of 10 mL, 0.08% APS, 0.037% TEMED) was pre-running at 100 V for 30 minutes, the reactions were incubated at 37°C for 20 minutes, followed by a 10 minute incubation on ice. Then, 10 µL of each reaction was run on the gel for 1 hour at 100 V, after which the gel was dried using a gel drier (Biorad). A phosphoimager plate (film) was then exposed to the gel overnight in an autoradiography cassette (Fisher Biotech). The film was then placed in the phosphoimager (Biorad) to visualize the gel-shift.

2.5 PrA-tagged Slr1p strain

PCR was set up using the pMO13 PrA Kan MX4 plasmid as the DNA template and SLR1 Tag For and SLR1 Tag Rev primers (see Table 2). The primers were designed to have sequence homology to the SLR1 gene, as well as the PrA tag and Kanamycin cassette. The PCR reaction and PCR Parameters outlined in Tables 3 and Table 4, respectively, were used with an annealing temperature of 55°C and an extension of 4 minutes. The PCR product was then cleaned up using the Omega E.Z.N.A MicroElute Cycle Pure Kit and following the manufacturer's protocol. Next, the DNA was transformed into the yeast strain yAS99.

2.5.1 Yeast Transformation, Lithium Acetate

The PCR amplified insert was transformed into the yeast strain yAS99. A single colony of yAS99 was inoculated in 10 mL of yeast extract with supplements (YES) rich complete media. The cells were grown at 32°C until stationary phase and then seeded down to OD_{600} 0.2 in 10 mL of YES media and grown to OD_{600} 0.5 – 0.6. The cells were harvested by centrifugation at 1,200 x g for 15 minutes and washed with 20 mL of sterile distilled water. Cells were then resuspended in 100 µL of chilled 1X TE-LiAc (1X Li-Ac, 1X TE) and 5 µL of salmon sperm DNA (10 mg/mL). 100 µL of cells was transferred to a new microfuge containing the 1 µg of insert DNA to be transformed and 700 µL of LiAc-TE PEG (1X LiAc, 1X TE, 40% PEG) was added. The tube was mixed by vortexing and the cells were heat shocked for 15 minutes at 42°C. The cells were pelleted at 7,500 x g

for 1 minute, resuspended in 200 μL of sterile distilled water, plated on YES agar plates and incubated at 32°C overnight.

The following day, the transformation was replica plated on a YES+G418 agar plate and the plate was incubated at 32°C for 5 days. Colonies that appeared were the new knock-in strain, a strain that consisted of a PrA tag integrated into the chromosomal ORF of SLR1. This strain was designated yLS001.

2.5.2 Isolation of Chromosomal DNA and Confirmation of PrA knock-in strain

The correct integration of the PrA tag was tested by PCR analysis. Genomic DNA was isolated from strain yLS001 which was used as the DNA template for PCR. In brief, a 10 mL yLS001 culture was grown to saturation in YES media. The cells were harvested by centrifugation at 1,200 x g for 10 minutes, resuspended in 500 μL of sterile distilled water, transferred to screw-cap microfuge tubes and centrifuged for 30 seconds to decant the supernatant. 200 μL of lysis buffer (2% Triton X-100, 1% SDS, 100 mM NaCl, 10 mM Tris-HCl pH 8.0, 1 mM EDTA), 200 μL of phenol:chloroform:isoamyl alcohol (25:24:1) and 0.3 g of acid-washed glass beads were added to the pellet. The cells were homogenized in a bead beater for 1 minute, after which 200 μL of 1X TE pH 8.0 was added and the tube was centrifuged for 5 minutes. The aqueous layer was transferred to a clean tube, 1 mL of 100% ethanol was added, and the tube was mixed by inversion and centrifuged for 2 minutes. The pellet was resuspended in 400 μL of TE, 1.5 μL of RNase A (10mg/mL) was added and this was incubated at 37°C for 5 minutes. 10 μL of 4M ammonium acetate and 1 mL of 100% ethanol were added. Again, the reaction was

mixed by inversion and centrifuged for 2 minutes. The pellet was resuspended in 50 µL TE pH 8.0.

3 different PCR reactions were set up to confirm the PrA tag integrated correctly into the SLR1 ORF. Primers SLR1 Int ORF For and SLR1 Int Tag Rev, SLR1 Int tag For and SLR1 Int 3UTR rev and Marker In For and SLR1 Int 3UTR Rev were used to set up 3 different PCR reactions (as per Table 3) and using the PCR parameters in Table 4. A 50°C annealing temperature was used with an extension of 3 minutes. The PCR reactions were analyzed for correct size on a 1% agarose gel and they were also sequenced at the molecular core facility (York University) for further confirmation.

2.6 Immunofluorescence

Overnight cultures of yAS99 and yLS001 strains were grown to saturation in YES media. Cultures were seeded down in 10 mL to OD_{600} 0.2 and grown to OD_{600} 0.6 at 32°C. Cells were harvested by centrifugation at 1,500 x g for 5 minutes and fixed in ice-cold 100% methanol. The cells were then spun down out of the 100% methanol and washed in 1 mL of 60% methanol/40% 1X PBS and washed in 1 mL of 1X PBS. Then, the cells were resuspended in 50 µL of sodium phosphate dibasic/50 mM citrate/ 1.2 M sorbital pH 5.6 to which 50 µL of zymolyase (G-Biosciences Catalogue # 786-036) was added and incubated at 37°C for 4 hours. Next, the cells were resuspended in 1 mL Triton X-100/1X PBS for 1 minute, washed three times in 1 mL 1X PBS and resuspended in 500 µL PBSBL (1X PBS,1% BSA,100 mM lysine-HCl). The cells were spun down and resuspended in 100 µL of PBSBL. 20 µL rabbit IgG at 12.5 mg/mL (Sigma Catalogue #

15006) was added and the tube was incubated on a nutator at room temperature overnight. The following day, the cells were washed four times with 200 µL of PBSBL and resuspended in 100 µL of PBSBL containing a 1:100 dilution of secondary Alexa Fluoro 488 antibody (Invitrogen Catalogue # A11008). The reaction was incubated with rotation for 4 hours with the tubes wrapped in aluminum foil to prevent light contact. Next, the cells were pelleted and washed four times, each with 200 µL PBSBL. Slides were coated with poly-L-lysine and cells were spread over the slide and air-dried for a few minutes. A drop of VECTASHIELD mounting medium with DAPI (Vector Laboratories Catalogue # H-1200) was added on top of the cells and a coverslip was placed on top. Nail polish was used to seal the coverslip and soon thereafter, the cells were visualized using a confocal microscope.

2.7 Co-immunoprecipitation

2.7.1 Harvesting cells, making noodles and cryogenic disruption of yeast cells

S. pombe yeast cells yAS99, yAS99ΔSLR1 and yLS001 were grown to an OD_{600} 0.6 and harvested by centrifugation at 4,000 x g for 10 minutes at 4 degrees. Cell pellets were washed two times with 50 mL of ddH_2O over ice and spun down at 2,600 x g for 5 minutes at 4°C. Pellets were resuspeneded, over ice, with a volume of resuspension buffer (1.2% PVP-40, 20 mM Hepes pH 7.4, 1 mM DTT, 1 mM PMSF and 1X Protease Inhibitor Cocktail (Sigma Catalogue # S8830) equal to the volume of the pellet. Cells were pelleted at 2,600 x g for 15 minutes and the buffer was aspirated. The pellet alone was centrifuged again at 2,600 x g for 15 minutes to ensure any residual buffer was

removed. To freeze the cells, liquid nitrogen was poured into a styrofoam container and covered with a styrofoam lid with a hole in the centre. A 50 mL conical tube was pushed through the hole in the lid and allowed to cool. The 50 mL conical tube was filled with liquid nitrogen. The cell paste was scooped into a 20 mL syringe and pressed out into the liquid nitrogen in the conical tube. Holes were poked on the cap of the conical tube and the liquid nitrogen was decanted from the tube by turning the tube upside down. The noodles were stored at -80°C.

Frozen yeast noodles were lysed using a planetary ball mill (Retsch PM 100). An ice bucket was filled about one quarter full with liquid nitrogen. Everything was pre-chilled by immersing the stainless steel grinding jars, stainless steel lid, grinding balls and storage tube with frozen yeast noodles in liquid nitrogen. Once everything was chilled, the noodles were poured into the grinding jar and 7-9 20 mm stainless steel balls were added to the jar. Grinding was performed in 8 cycles, each cycle being set in the following manner: 400 rpm, 3 minutes, 1 minute reverse rotation with no breaks between rotations. Between each cycle, the jar was removed and cooled in liquid nitrogen. Once the 8 cycles were complete, the frozen ground cells were scooped out into a 50 mL conical and stored at -80°C.

2.7.2 Conjugation of Dynabeads with rabbit IgG

Coupling of Dynabeads with rabbit IgG was necessary to produce magnetic beads which were capable of pulling out various Protein A tagged complexes. The entire vial of Dynabeads (2×10^{10} beads) was resuspended in 16 mL of 0.1 M $NaPO_4$ buffer – pH 7.4

and vortexed for 30 seconds. The bead suspension was divided equally across four 15 mL conical tubes and any remaining beads in the glass vial were washed with an additional 2 mL of 0.1 M $NaPO_4$ buffer and also divided equally amongst the four conical tubes. The bead suspension was placed on a nutator for 10 minutes. While the bead suspension was on the Nutator, the entire bottle of rabbit IgG (100 mg) was resuspended in 8 mL ddH_2O, resulting in a concentration of 12.5 mg/mL. 1 mL aliquots were stored at -20°C. 1 mL of rabbit IgG was centrifuged at 14, 000 rpm at 4°C for 10 minutes and the supernatant was saved. To prepare the AB mix, the following solutions were added to a 50 mL conical tube in the order listed: 1 mL of rabbit IgG (supernatant that was saved in the previous step), 9 mL 0.1 M $NaPO_4$ buffer and 10 mL 3M Ammonium Sulfate. The AB mix was then filtered using a .22 μm Millex GP filter. The conical tubes containing the bead suspension were then placed on a magnetic holder until the bead solution was clear. The buffer was aspirated off and the beads were washed again with 4 mL 0.1M $NaPO_4$ buffer. The tubes were vortexed 15 seconds, placed on a magnetic holder and the buffer was aspirated. 5 mL of AB mix was added to each tube and each tube was vortexed to completely combine the AB mix and the beads. The tubes were incubated overnight at 30°C on a nutator.

The following day, the beads were washed repeatedly with the following solutions: once with 3 mL of 100 mM Glycine HCl pH 2.5 (as quick as possible), once with 3 mL of 10 mM Tris pH 8.8, once with 3 mL of 100 mM Triethylamine (quickly), 5 washes with 1X PBS each 5 minutes on nutator, once with 1X PBS + 0.5% Triton X-100 for 5 min and finally once with 1X PBS + 0.5% Triton X-100 for 15 minutes on a

nutator. All the beads were then resuspended in a total of 2 mL of 1X PBS + 0.02% sodium azide and stored at 4°C.

2.7.3 Dynabead purification

Frozen cell powder (section 2.7.1) was weighed out into 50 mL conical tubes which were pre-cooled in liquid nitrogen. For the control strain yAS99, 0.5 g of frozen cell powder was used and for the Slr1p-PrA tagged strain, yLS001, 1.5 g of frozen cell powder was used. The powder was thawed slightly on ice to resemble soft ice cream. In the meantime, the conjugated dynabeads (section 2.7.2) were pre-washed 3 times with 1X RNP extraction buffer (20 mM Hepes pH 7.4, 110 mM KOAc, 0.5% Triton X-100, 0.1% Tween-20, 1:100 Protease Inhibitor Cocktail, 1 mM PMSF, Antifoam B, 1:5000 RNasein, 100 mM NaCl) by pipetting up and down and dividing them up into 15 mL conical tubes (25 µL beads/0.5 g cell powder). 4.5 mL of room temperature 1X RNP buffer per 0.5 g of cell powder was added to the pellet and mixed by vortexing for 30 seconds. 2x $1/200^{th}$ of sample was taken from each step of the purification for Western blot detection of Slr1p-PrA. Lysates were centrifuged at 3,500 rpm for 10 minutes at 4°C and the supernatant was poured onto the washed magnetic beads. For binding, the tubes were incubated on a nutator for 30 minutes at 4°C. After binding, the tubes were placed on a magnetic bar until the solution was clear. The supernatant was aspirated off and the beads were washed in 1 mL of 1X RNP buffer, mixed by pipetting and transferred to eppendorf tubes. The tubes were placed on the magnetic bar and the supernatant was aspirated. Three more washed followed in this manner. Then, the beads were washed

with 1 mL of Last Wash buffer (0.1 M NH_4OAc, 0.1 mM $MgCl_2$ and 0.02% Tween-20) for 5 minutes on a nutator. For mass spectrometry sample preparation, 4 more washes (3 short and one 5 min wash) were performed in Last Wash buffer without Tween-20. Lastly, the beads were eluted twice with 500 µL of Elution buffer (0.5 M NH_4OH and 0.5 mM EDTA pH 8.0) for 20 minutes each at room temperature on a nutator. The two eluates were pooled on ice, a hole was made on the lid of the tube and the elutions were spun in a speedvac overnight without heat or radiant cover. The lyophilized elutions were then subjected to mass spectrometry (in-solution trypsin digestion, LC-MS/MS), Western blot analysis as well as visualized by Coomassie staining.

2.7.4 Coomassie staining & Western Blotting of Slr1p-PrA

For gel analysis, the lyophilized elutions were resuspended in 8 µL of Solution A (0.5 M Tris pH 8, 5% SDS) and heated at 70 °C for 5 minutes. Then, 8 µL of Solution B (75% Glycerol, 0.05% Bromophenol blue, 0.1 µM DTT) was added and the tube was heated again at 80°C for 10 minutes.

For Coomassie staining, 14 µL of each elution was run on a 10% SDS-PAGE gel and incubated in stain solution (45% methanol, 10% acetic acid, 0.25% Coomassie Brilliant Blue, R-250) for 60 minutes, followed by detain solution (40% methanol, 10% acetic acid) overnight.

For Western blot analysis, 2 µL of each elution was diluted in 50 µL of yAS99 lysate (refer to Section 2.8.1) and 15 uL was loaded onto a 10% polyacrylamide gel. The gel was transferred to a nitrocellulose membrane for 1 hour and then incubated in

Blocking buffer (5% w/v skim milk powder, 1X TBS, 0.1% Tween-20) for 1 hour. The membrane was then probed with PAP antibody (1:5000 anti-PAP antibody (Sigma Catalogue # P1291), 1X TBS, 0.1% Tween-20) for another hour at room temperature. Four washes were then performed, 5 minutes each in 1X TBS + 0.1% Tween-20. To detect the proteins, the membrane was incubated with 2 mL of enhanced chemiluminescence (ECL) solution (Pierce) for 2 minutes with gentle agitation. The membrane was drained of excess developing solution, wrapped in Saran wrap and exposed to X-ray film with a 2 minute exposure.

2.7.5 RNA-Sequencing

For isolation of RNAs bound to Slr1p-PrA, after the Lash Wash 5 minute incubation (refer to Section 2.7.3), the beads were taken up again in 500 µL of Last Wash buffer to which 5 µL of 10% SDS and 5 µL Proteinase K (20 mg/mL) were added. RNAs from total lysate were also isolated from yAS99 and yAS99ΔSLR1 strains, by resuspending 0.1 g of frozen cell powder in 200 µL of 1X RNP buffer and adding 500 µL of Last Wash buffer, 5 µL of 10% SDS and 5 µL Proteinase K (20 mg/mL). From this point on, both totals and elutions were treated identically.

The samples were vortexed and incubated at 30°C for 30 minutes. Phenol chloroform extraction followed with the addition of 500 µL of phenol:chloroform:isoamyl alcohol (25:24:1) to each sample. The samples were vortexed and centrifuged at 13,000 x g for 5 minutes. The aqueous layer was ethanol precipitated overnight at -80°C. The following day, the samples were centrifuged at 13,000 x g for 15

minutes at 4°C, pellets were washed with 70% ethanol, air dried and resuspended in 11 µL of RNase free water. The samples were quantified using a nanodrop (eppendorf) and RNA-sequencing (Illumina) was performed at the Genome Quebec Innovation Center.

2.8 Cloning SLR1 associations factors

The following Slr1p associated factors were cloned into expression vectors in *S. pombe:* fatty acid synthase alpha subunit (Fas2), fatty acid synthase beta subunit (Fas1), eIF4G, eIF3B, eIF4A and aconitate hydrotase. Table 6 outlines the associated tags and vectors used.

Table 6 - Cloning of Slr1p-associated factors with their respective tags

Gene	C-terminal Tag	Vector
Fatty acid synthase alpha subunit (Fas2)	HA and FLAG	pREP42X
Fatty acid synthase beta subunit (Fas1)	HA	pREP41X
eIF4G	HA and FLAG	pREP41X
eIF3B	HA and FLAG	pREP41X
eIF4A	HA	pREP42X
Aconitate hydratase	HA and FLAG	pREP41X

yAS99 genomic DNA (refer Section 2.5.2) was used as the DNA template for insert amplification. The PCR reactions and PCR parameters used are outlined in Table 3 and Table 4, respectively. The annealing temperature was 55°C and extension was 4.5 minutes. The primers used (refer to Table 2) contained overhangs for the restriction enzymes XhoI and XmaI or SalI and XmaI which were the restriction sites used for ligating insert and vector. Refer to section 2.2 and 2.2.1 for the detailed cloning procedure.

Section 2.8.1 – *S. pombe* whole cell lysis

Yeast transformations were performed as outlined in Section 2.5.1. pREP41X + Fas1-HA and pREP42X+Fas2-FLAG were sequentially transformed into the strain yAS99ΔSLR1. An overnight culture was prepared by inoculating a single colony of yAS99ΔSLR1+ pREP41X-Fas1-HA + pREP42X-Fas2-FLAG in 10 mL of Edinburgh minimal media lacking uracil and leucine (EMM-ura-leu). The culture was grown to stationary phase at 32°C and used to seed down to an OD_{600} 0.2 in a final volume of 50 mL of EMM-ura-leu. When the cells reached OD_{600} 0.6, they were pelleted by centrifugation at 3,000 rpm for 5 minutes, washed with 1 mL of ddH_2O, resuspended in residual ddH_2O and transferred to a 2 mL screw cap tube. Cells were resuspended in 100 µL of cell lysis buffer (20 mM Hepes pH 7.6, 10% glycerol, 200 mM KOAc, 1 mM EDTA, 1 mM DTT, 10X Protease Inhibitor Cocktail and 1 mM PMSF) and 0.3 g of acid-washed glass beads were added. A bead beater was then used in the cold room to lyse the cells by vortexing for 1 minute on "homogenize". Another 100 µL of ice cold cell lysis buffer was added and the tube was vortexed to mix. The debris was sedimented at 14,000 x g for 10 minutes at 4°C and the supernatant was transferred to a new tube. Another 100 µL of cell lysis buffer was used to rinse the beads and was transferred to the supernatant tube. The supernatant was centrifuged at 14,000 x g for 30 minutes at 4°C and the supernatant was then once again transferred to a new tube. To quantify the lysate, Bradford assay was performed as per the manufacturer's protocol. Lysates were stored at -80°C.

2.9 Co-Immunoprecipitation of Fas1 and Fas2

2.9.1. Co-precipitation using cobalt beads

For each co-precipitation reaction, yAS99ΔSLR1 + pREP41X- Fas1-HA + pREP42X-Fas2-FLAG cell lysate (Section 2.8.1) was diluted to 2.5 mg/mL in a final volume of 220 µL. Approximately 5 µg of recombinant protein was added to the lysate and the sample was incubated on a nutator at 4°C for several hours. After the incubation, 12 µL of the sample was transferred to a new tube and labeled 'Input'. 50 µL of cobalt beads were prewashed three times with Wash Buffer (50 mM Tris-HCl pH 7.5, 150 mM NaCl, 0.05% IGEPAL, 10 mM Imidazole, 0.1 mM β-mercaptoethanol, 0.1 mM PMSF, 10X Protease Inhibitor Cocktail) and 200 µL of the lysate was transferred to the tube containing 50 µL of prewashed beads for binding. For binding to occur, the sample was incubated on a nutator for 30 minutes at 4°C, briefly centrifuged and the beads were washed 3 times with 700 µL of Wash Buffer each time. The supernatant was discarded and 250 µL of Elution Buffer (50 mM Tris-HCl pH 7.5, 150 mM NaCl, 1 mM EDTA, 1 mM EGTA. 0.1 mM β-mercaptoethanol, 150 mM Imidazole, 10X Protease Inhibitor Cocktail, 0.1 mM PMSF) was added to the beads. The sample was incubated on the nutator for 5 minutes at 4°C and then centrifuged at 10, 000 rpm for 1 minute. The supernatant was transferred to a new tube, and a second elution was performed again with 250 µL of Elution Buffer. The 2 elutions were pooled and Trichloroacetic acid (TCA) precipitated by adding an equal amount of cold 50% TCA. The reaction was set on ice for 10 minutes and then centrifuged for 10 minutes at 14, 000 rpm at 4°C. 500 µL of ice-cold acetone was added to the pellet and the sample was incubated at -20°C overnight. The

following day, the sample was centrifuged at 14, 000 rpm for 10 minutes at 4°C, supernatant was aspirated, pellet was air dried and resuspended in 8 µL of Solution A and 8 µL of Solution B. The samples were then analyzed by Western Blot Analysis by running the samples on a 10% SDS-PAGE gel, transferring to a nitrocellulose membrane and following a specific protocol based on the antibody used and tag being detected (refer to Section 2.9.3).

2.9.2 Co-IP using Protein G magnetic beads

For each co-IP reaction, yAS99ΔSLR1 + pREP41X-Fas1-HA + pREP42X-Fas2-FLAG cell lysate (Section 2.8.1) was diluted to 2.5 mg/mL in a final volume of 220 µL. Approximately 5 µg of recombinant protein was added to the lysate and the sample was incubated on a nutator at 4°C for several hours. After the incubation, the lysate was pre-cleared by adding 20 µL of magnetic Protein G beads (NEB Catalogue # S1430S) and incubating at room temperature for 30 minutes. A magnetic separation rack was used to separate the beads from the lysate and the pre-cleared lysate was transferred to a new tube. Primary antibody was added to the lysate (1:10 dilution (12CA5 DSHB, University of Iowa) or 1:50 dilution anti-FLAG (Cell Signaling Catalogue #2366S)) and the sample was incubated on a nutator at 4°C overnight. The next day, the Protein G beads were pre-washed by adding 40 µL of bead slurry to a tube containing 500 µL of cell lysis buffer (150 mM NaCl, 50 mM Tris pH 7.5, 0.05% IGEPAL, 1 mM PMSF, 10X Protease Inhibitor Cocktail). The tube was vortexed and placed on the magnetic separation rack and once the solution appeared clear, the supernatant was removed. The lysate and

antibody immunocomplex solution was transferred to the tube containing the washed magnetic beads and incubated on a nutator for 30 minutes at room temperature. After binding, the beads were washed 3 times with 500 µL of cell lysis buffer and then resuspended with 25 µL of 3X Laemmli buffer and vortexed. . The samples were analyzed by Western Blot analysis by running the samples on a 10% SDS-PAGE gel, transferring to a nitrocellulose membrane and following a specific protocol based on the antibody used and tag being detected (refer to Section 2.9.3).

2.9.3 Western Blot Analysis – probing with anti-his, anti-HA, anti-FLAG

6xHis Monocolonal Antibody – The blot was incubated in 20 mL Blotto (0.01 M Tris pH 7.4, 0.15 M NaCl, 0.075% Tween-20 and 0.5% skim milk powder) at room temperature for 40 minutes with shaking. Next, the membrane was incubated with 6xHis monoclonal anitobody (diluted 1:10,000 with Blotto) at room temperature for 1 hour with shaking. Three 10 minute washes in Blotto followed. The blot was then incubated with secondary anti-mouse HRP-linked antibody (diluted 1:5000 in Blotto) at room temperature for 1 hour. The following washes followed: one 10 minute wash in Blotto, two 10 minute washes in TST (0.01 M Tris pH 7.4, 0.15 M NaCl and 0.075% Tween-20) and one 5 minute wash in TSM (0.1 M Tris pH 9, 0.1 M NaCl, 5 mM $MgCl_2$). To detect the proteins, the membrane was incubated with 2 mL of ECL solution (Pierce) for 2 minutes with gentle agitation. The membrane was drained of excess developing solution, wrapped in Saran wrap and exposed to X-ray film with a 1 minute exposure.

Anti-FLAG and anti-HA: The same procedure was followed for probing with anti-FLAG

and anti-HA antibody, the only difference being the primary antibody dilution. After electrotransfer to nitrocellulose membrane, the blot was incubated with Blocking buffer (5% w/v skim milk powder, 1X TBS, 0.1% Tween-20) for 1 hour, followed by three 10 minute washes in 1X TBS + 0.1% Tween-20. Next, the membrane was incubated for 1 hour with primary antibody (anti-FLAG 1:1000 or anti-HA 1:50) diluted in 3% BSA, 1X TBS and 0.1% Tween-20. Three washes were then performed, 10 minutes each in 1X TBS + 0.1% Tween-20. The blot was then incubated with secondary antibody (anti-rabbit HRP-linked antibody for anti-FLAG (1:5000) or anti-mouse HRP-linked antibody for anti-HA (1:5000) in 3% skim milk powder, 1X TBS, 0.1% Tween-20) for 1 hour and three 10 minute washes thereafter in 1X TBS + 0.1% Tween-20. To detect the proteins, the membrane was incubated with 2 mL of ECL solution (Pierce) for 2 minutes with gentle agitation. The membrane was drained of excess developing solution, wrapped in Saran wrap and exposed to X-ray film with a 2 minute exposure.

2.10 Lipid Extraction

Total lipid extraction in *S. pombe* cells was performed using strains yAS99 and yAS99ΔLR1, each grown at 16°C and 32°C for a total of 4 samples. 50 mL of cells were seeded to OD_{600} 0.2 and allowed to grow to OD_{600} 0.6-0.8 in YES media. Cells were then harvested by centrifugation at 1,500 x g for 5 minutes at 4°C and pellets were washed twice with 30 mL of ice-cold 1X PBS and centrifuged at 1,500 x g for 5 minutes at 4°C. The cell pellets were resuspended in 200 µL of ice-cold 1X PBS and transferred to 2 mL screw cap tubes. 0.3 g of acid-washed glass beads were added to each tube and the

samples were lysed in a bead beater for 2 minutes. A hole was punctured in the bottom of each tube with a 25 gauge needle and placed on top of a 1.5 mL microfuge. This was placed into a 50 mL conical and centrifuged at 5,000 x g for 2 minutes at 4°C. The supernatant was transferred to 2 mL Teflon screw-cap tubes, the glass beads were washed with 100 µL of 1X PBS which was also transferred to the Teflon tubes and 900 µL of ice-cold Chloroform:Methanol (1:2) was added. The samples were incubated for 2 hours at 4°C with vigorous agitation. Then, 300 µL of ice-cold Chloroform and 300 µL of ice-cold water was added, samples were vortexed 15 seconds and incubated on ice for 2 minutes, twice. They were then centrifuged at 7,000 x g for 2 minutes at 4°C and the lower organic phase was transferred to a new Teflon tube. 500 µL of ice-cold Chloroform was added for re-extraction and samples were incubated once again for 2 hours at 4°C with vigorous agitation. The layers were separated by centrifugation at 7,000 x g for 2 minutes and the two organic extracts were combined. The supernatant was then evaporated with argon gas and dried samples were stored in -80°C until lipid analysis was performed by LC-MS/MS.

RESULTS

3.1 Slr1p Belongs to a Novel Class of La motif Containing Proteins

In addition to the La homolog in *S. pombe,* Sla1p, another gene in fission yeast has been identified which contains the La motif. Located on chromosome I, SPAC1527.03, is the only other gene in fission yeast to contain a La motif, therefore we suggest that it be called *S. pombe* La-related protein 1 (Slr1p). Comprised of 1428 base pairs, 475 amino acids, the protein has a molecular weight of 53.2 kDa and a pI of 9.10 (http://old.genedb.org/genedb/Search?name=SPAC1527.03&organism=pombe).

Although Slr1p shares a domain common to the La family of proteins, the position of the La motif within Slr1p is different from genuine La proteins and La-related proteins (Figure 10A). Genuine La proteins contain a highly conserved N-terminal La motif and adjacent RRM1 while the C-terminus is more divergent and increases in size from yeast to higher organism. In contrast, Slr1p contains a LAM located toward the C-terminus and lacks an RRM. Therefore, Slr1p does not resemble authentic La proteins outside the La motif.

Multiple sequence alignments of genuine La homologs in humans and yeast, as well as La-related proteins, suggests that Slr1p contains 5 out of the 6 conserved amino acid residues required for UUU-3'OH dependent binding (Figure 3B). Slr1p observes 43.48 % identity in its La motif when compared to the human La-motif and 45.65% when compared to human LARP1.

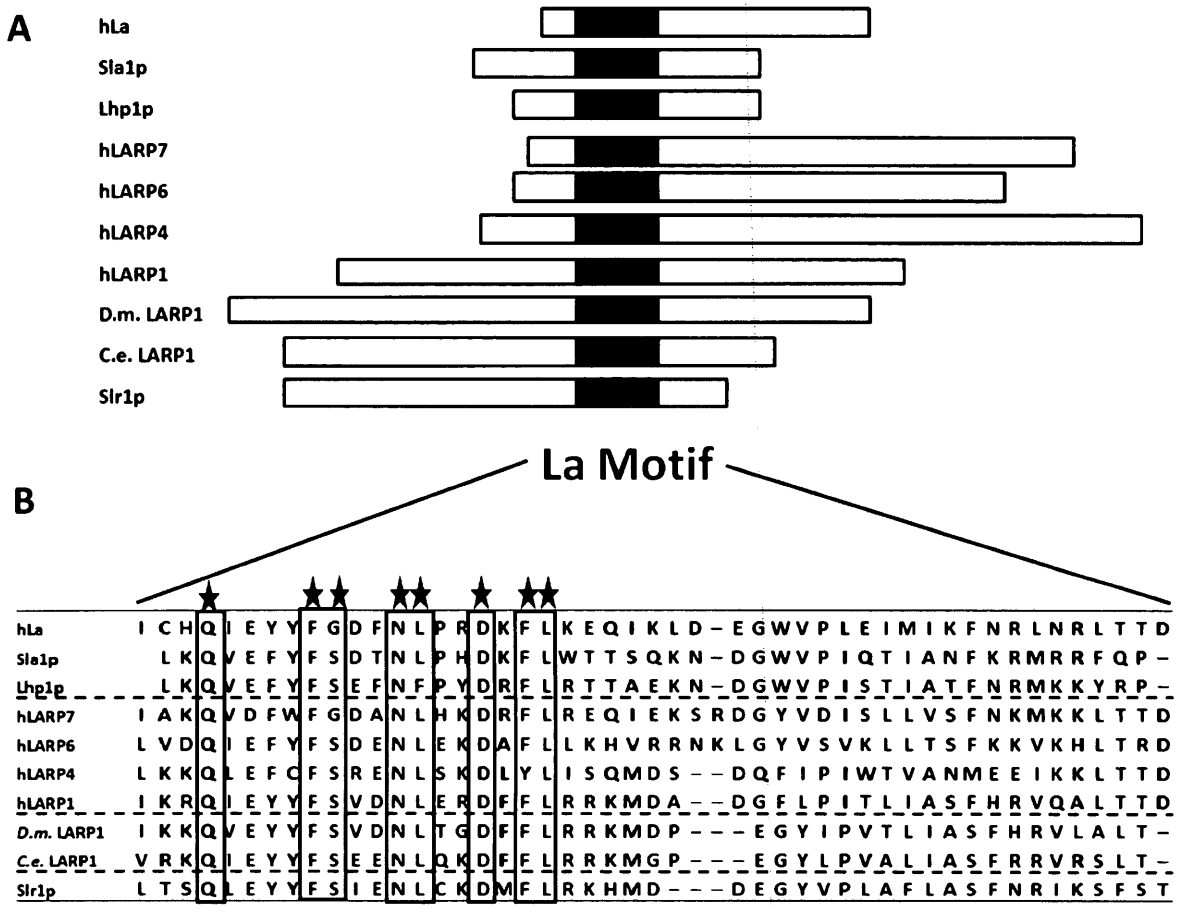

Figure 10 - Slr1p is a structural homolog of the evolutionarily conserved La-related family of proteins. (A) Domain structure of selected genuine La proteins: *Homo sapiens* (hLa), *Schizosaccharomyces pombe* (Sla1p), *Saccharomyces cerevisae* (Lhp1p) and La-related proteins in Homo sapiens, *Drosophila melanogaster* and *Caenorhabditis elegans*. La motifs are depicted in black boxes. B) Multiple-sequence alignment of La motifs of Slr1p, genuine La homologs and LARPs. Residues that are conserved across most species are outlined in red boxes. The identity and position of residues critical for UUU-3'OH binding in La proteins are shown on the top by stars. Species name abbreviations are as follows: *D.m., Drosophila melanogaster*, *C.e., Caenorhabditis elegans.* Adapted from Schenk et al., *RNA* 2012.

3.2 Slr1p is an RNA chaperone

In order to determine whether RNA chaperone activity is conserved in the La-related protein in fission yeast, full length Slr1p was cloned for expression and purification in *E. coli.* The purified protein was analyzed and quantified on an SDS-PAGE gel, alongside known amounts of BSA were the band intensity of known amounts of BSA were compared to the unknown quantity of protein (Figure 11). The FRET assay was then optimized for Slr1p to determine what the optimal concentration of protein is to use. A titration of Slr1p was performed, testing three different protein concentrations; 20 nM, 100 nM and 500 nM. It was shown that 100 nM is the saturating concentration of Slrp1, thus the optimal concentration to use in the FRET assay (Figure 12). Therefore, 100 nM of protein was used for all subsequent trials in the FRET experiment which is not dissimilar to the concentration of La in human cells.

It was shown, that like hLa, Slr1p was active in both strand annealing (Phase I, k_{ann1}) and strand dissociation (Phase II, k_{SD}) activities (Figure 13). The negative controls, RNA alone and BSA, show that the observed RNA dynamics in phase I occur at a much lower rate in the absence of a bona fide RNA chaperone. In phase II of the assay, RNA alone and BSA are not capable of strand dissociation activity, thus display a second rate of annealing (k_{ann2}). However, in the presence of an RNA chaperone with strand dissociation activity, such as hLa and Slr1p, the dissociation of the Cy3 and Cy5 annealed RNA strands and their inability to reanneal in the presence of excess competitor causes a decrease in FRET index (Figure 13A).

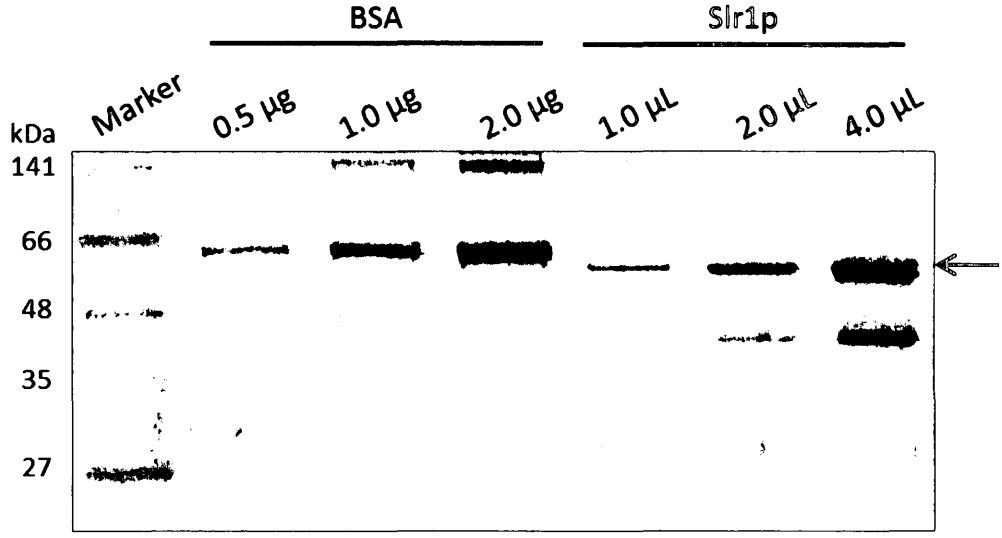

Figure 11 - Purification and quantification of Slr1p. Recombinant His-tagged Slr1p was expressed in *E. coli* Rosetta Blue (DE3) cells with 0.1 mM IPTG and purified by nickel affinity chromatography. The 53 kDa purified protein was analyzed by SDS-PAGE and Coomassie staining. Slr1p was quantified alongside BSA standards and calculated to have a concentration of approximately 0.5 µg/µL. Slr1p was also quantified using the Bradford assay, and a similar concentration was observed. The red arrow indicates purified Slr1p. The band below Slr1p is a degradation product of Slr1p. Molecular weight marker in kDa is depicted on the left.

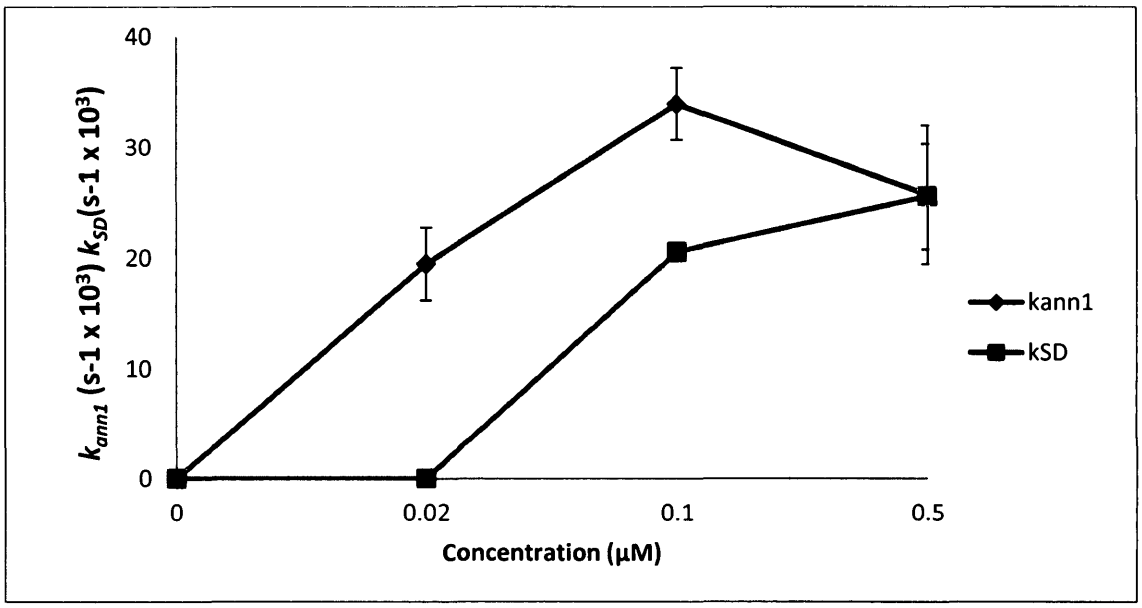

Figure 12 – 100 nM is the optimal concentration of Slr1p for FRET. A titration of Slr1p, using 20 nM, 100 nM and 500 nM of Slr1p was used in the FRET assay. Strand annealing (k_{ann1}, phase I) and strand dissociation (k_{SD}, phase II) rates are illustrated using three varying concentrations. The graph demonstrates that 100 nM is the optimal concentration to use, as there is a decrease in strand annealing activity after 100 nM Slr1p. The error bars show the standard deviation of three separate experiments.

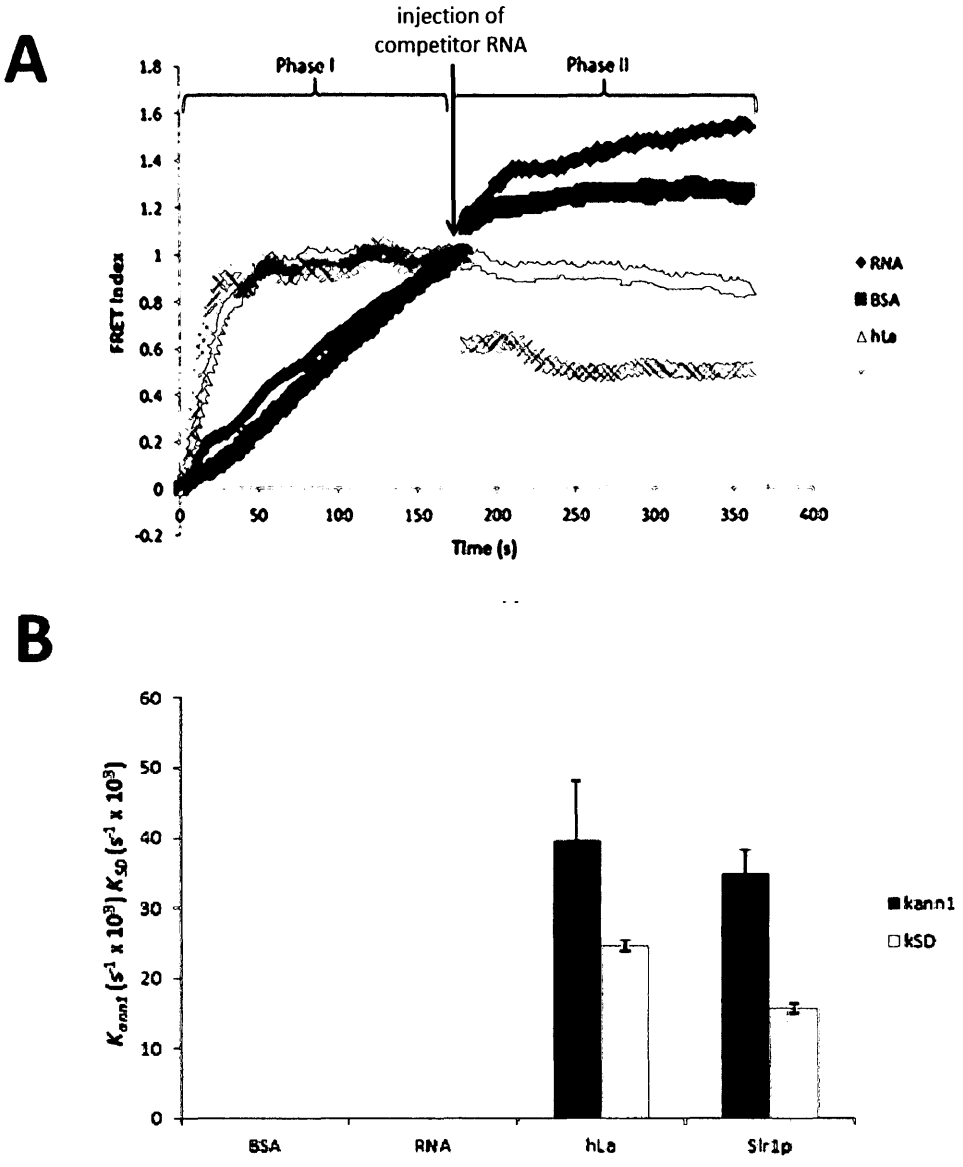

Figure 13 – Slr1p displays RNA strand association and strand dissociation activity. (A) RNA strand annealing (phase I) and strand dissociation (phase II) of Slr1p compared with hLa was measured as a change in FRET index (ratio of emission at 680nm/590nm) between complementary Cy5- and Cy3-labeled RNA strands over time. The representative curves shown are normalized at time 180 seconds. RNA and BSA were used as negative controls and hLa was the positive control. 100 nM protein concentrations were used for all the proteins. (B) Observed strand annealing rates (*k*ann1, phase I), strand dissociation rates (*k*S.D., phase II) and strand annealing rates in phase II in the absence of strand dissociation (*kann*2, phase II). Rates are given as mean ± standard deviation derived from three independent experiments.

3.2.1 The N- and C- terminal halves of Slr1p harbor both strand annealing and strand dissociation activity

Various regions of Slr1p were tested for RNA chaperone activity. Five Slr1p mutants were cloned for expression and purification in *E. coli*. Following, quantification, Slr1p mutants at 100 nM (the saturating concentration of full length Slr1p) were used in the FRET assay. Indeed we found that both the N-terminal half and C-terminal half was capable of strand annealing and strand displacement activity (Figure 14). Interestingly, we found that the RNA chaperone activity in the NTD is centered around residues 130-312 as residues 1-130 were inactive in the FRET assay (Figure 14A). The C-terminus also harboured RNA chaperone activity, however, the predicted La motif, Slr1p mutant 312-414, showed limited strand annealing and strand displacement activity. However, once the amino acids C-terminal to the LAM were added, in Slr1p mutant 312-475, there was a significant gain in strand annealing and strand displacement activities which were comparable to full length Slr1p and the positive control human La. This observation is reminiscent of human La and the human LARPs, where the RNA chaperone activity was enhanced by the inclusion of amino acids C-terminal to the La module. Another consistency with human La and human LARPs is that the LAM in isolation is inactive in strand annealing and strand displacement activity, suggesting that the Slr1p LAM acts similar to the LAM of other La proteins and LARPs.

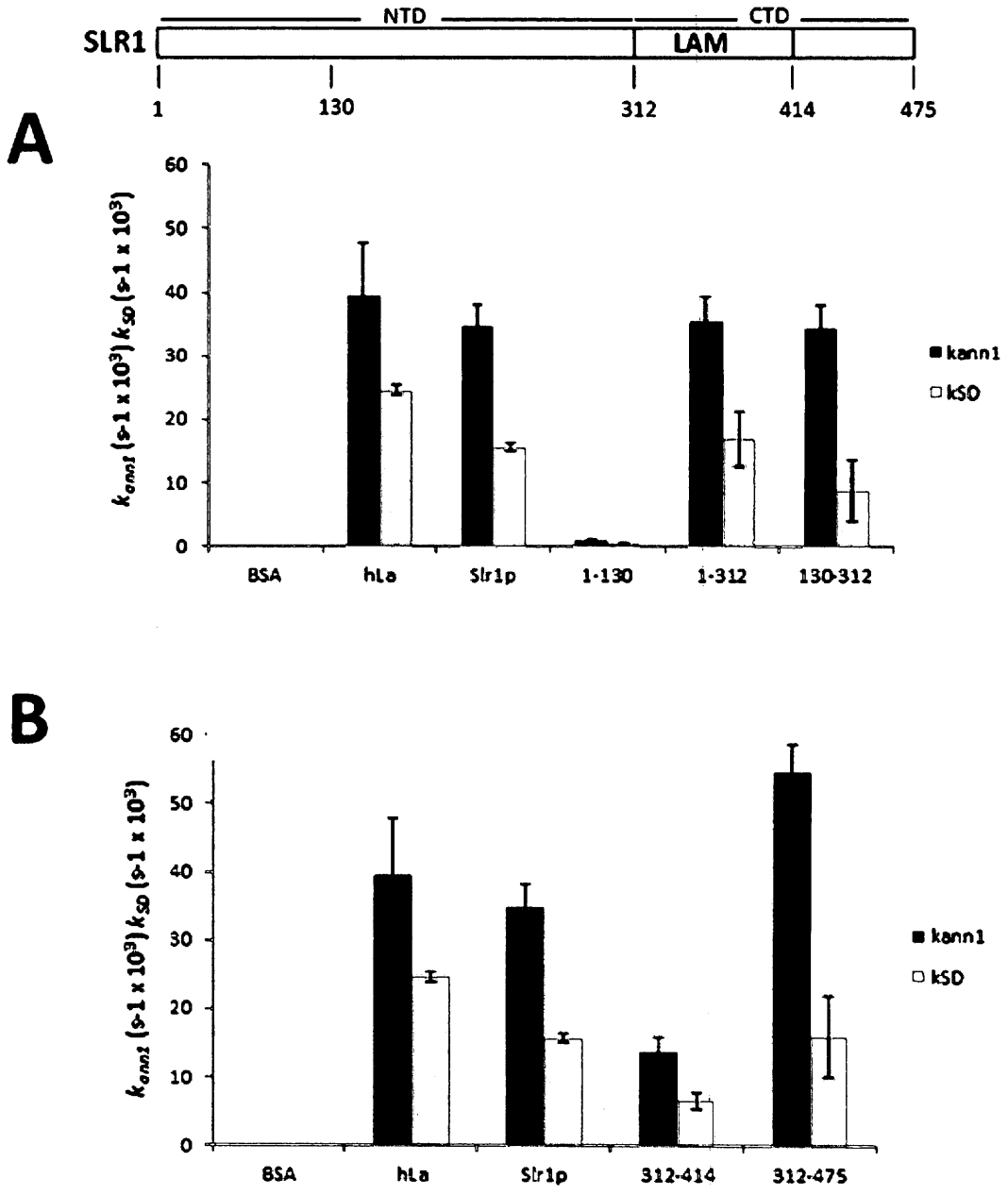

Figure 14 – Slr1p NTD and CTD can independently carry out RNA chaperone activity. *k*ann1 and *k*S.D. rates for indicated Slr1p mutants at 100 nM in comparison to the positive controls, full length Slr1p, hLa, and the negative control BSA. Error bars show the standard deviation of a minimum of three separate experiments. (A) Slr1p exhibits NTD associated RNA chaperone activity. Mutant 1-130 was inactive in the FRET assay and mutants 130-312 and 1-312 both displayed strand annealing and strand displacement activities. (B) Slr1p exhibits CTD associated RNA chaperone activity. RNA chaperone activity is greatly enhanced with the addition of the predicted disordered region immediately after the La motif (comparing mutant 312-414 and 312-475).

3.3 Slr1p has a UUU-3'OH independent mode of binding to its RNA substrate(s)

Since Slr1p has nearly complete identity of the conserved residues in the La motif associated in human La with UUU-3'OH dependent RNA binding, we tested if Slr1p has a similar binding mode to that of human La. RNA homopolymers that were either 10-mer or 20-mer; poly (U), poly (A), poly (C) and poly (G) were used in gel shifts with increasing concentrations of Slr1p to test Slr1p's binding capabilities (Figure 15). It was found that Slr1p did not bind to poly (A), poly (C) and poly (G) and had a weak binding with poly (U). Slr1p bound to the poly (U) 20 mer RNA with a weak affinity where binding was observed at about 1600 nm. Since Slr1p needs to be present at such a high concentration to see a relatively weak binding with the 20-mer poly (U) RNA (Figure 15(i)), suggests that Slr1p has a UUU-3'OH independent mode of RNA binding to its substrate.

We then tested whether Slr1p binds a tRNA substrate, as this a well characterized substrate for Sla1p, the fission yeast La homolog. Interestingly, Slr1p did bind to the tested $tRNA^{Ala}AGC$ substrate. Sla1p was used as the positive control, and it showed that Sla1p bound $tRNA^{Ala}AGC$ starting at approximately 200 nM. Binding for Slr1p was observed at about 800 nM, a significantly higher concentration when compared to Sla1p (Figure 16).

To determine if Slr1p has specific RNA targets or whether it binds to any RNA that bears a secondary structure needs to be determined. To address this question, we performed RNA-sequencing to identify Slr1p's endogenous RNA targets.

(i)

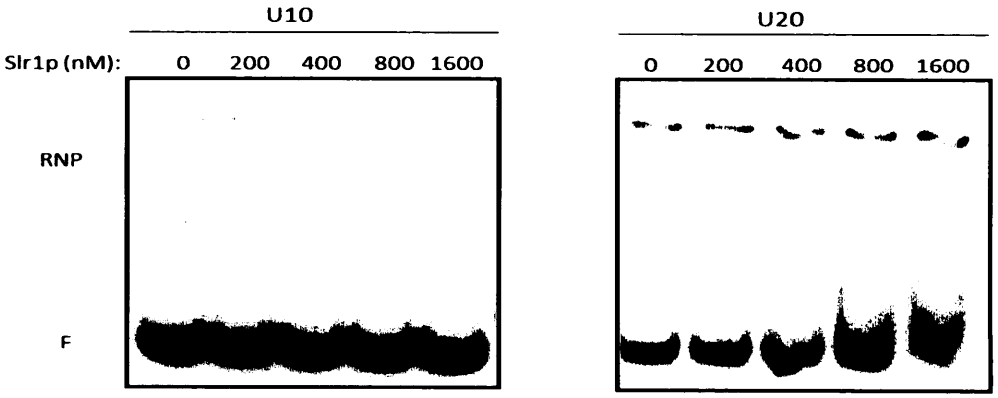
U10
U20
Slr1p (nM): 0 200 400 800 1600
0 200 400 800 1600
RNP
F

(ii)

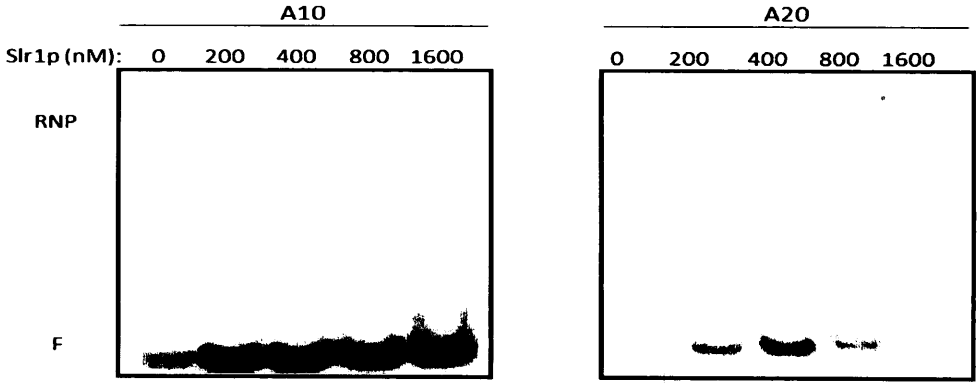
A10
A20
Slr1p (nM): 0 200 400 800 1600
0 200 400 800 1600
RNP
F

(iii)

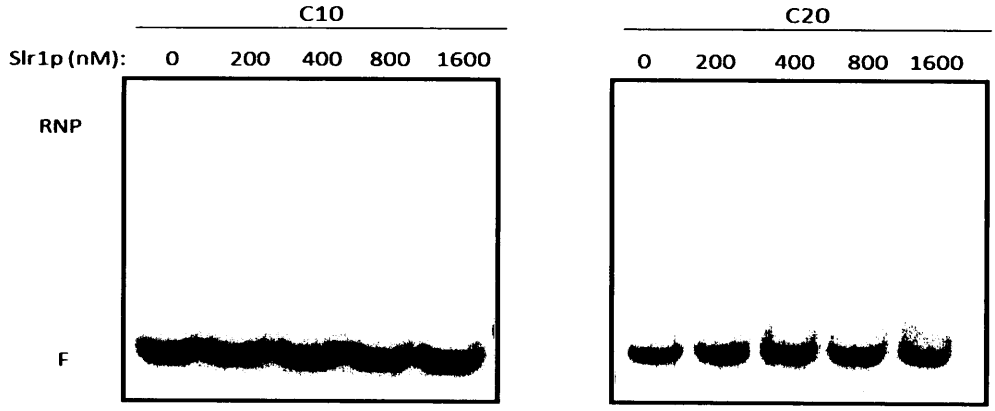
C10
C20
Slr1p (nM): 0 200 400 800 1600
0 200 400 800 1600
RNP
F

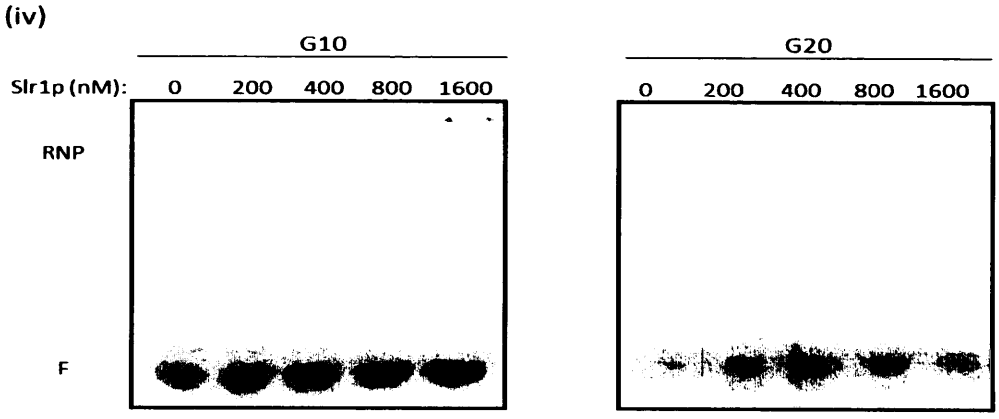

Figure 15 – Slr1p binding to 10-mer and 20-mer RNA homopolymers. Gel mobility shift assays of increasing amounts of full length Slr1p binding to 10mer and 20mer RNA homopolymers (i) poly (U), (ii) poly (A), (iii) poly (C) and (iv) poly (G) visible as RNP (RNA-bound protein) and F (free RNA). Weak binding was observed with poly (U) 20-mer RNA, however, this was relatively insignificant compared to binding to a tRNA substrate. Slr1p did not bind to the poly (A), poly (C) and poly (G) RNA homopolymers.

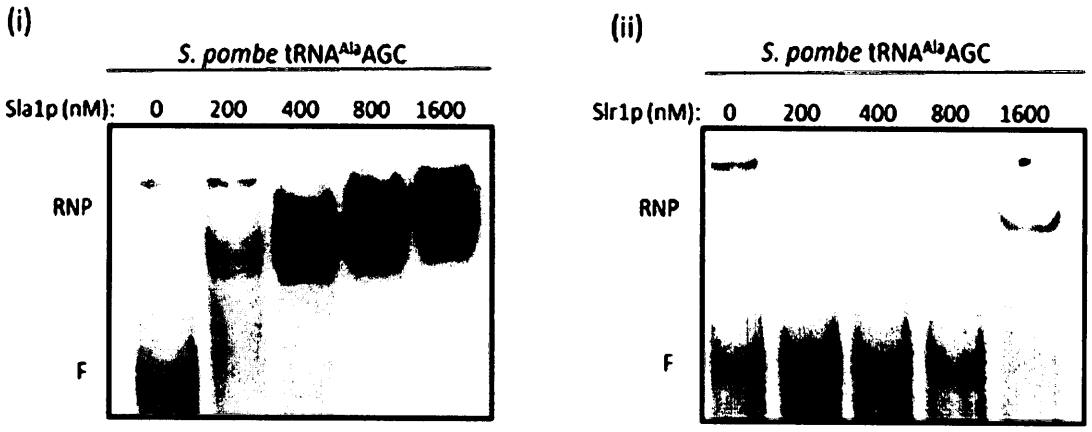

Figure 16 – Slr1p binds to a tRNA substrate. EMSAs illustrating binding reactions between varied concentrations of (i) Sla1p (control) and (ii) Slr1p and trace amounts of ^{32}P-labelled tRNA^{Ala}AGC, visible as RNP (RNA-bound protein) and F (free RNA). Sla1p binds to the tRNA substrate with a high affinity (at about 200 nM), while Slr1p binds to the tRNA substrate with a much lower affinity (at about 800 nM).

3.3.1 Identification of Slr1p RNA-targets

RNA-sequencing was performed to identify Slr1p's endogenous RNA targets by performing co-IPs and isolating RNAs that were pulled down with Slr1p-PrA. While bioinformatic analysis is still in the process of being completed, we have received some preliminary results. Out of the top 10 RNAs bound to Slr1p, 4 of them were involved in translation, 3 were associated with ubiquitination and 3 were mRNAs coding for unknown proteins. From this, we can speculate a general role for Slr1p that is also supported by the mass spectrometry results. We hypothesize that Slr1p has a function in translation and its primary RNA targets are coding RNAs, which is consistent with human LARPs 1, 4 and 6. Further analysis is required to establish these results in greater detail.

3.4 Slr1p is primarily cytoplasmic

Intracellular localization of Slr1p was determined by immunostaining with rabbit IgG coupled to Alexa Fluor 488 secondary antibody. DNA was visualized by DAPI staining. Alexa Fluor excites at 488 nm and emits at 519 nm (green), while DAPI absorbs at a maximum wavelength of 358 nm and emits at approximately 460 nm (blue). Observations were compared to those observed in the wild-type yA99 strain, bearing no tagged proteins. As seen in Figure 17, there is a significant difference in the signal level of Alexa Fluor 488 between the two strains. In the Slr1p-PrA tagged strain, the antibody binds to the PrA tag which appears to be located throughout the cytoplasm, whereas in yAS99, it seems to have non-specifically diffused throughout the cell, producing a much

weaker signal observed as background. DAPI exposure was at 1050 ms and Alexa Flour 488 was 450 ms. These results suggest that Slr1p is localized to the cytoplasm under normal growth conditions.

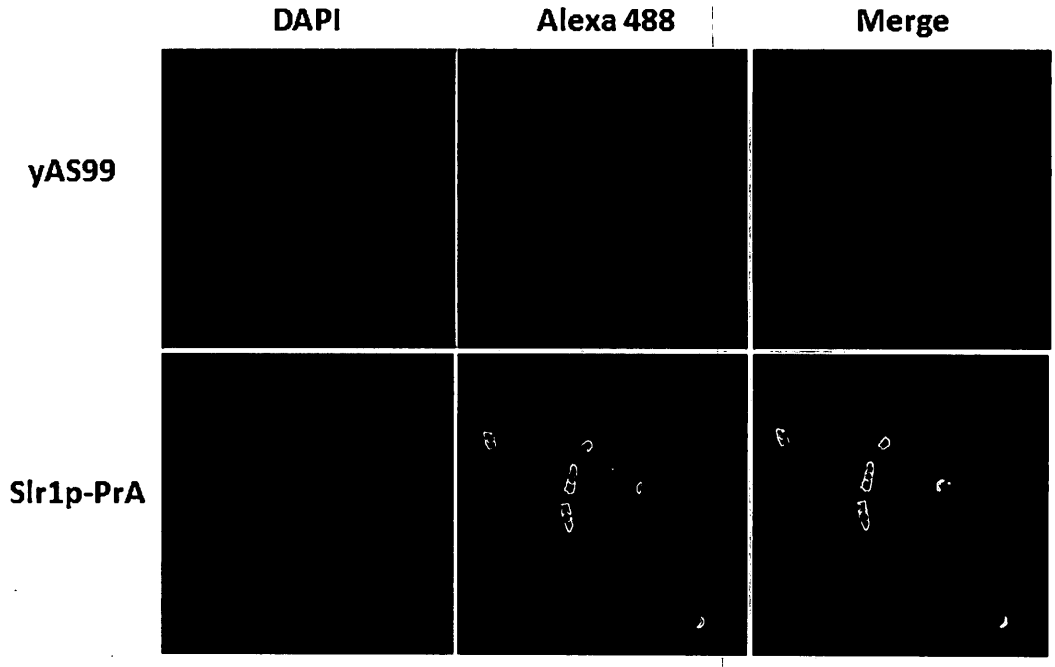

Figure 17 – Slr1p is localized in the cytoplasm. Subcellular localization was determined by immunostaining yAS99 wild type (control) cells and Slr1p-PrA cells with rabbit IgG and Alexa 488 secondary antibody. DNA was visualized by DAPI staining. Merged image of DAPI and fluorescence can be visualized on the far right.

3.5 Co-immunoprecipitation of Slr1p associated protein complexes

In order to determine Slr1p associated protein complexes, Slr1p needed to be tagged in a wild type strain for subsequent co-immunoprecipitation experiments. Protein A tagged Slr1p was generated from a wild type parent strain of *S. pombe,* yAS99. The strategy for integrating the PrA tag into the endogenous chromosomal open reading frame of SLR1 is illustrated in Figure 18A. Primers were strategically designed with regions complementary to SLR1, PrA tag and the Kanamycin cassette. The DNA of interest was PCR amplified to produce an end result as outlined in Figure 18B. Following homologous recombination, genomic DNA was isolated and PCR amplification was performed using various primers (depicted by black arrows in Figure 18B). The expected bands; #1 – 400 to 500 bp, #2 – 500 to 600 bp and #3 – 1.7 kb are presented in Figure 18C. In addition, Western blot analysis was performed to confirm the cells were expressing PrA-tagged Slr1p (data not shown). The Slr1p-PrA strain was designated yLS001.

In an attempt to identify novel protein-protein interactions of Slr1p, co-immunoprecipitation was performed and the lyophilized elutions were subjected to mass spectrometry. Co-immunoprecipitation of PrA-tagged Slr1p using magnetic Dynabeads was initially performed from *S. pombe* yAS99 (control, untagged strain) and yLS001 (Slr1p-PrA) and optimized prior to mass spectrometry analysis. Varying salt and buffer conditions were tested to determine the optimal buffer to use that preserves majority of the protein complexes. The procedure was optimized to using 100 mM NaCl in 1X RNP buffer (see Methods) for subsequent purifications (data not shown).

Slr1p-PrA was re-purified using the optimized condition, resolved on an SDS-PAGE gel and visualized by Coomassie staining (Figure 19A). Multiple bands were visible in the elution lane of yLS001 and many of these were specific to that strain, as indicated by their absence in the yAS99 control strain. In addition, Western blot analysis was performed for elutions yAS99 and yLS001, and Slr1-PrA was detected with PAP (anti-PrA) antibody at about 84 kDa (Figure 19B). These data provided confidence in the purification procedure and illustrated that proteins which associate with Slr1p *in vivo* could be analyzed by mass spectrometry.

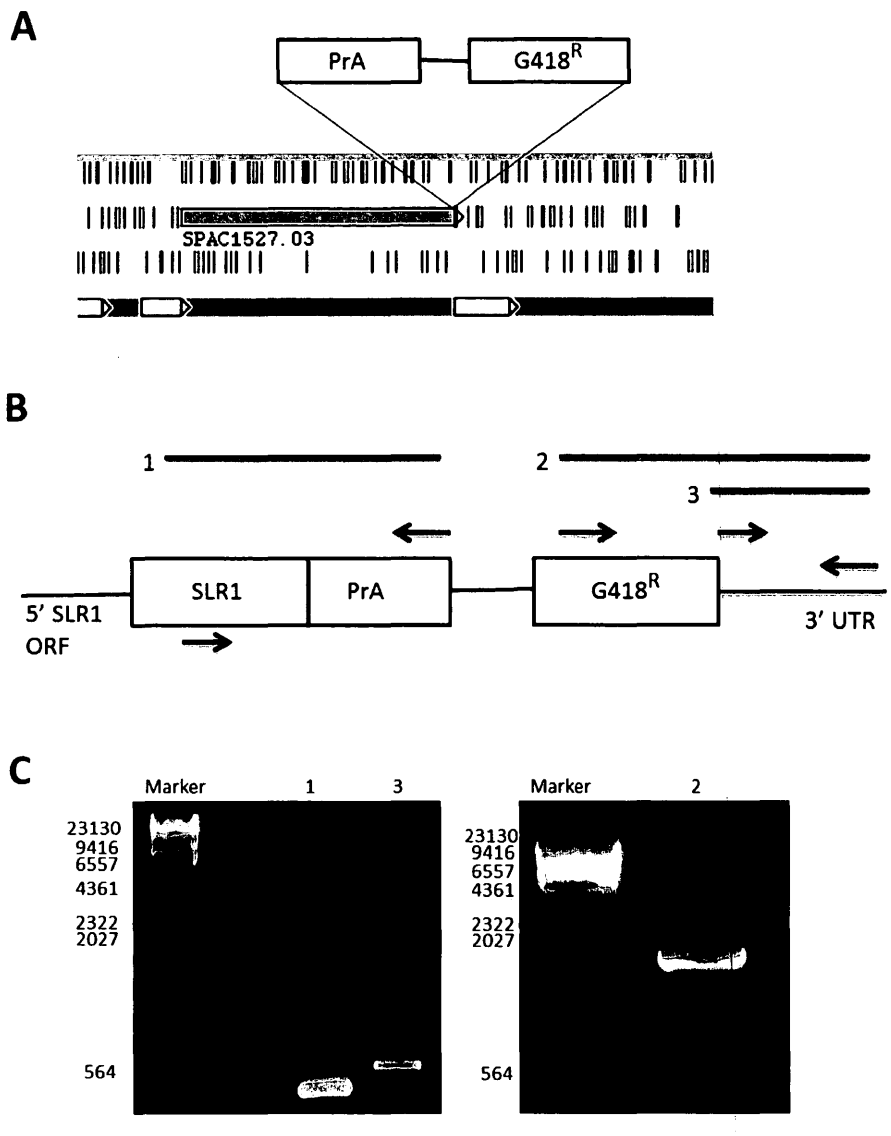

Figure 18 - Integrating a Protein A tag into the chromosomal ORF of Slr1p. (A) Schematic diagram of the strategy of creating Slr1p-PrA by inserting an in-frame PrA tag into the SLR1 genomic locus via a G418 Kan^R cassette. (B) Schematic diagram of the genomic locus of SLR1 after integration of the PrA tag and adjacent Kan^R cassette. PCR analysis was performed using the primers denoted by black arrows to confirm correct integration. Pink lines represent the expected PCR products with the following expected sizes; 1 – 400 to 500 bp, 2 – 1.7 kb, 3 – 500 to 600 bp. (C) PCR confirmation of correct integration of PrA tag into the ORF of SLR1 in the parent *S. pombe* strain yAS99. Bands 1,2 and 3 correspond to the expected PCR products denoted in (B).

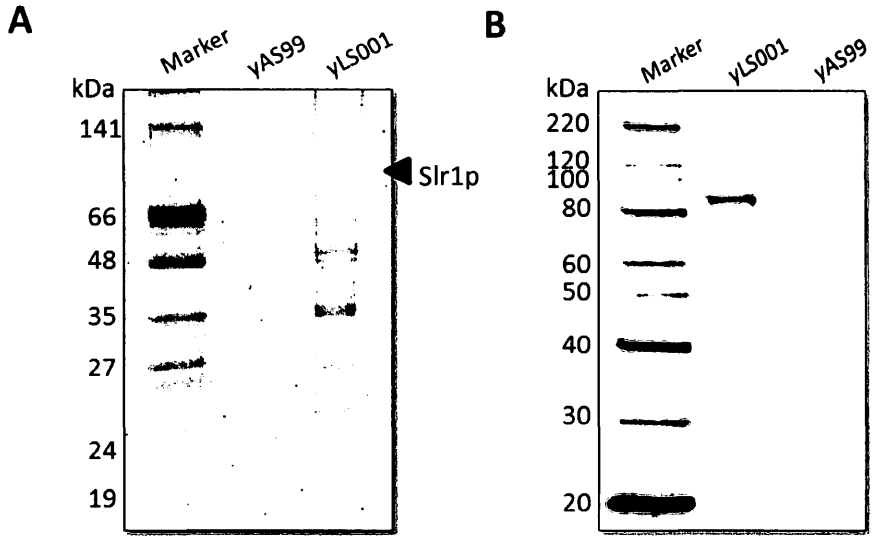

Figure 19 - Isolation of PrA-tagged Slr1p complexes. (A) Slr1p associated complexes were affinity purified via the PrA tag, and associated proteins were resolved by SDS-PAGE and visualized by staining with Coomassie blue. Purification was also carried out from yAS99, the negative, untagged strain. (B) Slr1p-PrA was expressed under the control of its endogenous promoter and affinity purified using IgG-conjugated magnetic beads. Western blot analysis using PAP antibody (1:5000) detects Slr1p in the elution of yLS001 (Slr1p-PrA), but not the negative control, yAS99.

3.5.1 Mass spectrometry analysis illustrates the potential physical interactors of Slr1p

Lyophilized elutions of yAS99 and yLS001 from co-immunoprecipiation were analyzed by tandem mass spectrometry. Mass spectrometry analysis of Slr1p associated proteins returned 735 hits of which 502 were common to both strains. The Scaffold 3 program (Proteome Software) was used to analyze the large volume of data and identify potential binding partners of Slr1p. 54 hits were specific to the yLS001 strain and those were the hits we were mainly interested in. As expected, the most robust hit represented the bait, Slr1p itself, further validating the effectiveness of the purification process. Proteins that were much more pronounced in the yLS001 strain than in the yAS99 strain included components of larger complexes involved mainly in translation, including multiple subunits of the eIF3 translation initiation factor, components of eIF4F (eIF4G (very high) and eIF4E (lower)), as well as cytoplasmic poly-A binding protein (PABP) (see Table 8). Also of interest were both alpha and beta subunits of fatty acid synthase which were pulled down very robustly. Since the majority of the proteins pulled down with Slr1p are mainly cytoplasmic, these results are consistent with the intracellular localization of Slr1p where immunostaining via indirect immunofluorescence showed that it is localized to the cytoplasm.

Some of the mass spectrometry hits were validated by co-IPs followed by Western blot analysis. Beads alone and Sla1p were used as negative controls for two different co-IPs. The first co-IP was a repeat of the mass spectrometry results, confirming that Fas1/Fas2 complex was pulled down when precipitated with cobalt beads specific to recombinant His-tagged Slr1p (Figure 20A). As expected, beads alone and Sla1p did not

pull down Fas1/Fas2, further indicating that the proteins in the mass spectrometry analysis are specific for Slr1p and do not bind to any La-motif containing protein, such as Sla1p. The second co-IP was the reversal co-IP which produced the same results. In this case, Fas2 was immunoprecipitated with anti-FLAG antibody and the goal was to see if Fas2 would pull down recombinant Slr1p. Indeed, Fas2 was able to pull down Fas1 and recombinant Slr1p, but not recombinant Sla1p (Figure 20B). Therefore, these co-IPs further confirm the mass spectrometry results that what we are seeing is indeed true and specific for Slr1p.

Table 7 - Proteins identified by mass spectrometry that associate with Slr1p. 10 top hits identified by tandem mass spectrometry (LC-MS/MS) are listed with the number of spectral counts in yAS99 and yLS001. The *P*-values were calculated with Fisher's exact test.

Identified Proteins	Fisher's Exact T-Test (P-Value)	yAS99	yLS001
RNA binding protein (Slr1p)	0	0	148
Translation initiation factor eIF4G	3.0×10^{-26}	6	98
Fatty acid synthase alpha subunit (Fas2)	1.2×10^{-26}	39	172
Fatty acid synthase beta subunit (Fas1)	1.3×10^{-24}	32	151
aconitate hydratase / mitochondrial ribosomal protein subunit L49, fusion protein	4.0×10^{-8}	0	22
Translation initiation factor eIF3C	6.0×10^{-8}	8	41
Translation initiation factor eIF3B	1.1×10^{-7}	8	40
Translation initiation factor eIF3A	3.4×10^{-7}	18	55
Poly-A binding protein (PABP)	4.1×10^{-6}	25	60
DNA-directed RNA Polymerase I complex subunit Rpa34	2.0×10^{-3}	0	8

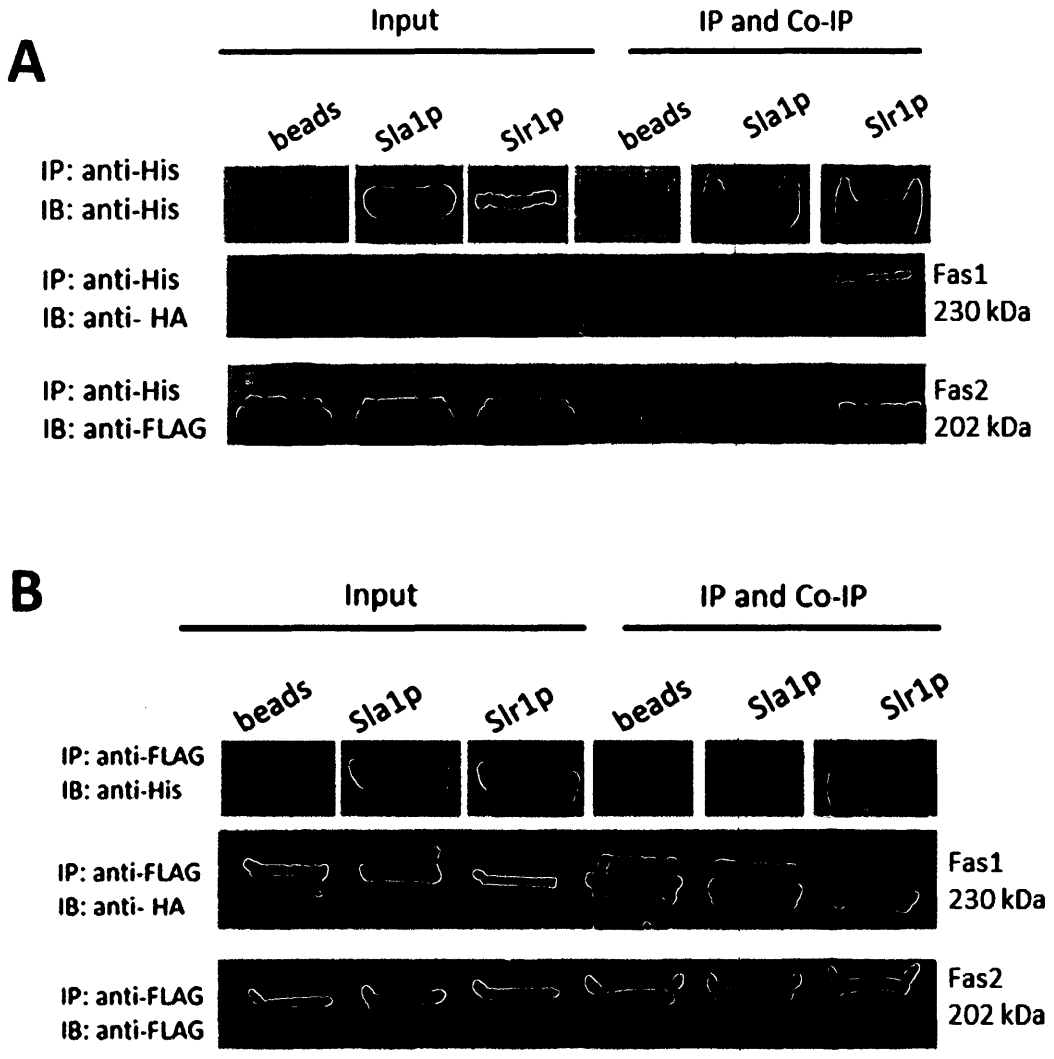

Figure 20 – Validation of mass spectrometric results. The identification of some of the interacting proteins identified by mass spectrometry were confirmed by Western blotting. Co-immunoprecipitation studies were carried out with an SLR1 knock-out yeast strain coexpressing pREP41X+ Fas1-HA and pREP42X+Fas2-FLAG (strain: yAS99ΔSLR1 + Fas1-HA + Fas2-FLAG). (A) Recombinant His-tagged Sla1p (negative control) and His-tagged Slr1p that were produced in *E.coli* and purified, were added to the lysate and immunoprecipitated with (A) cobalt beads and (B) Protein G magnetic beads bound to anti-FLAG (1:50) antibody. Recombinant proteins present in starting lysate (left) and co-immunoprecipitates (right) were detected with anti-His (1:10 000), anti-HA (1:50) and anti-FLAG (1:1000). Input represents 5% of the total cell extract used for each immunoprecipitation.

3.6 Mapping of Slr1p mutants required for binding fatty acid synthase

Since fatty acid synthase was found to associate with Slr1p, this result was quite interesting and we decided to study it in more detail. First, we wanted to determine whether the interaction between FAS and Slr1p was specific to the NTD or CTD of Slr1p. Therefore, we performed recombinant co-IPs testing full length Slr1p, Slr1p mutant 1-312 (NTD) and Slr1p mutant 312-475 (CTD). These recombinant His-tagged proteins were added to the lysate containing tagged Fas1 and Fas2 and precipitated with cobalt beads specific for the His tag. As expected, full length Slr1p bound Fas1 and Fas2 and mutant 1-312 also bound Fas1 and Fas2 but mutant 312-475 did not (Figure 21A). This suggests that only the NTD of Slr1p interacts with FAS.

We then tested three different mutants in the NTD: mutant 1-130, 130-312 and 1-312 in similar co-IPs to those previously described. These recombinant His-tagged proteins were added to the lysate containing tagged Fas1 and Fas2 and precipitated with cobalt beads specific for the His tag. It can be seen in Figure 21B, that only mutant 1-312 binds Fas1 and Fas2, but neither mutants 1-130 and 130-312 bind to the FAS subunits.

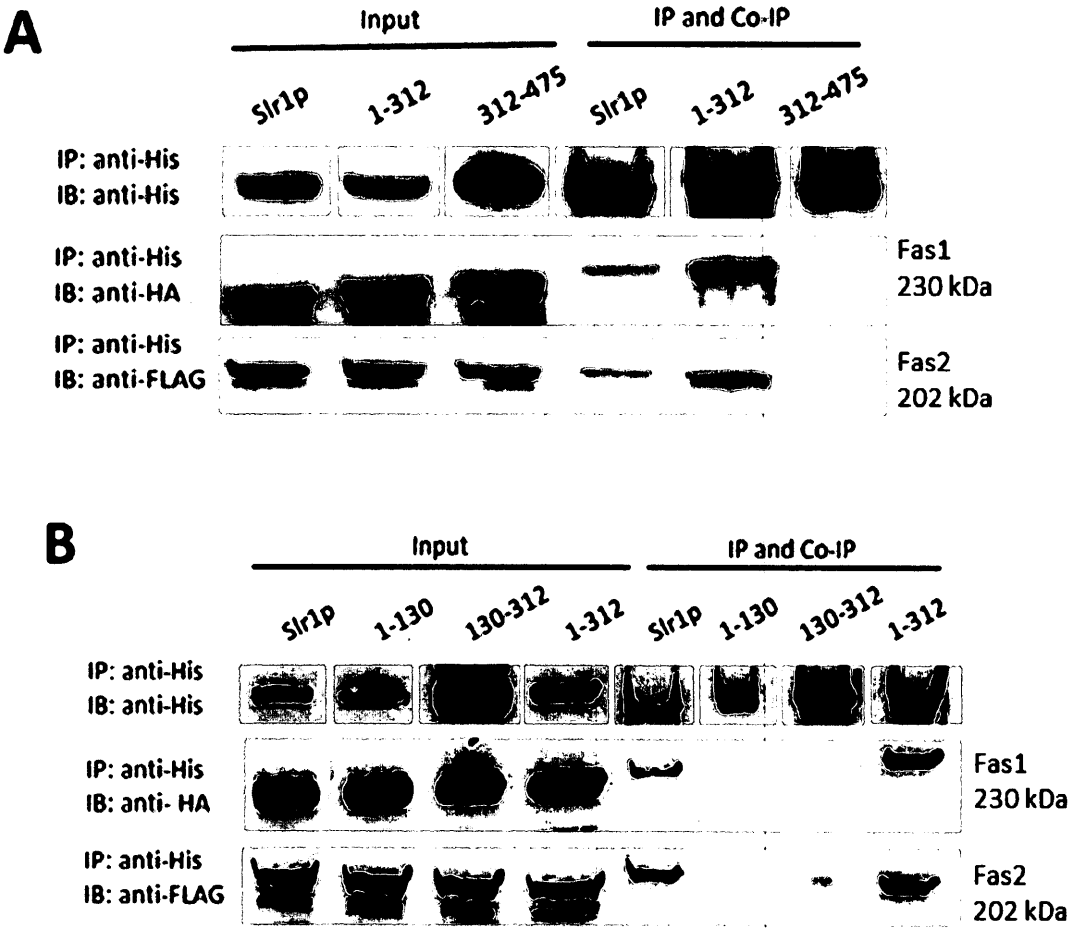

Figure 21 - The N-terminal domain of Slr1p interacts with FAS. Co-precipitation studies were carried out with an SLR1 knock-out yeast strain coexpressing pREP41X+ Fas1-HA and pREP42X+Fas2-FLAG (strain: yAS99ΔSLR1 + Fas1-HA + Fas2-FLAG). (A) Recombinant His-tagged Slr1p full length, His-tagged Slr1p mutant 1-312 (NTD) and His-tagged Slr1p mutant 312-475 (CTD) and (B) His-tagged Slr1p mutant 1-130, His-tagged Slr1p mutant 130-312 and His-tagged Slr1p mutant 1-312, that were produced in *E.coli* and purified, were added to the lysate and precipitated with cobalt beads. Recombinant proteins present in starting lysate (left) and co-precipitates (right) were detected with anti-His (1:10000), anti-HA (1:50) and anti-FLAG (1:1000). Input represents 5% of the total cell extract used for each precipitation.

3.7 Profiling lipids in a wild type and SLR1 null strain

Since FAS, the multienzyme complex that is responsible for bulk fatty acid synthesis (Tehlivets et al., 2006) was pulled down with Slr1p as discovered through mass spectrometric analysis, we were interested in seeing whether there were any differences in the lipid profile patterns and free fatty acids. As it has previously been shown that fatty acid chain length can change with temperature via mechanisms that are not known (Okuyama and Saito, 1979), we performed lipid analysis on a wild type *S. pombe* strain, yAS99 and an SLR1 knock-out strain, yAS99ΔSLR1, at a normal growth temperature of 32 °C and a reduced temperature of 16°C. Table 8 demonstrates the abundance of each lipid component in the four samples tested. It can be seen that at 32°C and 16°C, there is less total polar lipids in the knock-out strain when compared to the control strain. It can also be observed that in the control and the knockout strain there is less PC being produced at 16°C when compared to 32°C. Contrary to this, there is an increase in PG levels at 16°C when compared to 32°C. Another interesting difference is in the pattern of PS when shifting temperatures. There is no significant difference in PS levels in the control strain at both temperatures, however, when analyzing the knock-out strain, the PS level drops about 55% when comparing 32°C and 16°C incubation temperatures.

Table 9 illustrates the fatty acid composition of the four samples tested. Significant differences can be observed in the 18:0 and 18:1 free fatty acids. There is significantly more 18:0 fatty acids at 32°C in the knock-out strain than in the control strain. Also, there is less 18:1 in the knockout strain at 32°C which substantially decreases at 16°C, while in the control strain it increases at 16°C.

When looking at the fatty acid synthesis pathway, phosphatidic acid is the closest to the step catalyzed by fatty acid synthase which we are predominantly interested in. Therefore, we analyzed several PA species and noted significant differences in Figure 22. At low temperature more PA(36:2) is made compared to PA(34:1), relative to their amounts at high temperature for both the wild type strain and the SLR1 null strain. At high temperatures, more PA(34:1) is made for both strains, relative to their amounts at low temperatures. However, when comparing the control strain and SLR1 null strain, the changes observed are significantly amplified in the absence of Slr1p (Figure 22). In the SLR1 knock-out strain, the swing to PA(36:2) at low temperature is more extreme. In this strain there is also more PA(34:1) and less PA(36:2) at high temperature and this composition reverses at low temperature where you see less PA(34:1) and more PA(36:2).

Table 8 – Mass spectrometric analysis of each lipid component. Values are means ± SD of two independent experiments based on picomol per mg dry weight.

	32°C control	32° ΔSLR1	16°C control	16° ΔSLR1
PC	1950 ± 679	1207 ± 557	1610 ± 16	1081 ± 397
PE	323 ± 100	207 ± 86	310 ± 48	214 ± 139
PI	391 ± 192	295 ± 225	340 ± 70	257 ± 72
PS	71 ± 18	89 ± 44	72 ± 8	49 ± 7
PA	12 ± 8	7 ± 7	10 ± 4	6 ± 4
PG	26 ± 21	20 ± 10	46 ± 10	26 ± 3
Total polar lipids	2804 ± 961	1841 ± 923	2421 ± 133	1653 ± 639

Table 9 – Fatty acid composition of *S. pombe* strains yAS99 (control) and yAS99ΔSLR1 at 32°C and 16°C determined by mass spectrometric analysis. Values are means ± SD of two independent experiments based on picomol per mg dry weight.

	32°C control	32° ΔSLR1	16°C control	16° ΔSLR1
16:0	75 ± 37	72 ± 8	25 ± 16	25 ± 35
18:0	190 ± 48	251 ± 25	138 ± 54	135 ± 87
18:1	165 ± 25	137 ± 122	179 ± 77	89 ± 58
22:0	3.4 ± 4.8	0.03 ± 0.04	0.86 ± 1.22	0.53 ± 0.74
22:1	4 ± 3.6	2.1 ± 1.5	0.52 ± 0.7	0.51 ± 0.7
Total fatty acids	451 ± 85	464 ± 156	345 ± 4	251 ± 182

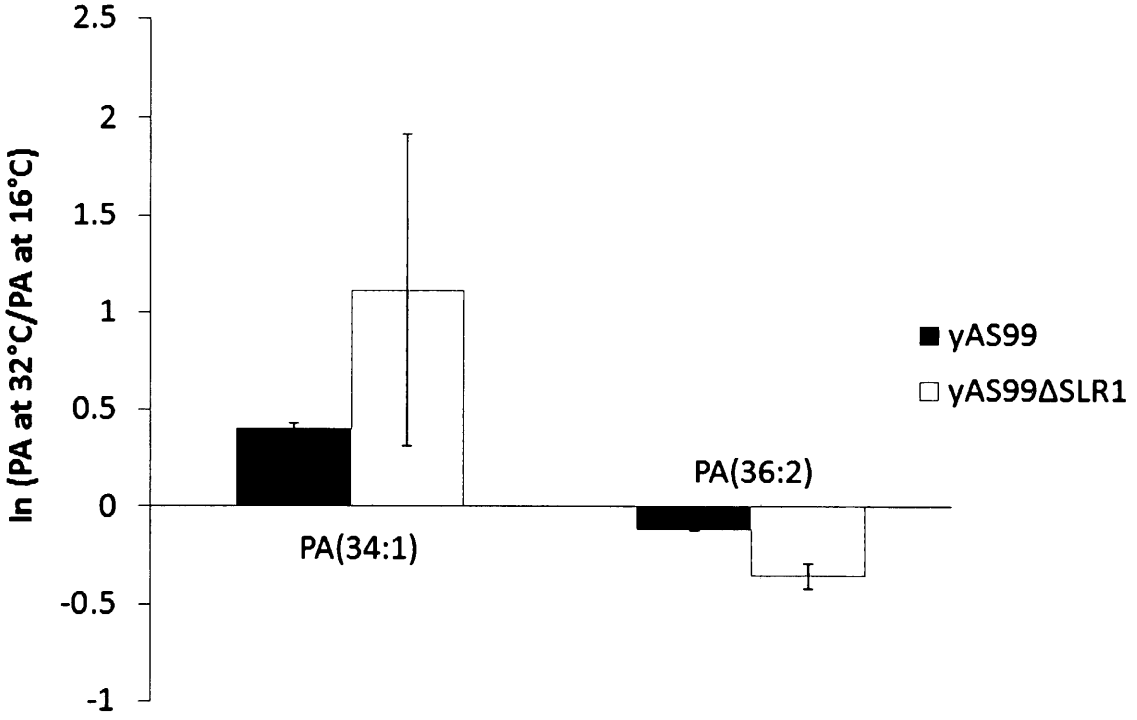

Figure 22 - Phosphatidic acid composition in *S. pombe* cells. PA (34:1) and PA(36:2) composition of wild type strain yAS99 and SLR1 knock-out strain yAS99ΔSLR1 at 32°C and 16°C, analyzed by LC-MS/MS. Values are represented as In (PA at 32°C/PA at 16°C). At 32° there is more PA(34:1) and at 16°C there is more PA(36:2) for both yAS99 and yAS99ΔSLR1, but it is exacerbated in the knock-out strain. Ratios are represented as mean ± SD derived from two independent experiments.

DISCUSSION

Slr1p is a member of a novel family of proteins characterized by the presence of a highly conserved La-motif. Very little is known about La-related proteins and specification of a general role for these proteins is made difficult by the high degree of structural variability among them. *S. pombe* proves an efficient system for studying this group of proteins, as *S. pombe* only has one LARP that shares the highly conserved motif with genuine La proteins. The goal of this study was to use several methodologies to resolve the function of Slr1p that may be pertinent to LARPs in higher eukaryotes.

A new class of La motif containing proteins

The main functional class of La proteins consists of genuine La homologs in nearly all eukaryotic species, which are nuclear phosphoproteins that bind nascent RNA polymerase III transcripts (Bayfield et al., 2010). However, *H. sapiens, C. elegans, D. melanogaster* and *S. cerevisiae* all have La motif containing proteins that are distinct from the authentic La protein in each organism. Since the La motifs of these organisms are more similar to each other than genuine La proteins, these proteins may constitute a new functional class of RNA-binding proteins. Slr1p has been identified as a member of the La-related family of proteins based on its sequence homology in its La-motif and we propose it constitutes a functional ancestor to all the other LARPs. Although LARPs bind to a wide variety of RNAs and the mechanisms by which they discriminate their RNA targets are unknown, characterization of Slr1p will hopefully provide information that could enhance our understanding of its relatives. Thorough understanding of the LARPs' role in cellular function and regulation may prove necessary to further understand RNA-

involving processes in the cell. Based on what is known so far, we may expect them to have implications in human disease, as emphasized by the tumor suppressing activity reported for human LARP7 (He et al., 2008).

Budding and fission yeast are one of the simplest model organisms where La proteins and LARPs can be manipulated and deleted to perform various experiments in the hopes of characterizing these proteins in greater detail. Consequently, Slr1p, the single LARP in fission yeast was studied. Sequence analysis demonstrates that Slr1p harbours a La motif that is more C-terminal in comparison to other LARPs, and it lacks an RRM (Figure 10). In comparison to the five families of LARPs, Slr1p shows closest resemblance to LARP1. Despite Slr1p having a La-motif, it can be concluded that Slr1p is distinct from authentic La proteins by several criteria; the La motif is located more C-terminally, rather than at the N-terminus, the La motif is phylogenetically divergent from that of genuine La and Slr1p lacks homology to genuine La proteins outside the La motif. Therefore, we conclude that Slr1p likely does not classify into one of the five LARP families identified thus far and may represent a progenitor or ancestor for these more specialized LARPs found in higher systems.

Slr1p is an RNA Chaperone

FRET based analysis shows that full length Slr1p harbours RNA chaperone activity, as previously demonstrated for human La. Figure 13 illustrates that like hLa, but unlike RNA and BSA, Slr1p was active in both strand annealing and strand displacement activities. In phase I of the assay, the increasing FRET index corresponds to the annealing of the two RNA 21mers, a reaction that was accelerated by Slr1p and human La. After

injection of an excess of non-labelled competitor RNA in phase II of the assay, the FRET index decreased, indicating the efficient strand displacement activity of Slr1p (Figure 13). Based on the observation made with the crystal structure of human La, contacts with RNA are speculated to be mediated by the La motif and RRM (Teplova et al.,2006). However, the RNA chaperone activity of Slr1p is surprising considering that Slr1p lacks an RRM, which has been shown to convey the chaperone activity associated with the La module of human La. This result suggests that there may be multiple mechanisms by which La and LARPs engage their substrate(s). In addition, the 2nd prediction model (see Appendix; Figure 1) suggests Slr1p has intrinsically unstructured regions which is advantageous for RNA chaperones since it can easily interact with a range of many different partners and is not limited to a single binding pocket. Disordered regions might also provide a folding platform for the RNA as the chaperone holds the RNA molecule in close proximity.

We also found that both the N- and C-terminal halves are capable of strand annealing and strand displacement activity (Figure 14). Mutational analysis showed that Slr1p mutant 1-130 was inactive in the FRET assay and mutant 130-312 was active, suggesting that residues 130-312 are important for RNA chaperone activity in the N-terminal domain. The predicted La motif, mutant 312-414, had minimal strand annealing and strand displacement activity, but this was enhanced with the addition of the predicted disordered region C-terminal to the La motif. This is consistent with human La, as it was shown that predicted disordered regions C-terminal to the canonical RRM are important for the capacity of hLa to function as an RNA chaperone (Naeeni et al., 2012). These data

propose that RNA chaperone activity is a conserved function of genuine La proteins and most LARPs, and as for human La, the predicted disordered regions after the RRM and in this case the La motif, are important for this function *in vitro*.

Unfortunately, the FRET assay measures merely the kinetics of strand annealing and strand displacement and provides no information to its *in vivo* activity. Therefore, other methods may be more effective in determining the molecular basis for the specific mechanism *in vivo*. Furthermore, understanding the physiologically relevant implications of these findings requires knowledge of the function of Slr1p and Slr1p's RNA targets which have been recently identified by co-immunoprecipitation of ribonucleoprotein complexes and analysis of these by RNA-sequencing. As a result, further experimentation is required with testing specific RNAs that are bound to Slr1p *in vivo.*

Slr1p binds to a tRNA substrate and identification of Slr1p's RNA targets

Gel shift analysis revealed that Slr1p did not bind to poly (A), poly (C) and poly (G) 10-mer and 20-mer RNA homopolymers and weak binding was observed with the 20 mer poly (U) RNA but not the 10-mer poly (U) RNA (Figure 15). Also, Slr1p did bind to a tRNA with a low affinity when compared to Sla1p (Figure 16). In order to gain a better understanding of Slr1p's endogenous RNA targets, RNA was isolated that was pulled down with Slr1p-PrA in co-IP experiments and Illumina RNA sequencing was performed. Since bioinformatic analysis is still being processed, definite conclusions of the RNAs bound to Slr1p cannot be made. However, preliminary data suggests that some of the predominant RNAs that associate with Slr1p are involved in translation. This is consistent with human LARPs 1, 4 and 6 substrates, which are primarily coding RNAs,

thus, implicating Slr1p and human LARPs 1, 4 and 6 to have a function in mRNA metabolism.

Sr1p1 interacts with translation initiation machinery and fatty acid synthase in the cytoplasm

Co-immunoprecipitation, a common biochemical technique used to study protein-protein interactions was used to determine Slr1p associated protein complexes. A rapid affinity-purification method was used, which had been shown to produce efficient isolation of RNP complexes. This method aims to overcome many of the previous limitations experienced in protein purifications and studies of protein-protein interactions in yeast (Oeffinger et al., 2007). Different from traditional affinity purifications, this method produces efficient cell lysis in the solid phase by milling with cells being rapidly frozen in liquid nitrogen to avoid any damage by released nucleases and proteases, as well as redistribution of proteins within the extract (Oeffinger et al., 2007). In addition, tagged complexes are isolated using antibody-conjugated magnetic beads that significantly reduce the pullout time which is of crucial importance to achieve high yields. Prolonged incubations are likely to result in loss of transiently interacting molecules and retention of only tightly bound proteins. Furthermore, we optimized for efficient isolation of Slr1p associated proteins by testing different buffers and buffer conditions. As a result, we have successfully adapted a novel method for protein purification from *S. pombe*.

Having generated a knock-in construct with a Protein A tag integrated into the chromosomal open reading frame of SLR1, co-immunoprecipitation was performed to

isolate Slr1p associated factors (Figure 19A). The data suggest that Slr1p-PrA is a soluble protein that is being expressed, as a bright band is observed at approximately 82 kDa on the Western Blot (Figure 19B). Since Slr1p was being expressed from its endogenous promoter, more cells may be required to observe a higher level of expression and therefore a more prominent band around 82 kDa in the Coomassie stain. By means of co-IP, we have demonstrated the existence of several physical interactors of Slr1p. All associated proteins were identified by mass spectrometry and the results significant to Slr1p were analyzed (see Table 7). Interestingly, both fatty acid synthase alpha and beta subunits were pulled down with Slr1p, as well many of the translation initiation subunits of eIF3 and eIF4F. Fatty acid synthase is a multienzyme complex responsible for the *de novo* synthesis of saturated long chain fatty acids (Lomakin et al., 2007). Translation initiation factors function in positioning the ribosomal subunits on the mRNA transcript to allow translation, hence association with these proteins, strongly suggests a role for Slr1p in translation. This is interesting yet not unique to Slr1p, as other LARPs have been shown to interact with these translation initiation factors. Human LARP1 and LARP4 have been shown to bind eIF4G and PABP (Burrows et al., 2010; Schaffler et al., 2010) suggesting a role in mRNA metabolism, however, the mechanisms are unknown. Thus far, the fatty acid synthase mass spectrometry hits have been validated through co-IP experiments (Figure 20), yet the mechanism by which Slr1p functions in translation still needs to be determined.

Furthermore, having studied the interaction between Slr1p and FAS in a little bit more detail, it is hypothesized that Slr1p is involved in the regulation of what type of

long chain fatty acids FAS makes. The interaction between FAS and Slr1p has been mapped to the NTD, specifically Slr1p mutant 1-312 (Figure 21). This suggests that the binding of Slr1p to FAS is not mediated by its La-motif, and is specific for Slr1p.

In addition, lipid analysis demonstrates that several differences can be observed between a wild type strain and an SLR1 null strain. At low incubation temperatures there is more PA(36:2) and at high temperatures there is more PA(34:1) in both the wild type strain and SLR1 null strain. However, the temperature dependant swing from PA(34:1) to PA(36:2) is amplified in the knock-out strain when Slr1p is absent (Figure 22). Therefore, it seems as if though Slr1p is a counterforce or negatively repulses the normal distribution of PA species in *S. pombe*. Also, there is a much greater drop in the total number of fatty acids in the knockout strain when shifting from 32°C to 16°C when compared to the wild type strain. Overall, these results suggest that differences can be seen between the two strains, however, the experiment needs to be repeated several more times to conclude that the results are true.

Intracellular localization plays a major role as a means of spatial restriction in regards to protein function. Some cellular activities are localized to a particular region within the cell, which dictates the distribution of molecules involved. Indirect immunofluorescence of Slr1p-PrA has demonstrated that it is primarily cytoplasmic, which is consistent with the protein complexes pulled down with Slr1p, as majority of them are cytoplasmic. Slr1p's cytoplasmic localization is also consistent with the *S. cereviasie* LARPs, Sro9p and Slf1p, as these have been also shown to be localized to the cytoplasm (Rother et al., 2010).

Conclusion

The main research objective of this Master's thesis was to employ several methodologies to characterize Slr1p, a member of a larger family of La-related proteins. A better understanding of this protein could provide further insight into LARPs in higher eukaryotes which could have implications in human disease.

To date, progress has been made in terms of specification of Slr1p involvement in a particular biological process. Through our experiments, we have shown that Slr1p interacts with other factors in the cell, including translation initiation factors and fatty acid synthase. Slr1p interacts with FAS via its N-terminus, however, further experimentation is required to establish a mechanism and define Slr1p's involvement in this process. Slr1p is a cytoplasmic RNA-binding factor capable of RNA chaperone activity. The NTD and CTD halves both harbour RNA chaperone activity and the CTD associated strand annealing and strand displacement activity is enhanced with the addition of the subsequent disordered region C-terminal to the La motif. Based on these observations, we propose that Slr1p functions in the regulation of fatty acids within the cell as well as in RNA stability, possibly associated with translation initiation. Further experimentation is required to validate the hypothesis and gain a better understanding of the complete function of Slr1p in the cell.

Future Perspectives

Taken together, we have engaged a variety of biochemical methodologies to characterize Slr1p. Although an abundance of information regarding Slr1p has been obtained thus far, further experimentation is required to fully characterize this protein and establish a working model for this protein. To follow upon the progress made so far, future work will focus primarily on verifying the RNA-sequencing data and performing specific experiments that will provide insight into the mechanism(s) Slr1p is involved in.

First, the RNA-sequencing data needs to be validated by selecting several candidate RNAs that have been shown to preferentially bind to Slr1p and perform specific experiments for these RNAs. Gel shift analysis should also be performed to determine binding affinities, as well as FRET assays using Slr1p's endogenous substrates. In addition, mutational analysis would be useful to determine the binding characteristics associated with its substrate(s).

In order to complete the model for Slr1p's interaction and involvement with fatty acid synthase, the multienzyme complex will need to be purified for the purpose of performing enzyme activity assays in the presence and absence of Slr1p. Fas1 will be cloned into an expression vector with a 8xHis tag and purified by affinity chromatography. Moreover, different factors can be introduced into the assay to see changes in enzyme activity and the affect they may or may not have. Furthermore, mass spectrometry revealed that serine on residue 130 is phosphorylated. As seen in the co-IPs, neither halves of the NTD (mutants 1-130 and 130-312) interacted with the Fas1/Fas2 complex, however, mutant 1-312 did. This indicates that the region around serine 130,

and possibly the phosphorylation status of this residue, may be critical for this interaction. Therefore, new Slr1p mutants should be designed, one including the phosphorylation site and one mutating the serine on residue 130 to an alanine or glutamic acid and see whether phosphorylation may play a role in the interaction. Additional Co-IPs should also be performed to determine if Fas1 and Fas2 subunits independently bind Slr1p or if they form a complex with Slr1p and only one of the subunits makes the interaction. It is also essential to perform subsequent trials of lipid extraction to validate the lipidomics data and obtain significant error bars.

Some focus should also be placed on translation initiation since Slr1p pulled down many of these factors and is therefore presumed to have some role in this process. Various experiments should be performed regarding translation and protein levels could be detected by reverse transcriptase-PCR and Western blotting. Furthermore, genetic knockdowns may be applied to investigate possible relationships among these proteins. In addition, mass spectrometry revealed that Slr1p pulled down more than one subunit of the DNA-directed RNA Polymerase I complex. We thought this was an interesting hit since it is very different from substrates that authentic La proteins engage, therefore, it may be worthwhile to investigate this interaction in greater detail.

If a defined mechanism can be identified for the activity of Slr1p, other LARPs would also have to be evaluated in terms of similarities in their activity. In the end, we hope to be able to characterize Slr1p functionally as well as structurally and to be able to extend those finding onto other members of the LARP family.

References

Aigner, S., Lingner, J., Goodrich, K.J., Grosshans, C.A., Shevchenko, A., Mann, M. and Cech, T.R. (2000). Euplotes telomerase contains an La motif protein produced by apparent translational frameshifting. *EMBO J*, **19**, 6230–6239.

Alfano, C., Sanfelice, D., Babon, J., Kelly, G., Jacks, A., Curry, S. and Conte, M.R. (2004). Structural analysis of cooperative RNA binding by the La motif and central RRM domain of human La protein. *Nat Struct Mol Biol*, **7-14**, 7-12.

Ali, N. and Siddiqui, A. (1997). The La antigen binds 5' noncoding region of the hepatitis C virus RNA in the context of the initiator AUG codon and stimulates internal ribosome entry site-mediated translation. *PNAS*, **94**, 2249-2254.

Ali, N., Pruijn, G.J., Kenan, D.J., Keene, J.D. and Siddiqui, A. (2000). Human La antigen is required for the hepatitis C virus internal ribosome entry site (IRES)-mediated translation. *J Biol Chem*, **275**, 27531-27540.

Alspaugh, M.A. and Tan, E.M. (1975). Antibodies to cellular antigens in Sjogren's syndrome. *J Clin Invest*, **55**, 1067-1073.

Aoki, K., Adachi, S., Homoto, M., Kusano, H., Koike, K. and Natsume, T. (2013). LARP1 specifically recognizes the 3'terminus of poly(A) mRNA. *FEBS Letters*.

Ayukawa, K., Taniguchi, S., Masumoto, J., Hashimoto, S., Sarvotham, H., Hara, A., Aoyama, T. and Sagara, J. (2000). La autoantigen is cleaved in the COOH terminus and loses the nuclear localization signal during apoptosis. *J Biol Chem*, **275**, 34465-34470.

Bai, C. and Tolias, P.P. (2000). Genetic analysis of a La homolog in Drosophila melanogaster. *Nucleic Acids Res*, **28,** 1078–1084.

Basi, G., Schmid, E. and Maundrell, K. (1993). TATA box mutations in the Schizosaccharomyces pombe nmt1 promoter affect transcription efficiency but not the transcription start point or thiamine repressibility. *Gene.* **123**, 131-136.

Bayfield, M. A., Kaiser, T. E., Intine, R. V. & Maraia, R. J. (2007). Conservation of a masked nuclear export activity of La proteins and its effects on tRNA maturation. *Mol. Cell. Biol,* **27**, 3303–3312.

Bayfield, M.A. and Maraia, R.J. (2009). Precursor-product discrimination by La protein during tRNA metabolism. *Nat Struct Mol Biol*, **16**, 430-437.

Bayfield, M.A., Yang, R. and Maraia, R.J. (2010). Conserved and divergent features of the structure and function of La and La-related proteins (LARPs). *Biochim Biophys Acta*, **1799**, 365-378.

Belisova, A., Semrad, K., Mayer, O., Kocian, G., Waigmann, E., Schroeder, R. and Steiner, G. (2005). RNA chaperone activity of protein components of human Ro RNPs. *RNA*, **11**, 1084-1094.

Blagden, S.P., Gatt, M.K., Archambault, V., Lada, K., Ichihara, K., Lilley, K.S., Inoue, Y.H. and Glover, D.M. (2009). Drosophila Larp associates with poly(A)-binding protein and is required for male fertility and syncytial embryo development. *Dev Biol,* **334**, 186-197.

Bousquet-Antonelli, C. and Deragon, J.M. (2009). A comprehensive analysis of the La-motif protein superfamily. *RNA*, **15**, 750-764.

Burrows, C., Latip, N.A., Lam, S.J., Carpenter, L., Sawicka, K., Tzolovsky, G., Gabra, H., Bushell, M., Glover, D.M., Willis, A.E. and Blagden, S.P. (2010). The RNA binding protein Larp1 regulates cell division, apoptosis and cell migration. *Nucleic Acids Res*, **38**, 5542-5553.

Cai, L., Fritz, D., Stefanovic, L. and Stefanovic, B. (2010). Binding of LARP6 to the Conserved 5' Stem-Loop Regulates Translation of mRNAs Encoding Type I Collagen. *J Mol Biol*, **395**, 309-326.

Cardinali, B., Carissimi, C., Gravina, P. and Pierandrei-Amaldi, P. (2003). La protein is associated with terminal oligopyrimidine mRNAs in actively translating polysomes. *J Biol Chem*, **278**, 35145-35151.

Chakshusmathi, G., Kim, S.D., Rubinson, D.A. and Wolin. S.L. (2003). A La protein requirement for efficient pre-tRNA folding. *EMBO J*, **22**, 6562–6572.

Chauvet, S., Maurel-Zaffran, C., Miassod, R., Jullien, N., Pradel, J. and Aragnol, D. (2000). dlarp, a new candidate Hox target in Drosophila whose orthologue in mouse is expressed at sites of epithelium/mesenchymal interactions. *Dev Dyn*, **218,** 401–413.

Costa-Mattioli, M., Svitkin, Y. and Sonenberg, N. (2004). La Autoantigen Is Necessary for Optimal Function of the Poliovirus and Hepatitis C Virus Internal Ribosome Entry Site In Vivo and In Vitro. *Mol Cell Biol*, **24**, 6861-6870.

Craig, A.W., Svitkin, Y.V., Lee, H.S., Belsham, G.J. and Sonenberg, N. (1997). The La autoantigen contains a dimerization domain that is essential for enhancing translation. *Mol Cell Biol,* **17**, 163-169.

Dong, G., Chakshusmathi, G., Wolin, S.L. and Reinisch, K.M. (2004). Structure of the La motif: a winged helix domain mediates RNA binding via a conserved aromatic patch. *EMBO J*, **23**, 1000-1007.

Forsburg, S. L. (1993). Comparison of different *Schizosaccharomyces pombe* expression systems. *Nucleic Acids Res*, **21**, 2955-2956.

He, N., Jahchan, N.S., Hong, E., Li, Q., Bayfield, M.A., Maraia, R.J., Luo, K. and Zhou, Q. (2008). A La-related protein modulates 7SK snRNP integrity to suppress P-TEFb-dependent transcriptional elongation and tumorigenesis. *Mol Cell*, **29**, 588–599.

Hershey, J.W., Asano, K., Naranda, T., Vornlocher, H.P., Hanachi, P. and Merrick, W.C. (1996). Conservation and diversity in the structure of translation initiation factor EIF3 from humans and yeast. *Biochimie*, **78,** 903- 907.

Holcik, M. and Korneluk, R.G. (2000). Functional characterization of the X-linked inhibitor of apoptosis (XIAP) internal ribosome entry site element: role of La autoantigen in XIAP translation. *Mol Cell Biol*, **20**, 4648 -4657.

Holcik, M. and Sonenberg, N. (2005). Translational control in stress and apoptosis. *Nat Rev Mol Cell Biol*, **6,** 318-327.

Ichihara, K., Shimizu, H., Taguchi, O., Yamaguchi, M. and Inoue, Y.H. (2007). A Drosophila orthologue of Larp protein family is required for multiple processes in male meiosis. *Cell Struct and Function*, **32**, 89-100.

Inada, M. and Guthrie, C. (2004). Identification of Lhp1p–associated RNAs by microarray analysis in *Saccharomyces cerevisiae* reveals association with coding and noncoding RNAs. *Proc Natl Acad Sci U S A*, **101**, 434–439.

Intine, R.V., Dundr, M., Misteli, T. and Maraia, R.J. (2002). Aberrant nuclear trafficking of La protein leads to disordered processing of associated precursor tRNAs. *Mol Cell,* **9,** 1113–1123.

Intine, R.V., Tenenbaum, S.A., Sakulich, A.S., Keene, J.D. and Maraia, R.J. (2003). Differential phosphorylation and subcellular localization of La RNPs associated with precursor tRNAs and translation-related mRNAs. *Molecular Cell*, **12**, 1301-1307.

Jacks, A., Babon, J., Kelly, G., Manolardis, I., Cary, P.D., Curry, S. and Conte, M.R. (2003). Structure of the C-terminal domain of human La protein reveals a novel RNA recognition motif coupled to a helical nuclear retention element. *Structure*, **11**, 833-843.

Johansson, P., Wiltschi, B., Kumari, P., Kessler, B., Vonrhein, C., Vonck, J., Oesterhelt, D. and Grininger, M. (2008). Inhibition of the fungal fatty acid synthase type I multienzyme complex. *PNAS*, **105,** 12803-12808.

Kotik-Kogan, O., Valentine, E.R., Sanfelice, D., Conte, M.R. and Curry, S. (2008). Structural analysis reveals conformational plasticity in the recognition of RNA 3' ends by the human La protein. *Structure*, **16**, 852-862.

Krueger, B.J., Jeronimo, C., Roy, B.B., Bouchard, A., Barrandon, C., Byers, S.A., Searcey, C.E., Cooper, J.J., Bensaude, O., Cohen, E.A., Coulombe, B. and Price, D.H. (2008). LARP7 is a stable component of the 7SK snRNP while P-TEFb, HEXIM1 and hnRNP A1 are reversibly associated. *Nucleic Acids Res*, **36**, 2219–2229.

Kucera, N.J., Hodsdon, M.E. and Wolin, S.L. (2011). An intrinsically disordered C terminus allows the La protein to assist the biogenesis of diverse noncoding RNA precursors. *Proc Natl Acad Sci U S A*, **108**, 1308-1313.

Lomakin, I.B., Xiong, Y. and Steitz T.A. (2007). The crystal structure of yeast fatty acid synthase, a cellular machine with eight active sites working together. *Cell*, **129,** 319-332.

Manojlovic, Z. and Stefanovic, B. (2012). A novel role of RNA helicase A in regulation of translation of type I collagen mRNAs. *RNA*, **18**, 321-334.

Maraia, R.J. and Bayfield, M.A. (2006). The La protein-RNA complex surfaces. *Mol Cell*, **21**, 149-152.

Maraia, R. J. and Intine, R. V. (2001). Recognition of nascent RNA by the human La antigen: conserved and divergent features of structure and function. *Mol Cell Biol,* **21**, 367–379.

Maris, C., Dominguez, C. and Allain, F.H. (2005). The RNA recognition motif, a plastic RNA-binding platform to regulate post-transcriptional gene expression. *Febs J*, **272**, 2118–2131.

Markert, A., Grimm, M., Martinez, J., Wiesner, J., Meyerhans, A., Meyuhas, O., Sickmann, A. and Fischer, U. (2008). The La-related protein LARP7 is a component of the 7SK ribonucleoprotein and affects transcription of cellular and viral polymerase II genes. *EMBO Rep*, **9**, 569-575.

Martino, L., Pennell, S., Kelly, G., Bui, T.T., Kotik-Kogan, O., Smerdon, S.J., Drake, A.F., Curry, S. and Conte, M.R. (2012). Analysis of the interaction with the hepatitis C virus mRNA reveals an alternative mode of RNA recognition by the human La protein. *Nucleic Acids Res*, **40**, 1381-1394.

Mattioli, M. and Reichlin, M. (1974). Heterogeneity of RNA protein antigens reactive with sera of patients with systemic lupus erythematosus. Description of a cytoplasmic nonribosomal antigen. *Arthritis Rheum*, **17,** 421–429.

McDonough, V.M. and Roth, T.M. (2004). Growth temperature affects accumulation of exogenous fatty acids and fatty acid composition in *Schizosaccharomyces pombe*. *Antonie Van Leeuwenhoek*, **86**, 349-354.

Meerovitch, K., Svitkin, Y.V., Lee, H.S., Lejbkowicz, F., Kenan, D.J., Chan, E.K., Agol, V.I., Keene, J.D. and Sonenberg, N. (1993). La autoantigen enhances and corrects aberrant translation of poliovirus RNA in reticulocyte lysate. *J Virol*, **67**, 3798-3807.

Merret, R., Martino, L., Bousquet-Antonelli, C., Fneich, S., Descombin, J., Billey, E., Conte, M.R. and Deragon, J.M. (2013). The association of a La module with the PABP-interacting motif PAM2 is a recurrent evolutionary process that led to the neofunctionalization of La-related proteins. *RNA*, **19**, 36-50.

Meyuhas, O. (2000). Synthesis of the translational apparatus is regulated at the translational level. *Eur J Biochem*, **267**, 6321-6330.

Naeeni, A.R., Conte, M.R. and Bayfield, M.A. (2012). RNA chaperone activity of the human La protein is mediated by a variant RNA recognition motif. *J Biol Chem*, **287**, 5472-5482.

Niwa, H., Katayama, E., Yanagida, M. and Morikawa, K. (1998). Cloning of the fatty acid synthase beta subunit from fission yeats, coexpression with the alpha subunit, and purification of the intact multifunctional enzyme complex. *Protein Expr Purif*, **13**, 403-413.

Nykamp, K., Lee, M.H. and Kimble, J. (2008). *C .elegans* La-related protein, LARP-1, localizes to germline P bodies and attenuates Ras-MAPK signalling during oogenesis. *RNA*, **14**, 1378-1389.

Oeffinger, M., Wei, K.E., Rogers, R., DeGrasse, J., Chait, B.T., Aitchison, J.D. and Rout, M.P. (2007). Comprehensive analysis of diverse ribonucleoprotein complexes. *Nat Methods*, **4**, 951-956.

Okuyama, H., Saito, M., Joshi, V.C., Gunsberg, S. and Wakil S.J. (1979). Regulation by temperature of the chain length of fatty acids in yeast. *J Biol Chem*, **254**, 12281-12284.

Park, J.M., Kohn, M.J., Bruinsma, M.W., Vech, C., Intine, R.V., Fuhrmann, S., Grinberg, A., Mukherjee, I., Love, P.E., Ko, M.S., DePamphilis, M.L. and Maraia, R.J. (2006). The multifunctional RNA-binding protein La is required for mouse development and for the establishment of embryonic stem cells. *Mol Cell Biol*, **26**, 1445–1451.

Peterlin, B.M. and Price, D.H. (2006). Controlling the elongation phase of transcription with P-TEFb. *Mol Cell*, **23**, 297–305.

Rajkowitsch, L. and Schroeder, R. (2007). Coupling RNA annealing and strand displacement: a FRET-based microplate reader assay for RNA chaperone activity. *Biotechniques,* **43**, 304, 306, 308.

Robaglia, C. and Caranta, C. (2006). Translation intiation factors: a weak link in plant RNA virus infection. *Trends Plant Sci*, **11**, 40-45.

Rother, S., Burkert, C., Brunger, K.M., Mayer, A., Kieser, A. and Straber, K. (2010). Nucleocytoplasmic shuttling of the La motif-containing protein Sro9p might link its nuclear and cytoplasmic functions. *RNA*, **16**, 1393-1401.

Schaffler, K., Schulz, K., Hirmer, A., Wiesner, J., Grimm, M., Sickmann, A. and Fischer, U. (2010). A stimulatory role for the La-related protein 4B in translation. *RNA*, **16**, 1488-1499.

Schenk, L., Meinel, D.M., Strasser, K. and Gerber, A.P. (2012). La-motif-dependent mRNA association with Slf1p promotes copper detoxification. *RNA*, **18**, 449-461.

Semrad, K. (2011). Proteins with RNA chaperone activity: a world of diverse proteins with a common task-impediment of RNA misfolding. *Biochem Res Int*, **2011,** 532908.

Shui, G., Guan, X.L., Low, C.P., Chua, G.H., Goh, J.S., Yang, H. and Wenk, M.R. (2010). Toward one step analysis of cellular lipidomes using liquid chromatography coupled with mass spectrometry: application to *Saccharomyces cerevisiae* and *Schizosaccharomyces pombe* lipidomics. *Mol Biosyst*, **6,** 1008-1017.

Simons, F.H., Broers, F.J., Van Venrooij, W.J. and Pruijn, G.J. (1996). Characterization of cis-acting signals for nuclear import and retention of the La (SS-B) autoantigen. *Exp Cell Res*, **224**, 224-236.

Singh, M., Wang, Z., Koo, B.K., Patel, A., Cascio, D., Collins, K. and Feigon, J. (2012). Structural basis for telomerase RNA recognition and RNP assembly by the holoenzyme La family protein p65. *Cell,* **47,** 16-26.

Sobel, S.G. and Wolin, S.L. (1999). Two yeast La motif-containing proteins are RNA-binding proteins that associate with polyribosomes. *Mol Biol Cell*, **10**, 3849–3862.

Sonenberg, N. and Dever, T.E. (2003). Eukaryotic translation initiation factors and regulators. *Curr Opin Struct Biol*, **13,** 56-63.

Stefano, J. E. (1984). Purified lupus antigen La recognizes an oligouridylate stretch common to the 3' termini of RNA polymerase III transcripts. *Cell,* **36**, 145–154.

Svitkin, Y.V., Pause, A. and Sonenberg, N. (1994). La autoantigen alleviates translational repression by the 5' leader sequence of the human immunodeficiency virus type 1 mRNA. *J Virol,* **68**, 7001–7007.

Svitkin, Y.V., Evdokimova, V.M., Brasey, A., Pestova, T.V., Fantus, D., Yanagiya, A., Imataka, H., Skabkin, M.A., Ovchinnikov, L.P., Merrick, W.C. and Sonenberg, N. (2009). General RNA-binding proteins have a function in poly(A)-binding protein-dependent translation. *EMBO J,* **28**, 58–68.

Tehlivets, O., Scheuringer, K. and Kohlwein, S.D. (2006). Fatty acid synthesis and elongation in yeast. *Biochim Biophys Acta*, **1771**, 255-270.

Teplova, M., Yuan, Y.R., Phan, A.T., Malinina, L., Ilin, S., Teplov, A. and Patel, D.J. (2006). Structural basis for recognition and sequestration of UUU(OH) 3' temini of nascent RNA polymerase III transcripts by La, a rheumatic disease autoantigen. *Mol Cell*, **21**, 75-85.

Trotta, R., Vignudelli, T., Pecorari, L., Intine, R.V., Guerzoni, C., Santilli, G., Candini, O., Byrom, M.W., Goldoni, S., Ford, L.P. *et al.* (2003). BCR/ABL activates mdm2 mRNA translation via the La antigen. *Cancer Cell*, **I3**, 145-160.

Valavanis, C., Wang, Z., Sun, D., Vaine, M. and Schwartz, L.M. (2007). Acheron, a novel member of the Lupus Antigen family, is induced during the programmed cell death of skeletal muscles in the moth Manduca sexta. *Gene*, **393**, 101–109.

Van Horn, D.J., Yoo, C.J., Xue, D., Shi, H. and Wolin, S.L. (1997). The La protein in *Schizosaccharomyces pombe*: a conserved yet dispensable phosphoprotein that functions in tRNA maturation. *RNA*, **3**, 1434-1443.

Wolin, S.L. and Cedervall, T. (2002). The La protein. *Annu Rev Biochem*, **71**, 375-403.

Wolin, S. L. & Matera, A. G. (1999). The trials and travels of tRNA. *Genes Dev,* **13**, 1–10.

Yang, R., Gaidamakov, S.A., Xie, J., Lee, J., Martino, L., Kozlov, G., Crawford, A.K., Russo, A.N., Conte, M.R., Gehring, K. *et al.* (2011). LARP4 binds poly(A), interacts with poly(A)-binding protein MLLE domain via a variant PAM2w motif and can promote mRNA stability. *Mol Cell Biol*, **31,** 542-556.

Yoo, C.J. and Wolin, S.L. (1994). La proteins from *Drosophila melanogaster* and *Saccharomyces cerevisiae*: a yeast homolog of the La autoantigen is dispensable for growth. *Mol Cell Biol*, **14,** 5412–5424.

Yoo, C. J. and Wolin, S. L. (1997). The yeast La protein is required for the 3' endonucleolytic cleavage that matures tRNA precursors. *Cell,* **89**, 393–402.

Zhu, J., Hayakawa, A., Kakegawa, T. and Kaspar, R.L. (2001). Binding of the La autoantigen to the 5' untranslated region of a chimeric human translation elongation factor 1A reporter mRNA inhibits translation in vitro. *Biochim Biophys Acta*, **1521**, 19–29.

Appendix

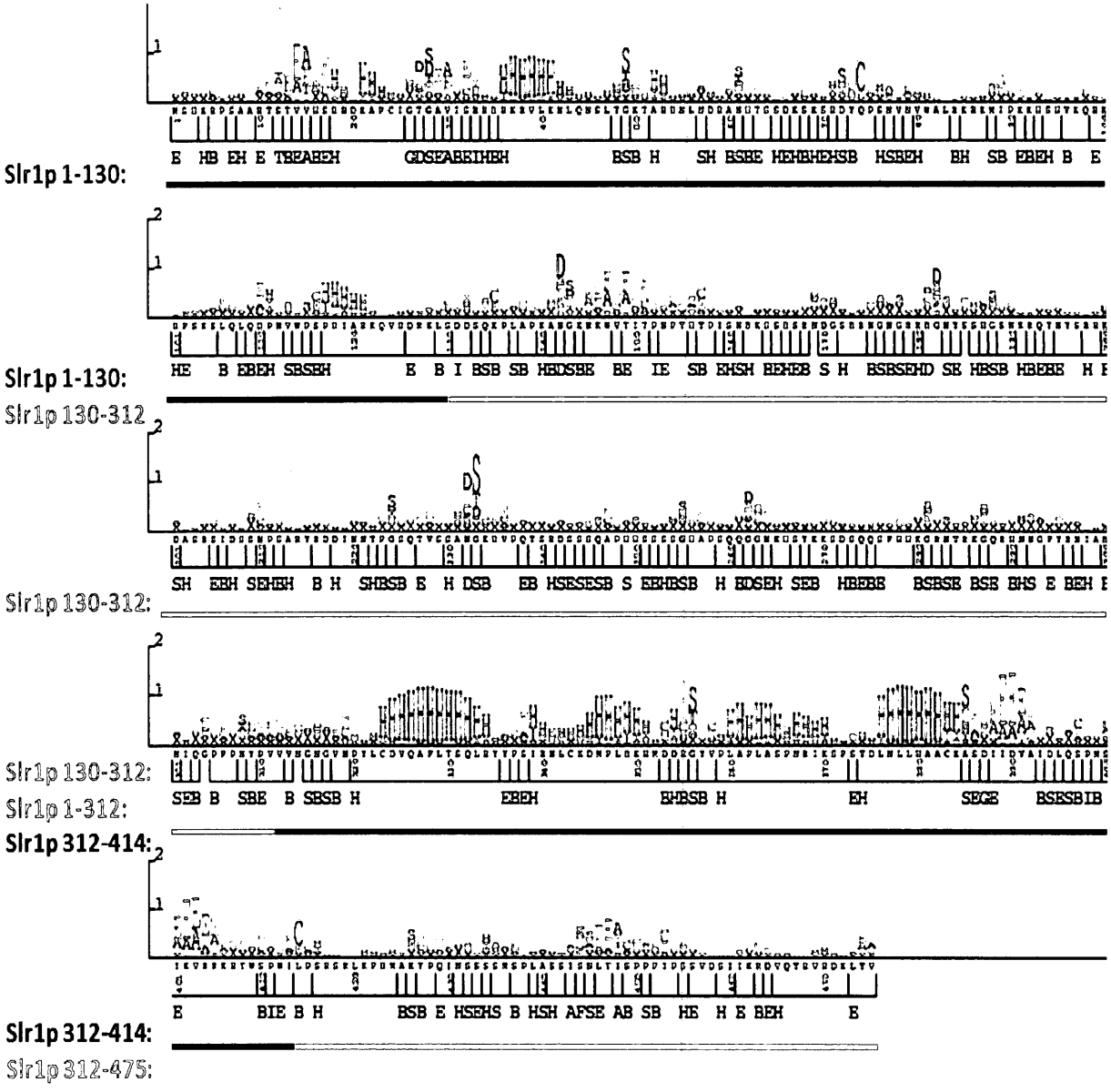

Figure 1: Primary structure and secondary structure prediction for Slr1p using the Predict-2nd program. The ALPHA alphabet was used, which is the torsion angle of the carbon alpha atoms along the backbone. The torsion angle is measured by the C_alpha(i-1), C_alpha(i), C_alpha(i+1), C_alpha(i+2) atoms. The alpha alphabet name and range is as follows: A, 165<=alpha<-170; B, -136<=alpha<-103; D, -68<=alpha<-17; E, -170<=alpha<-136; F, -17<=alpha<8; G, 8<=alpha<31; H, 31<=alpha<58; I, 58<=alpha<85; S, 85<=alpha<140; T, 140<=alpha<165. Slr1p mutant 1-130 is in blue, mutant 130-312 is in green and 1-312 is blue plus green. Secondary structure for the predicted LAM is in red and the CTD mutant 312-475 is red plus cyan. These are the mutants presented in this study.